1998

The Petrography of the Buck Creek Dunite Body, Clay County, NC: Implications about its Origin and Emplacement

Trista L. Thornberry
Oberlin College

The Petrography of the Buck Creek Dunite Body , Clay County, NC: Implications about its Origin and Emplacement

Submitted in partial completion of Honors in Geology
on May 1, 1998
by
Trista Thornberry
Oberlin College, class of 1998

ABSTRACT:

The Buck Creek dunite body, which is part of the Chunky Gal mafic and ultramafic complex, is well exposed on Corundum Knob in Clay County, North Carolina. These ultramafic rocks are surrounded here by mafic schists and gneisses. Gradational geochemical/mineralogical contacts between the mafic and ultramafic rocks of this complex imply the same protolith for both rock types. They may have originated as distinct parts of an ophiolitic suite beneath a mid-ocean spreading ridge. The metamorphic history of these ophiolitic rocks suggest further that they were subducted to depths of ~18km before being emplaced along fault zones in the present day Blue Ridge Province. Buck Creek dunites are generally unserpentinized, and display microstructures and crystallographic preferred orientations indicative of a simple shear deformation via dislocation creep. The degree of recrystallization in deformed olivines here implies elevated temperature/pressure conditions such as those found in collisional events. The large size of recrystallized grains and the apparently low dislocation densities in olivine indicates low differential stresses, also consistent with high temperature crustal deformation.

INTRODUCTION:

Some 300 ultramafic bodies occur among the metamorphic rocks of the Blue Ridge Province in the southern Appalachians. The Chunky Gal Mountain mafic/ultramafic complex is one of the larger complexes. Contained within the complex is the Buck Creek ultramafic body. At the southern-most end of this body is Corundum Knob (elev. 4000 ft), which is underlain mainly by dunite. As is true of most southern Appalachian ultramafic massifs, the Buck Creek body is encased in metamorphosed mafic plutonic rocks (see Map 1). Likewise, the origins of the Buck Creek body, like other ultramafic bodies in the southern Appalachians, is not known. If fact, it is not clear whether the mafic and ultramafic rocks are derived from the same protolith. The Buck Creek body exhibits typical characteristics of alpine ultramafic bodies. It is relevant to note that the contact between the Buck Creek body and the surrounding mafic country rock preserves no evidence of intrusive relations or contact metamorphism.

Because the dunites of the Buck Creek body are fairly unserpentinized, they may hold information critical to interpreting the origin of the complex. I undertook a comprehensive examination of their fabrics with the aim of placing limits on the conditions at which the body formed and/or was emplaced. In particular, olivine in dunite may preserve useful information such as: crystallographic preferred orientation, deformation microstructures, and grain size. By analyzing the *texture* of these deformed dunites, using texture in the sense defined by Wenk (1985), i.e. where it encompasses recognizing deformation microstructures and measuring any crystallographic fabric, I hope to provide constraints on hypotheses for the origin and emplacement of this body.

BACKGROUND ON ULTRAMAFIC ROCKS:

Ultramafic rocks are ferromagnesian rocks, usually containing less than 45% silica. Defining a particular rock as an ultramafic need not be based on chemical/mineralogical data, but merely color index. The color index of an ultramafic rock is 90-100 according to the International Union of Geological Sciences (IUGS) scale in which 100 is the darkest color index value, composed entirely of dark, ferromagnesian minerals (Streckeisen 1976, cited by Raymond 1995). Olivine is typically the most normative mineral in ultramafic rocks. Other common mineral phases include orthopyroxene, clinopyroxene, hornblende, chromite, magnetite, and anorthositic plagioclase. Magnesium is abundant in ultramafic rocks, often making up to 40% of the total rock. Most ultramafic rocks also have a relatively high iron content, typically 10%. Ultramafic rocks occur in six different geological settings. These are layered igneous bodies, zoned to irregularly shaped intrusions, komatiite flows, kimberlite pipes, alpine-type ultramafic complexes, and nodules such as xenoliths in igneous rocks. Layered bodies include ophiolites, dikes, sills, and lopolithic bodies (see Figure 1).

Intrusive ultramafic rocks are characteristically composite. Layering can be of three types: rhythmic (modally graded) layering, which is defined by differing plagioclase contents, uniform (isomodal) layering, which is less conspicuous, and cryptic layering ,which is only discerned geochemically (Nicolas 1988). Cumulate textures are most common, resulting from early crystallizing minerals settling out of a melt and forming a bottom layer with fluid filled interstices between these grains crystallizing later (Raymond 1995).

ALPINE ULTRAMAFICS:

Ultramafic rocks that are emplaced in mountain belts are called alpine ultramafic bodies. Alpine ultramafics are usually irregular, elliptical bodies. By definition alpine ultramafics contain primary olivine and orthopyroxene with a high Mg content, exhibit tectonite fabrics, have lenticular to lensoid shapes, lack chilled margins or contact metamorphism and are normally serpentinized. A tectonite is any rock with a fabric that reflects a history of deformation (Turner and Weiss 1963); in practice tectonites possess foliations, lineations, or both. Alpine ultramafics are emplaced early in the orogenic event, and are often highly metamorphosed. Metamorphic minerals include Ca-Mg amphiboles (tremolite, anthophyllite, hornblende), talc, chlorite, phlogopite, serpentines, and magnetite. The tectonite fabrics, the lack of chilled margins and metamorphism usually render their origins obscure. Alpine ultramafic bodies include ophiolites, magmatic crystal cumulates, mantle slabs, or crystallized/recrystallized diapirs (Raymond 1995).

Raymond (1995) placed the metamorphic textures in alpine ultramafic rocks into four categories (see Figure 2). Ultramafic rocks with a *protogranular* texture are coarse and non-foliated. Those with an *equigranular-mosaic* texture are weakly foliated with equant, polygonal grains whose curved to straight grain boundaries meet at 120° angles. *Equigranular-tabular* ultramafic rocks exhibit a semi-schistose fabric with elongate, deformed grains showing deformation bands and features such as: kink bands, undulose extinction, deformation lamellae, cleavage, etc. Alpine ultramafic rocks may be *porphyroclastic*, possessing a bimodal grain size distribution in which weakly deformed, fine-grained matrix grains surround large, deformed porphyroclasts (Raymond 1995). Each of these distinct textures are the result of a rock's response to the surrounding ambient physical and chemical conditions.

Protogranular textures result from a low stress/strain environment. Equigranular-mosaic textures form in high temperature, low stress environments. Equigranular-tabular textures have a high degree of grain elongation indicating high strain/stress shearing conditions and moderate to high temperatures. Raymond suggests that porphyroclastic texture indicates multiple deformation events. The supposed first event imposed strain and deformation features on the early large grains at high temperatures and stresses. Later deformation at high temperatures and low stresses allows nucleation and growth of new grains (neoblasts) which are a result of the crystals trying to lower strain energy. Documenting any of these textures in ultramafic rocks could help to constrain the conditions at which they were deformed and/or emplaced.

In some alpine ultramafic bodies, one may use distinctive properties to determine the sources of the ultramafic rocks. For instance, magmatic differentiates are distinguished by their relict igneous textures, low alumina chemistry and primary layering. Mantle slabs are characterized by high Mg content, an association with tectonic melanges, lineation defined by elongated grains, lattice preferred orientation, foliations, isoclinal folds, faults, etc. Finally, mantle diapirs are recognized by their high alumina content leading to specific minerals such as garnets, aluminous chromium spinel, and pyroxenes (jadeite or aegerine-rich clinopyroxene). This type of alpine ultramafic body also displays a contact aureole indicative of high temperature emplacement; this and other relationships between the diapir and the country rock are the most distinctive features of these alpine ultramafic bodies (Raymond 1995).

OPHIOLITES:

Ophiolites, which are included in the alpine ultramafics, should be discussed in depth considering (1) the composition of the Buck Creek Ultramafic rocks, as will be described later, and (2) their setting along an inferred terrane boundary. The primary rock types in an ophiolite include: basalt, gabbros, lherzolite, harzburgite and dunite. Ophiolites have a layered structure produced by distinct intrusive and extrusive processes above a mantle tectonite (Nicolas 1988).

Geologists have debated the origin of ophiolites since they were first described by Brongniart in 1813. Different models included a magma pouch extruded on the sea floor along deep faults, solid state emplacement through oceanic crust, uplifted remnants of oceanic floor, etc. By the early 1970's, after the widespread acceptance of plate tectonics, most geologists thought ophiolites only formed at mid-ocean ridges. Now, however, many geologists argue that they may also form in island arc settings and marginal basin ridges. However formed, an ophiolite is interpreted to be composed of oceanic crust and upper mantle. Today the term ophiolite does not imply origin, merely a distinct assemblage of rock. Starting at the bottom, this assemblage consists of: an ultramafic complex of harzburgite, lherzolite and dunite with a tectonic fabric, a gabbroic complex with cumulus peridotites and pyroxenites which are less deformed than the ultramafics, a mafic sheeted dike complex, a mafic volcanic complex (pillow basalts), and lastly, an overlying sediment section of typically deep marine deposits (i.e. cherts, shales, limestones) (Nicolas 1988). Entire sections of this assemblage may be missing due to erosion, incompleteness of formation, tectonic processes, or metamorphism beyond recognition. Some would call the resulting masses ophiolitic, but not true ophiolites.

The study of ophiolites is integral in understanding the oceanic lithosphere and asthenosphere as well as past plate tectonics. Structural measurements of ophiolite features such as: sheeted dike chill margins, foliations and flow planes, cross bedding structures in layered gabbros, and crystallographic preferred orientation of minerals in the tectonite can give a sense of where the ophiolite originated geographically and tectonically (Nicolas 1988).

Olivines, typically Fo_{94-85}, and pyroxenes, also typically Mg-rich, are essential components of ophiolitic ultramafic rocks. Crystallized calcic plagioclase, formed early in the parent melt, is often found in association with ophiolitic ultramafic rocks. Plagioclase is found in the ultramafic tectonite as well as the gabbroic plutonic complex. Given plagioclase's buoyancy in contrast with that of most ultramafic magmas it is difficult to explain how it ends up as a cumulative mineral; no satisfactory hypothesis exists to explain this enigmatic occurrence. The ultramafic component of an ophiolite is a metamorphosed rock upon which the rest of the complex lies. Usually serpentinized, the tectonite contains relict blocks of the original dunite, peridotite and pyroxenite. The tectonite is usually fault-bounded and lacks chill margins and contact aureoles, indicating tectonic emplacement possibly during collision (Raymond 1995).

Inherent in ophiolitic peridotites is plastic deformation resulting first from mantle flow and later, usually at the base of the peridotite, from high stresses and/or temperatures such as those found in orogenic or subduction events. The dominant microstructure is porphyroclastic with (100) tilt walls and subgrains abundant in the olivine grains. Large, homogeneous deformation approaching a simple shear regime is a naturally common occurrence. Slip planes and slip lines of olivine and pyroxene become oriented during flow parallel to the plane of simple shear manifested in a preferred orientation of these minerals. By studying the obliquity between foliation/lineation and lattice fabrics, a rotation to bring these two into accordance can allow a sense of shear to be deduced as well as shear strain -thus, deformation regime- theoretically (Nicolas 1988). Deformation structures and processes will be discussed later in detail.

In peridotites with minimal serpentinization the ultramafic section tends to behave like a homogenous block. Structures in the ultramafic section are difficult to discern in the field, since the compositional layering that would render structures visible is scant and olivine grains, unless mylonitic, tend to appear equigranular ("sugary"). The tectonic structure is defined by a mineral flattening foliation and a lineation parallel to the longest axis of the deformation ellipsoid. Compositional layering is usually parallel to foliation except where folding has occurred. Other definitive features seen in peridotites include indigenous dikes. These leave relict dunite veins and bodies. They were injected when the peridotite was partially melted as indicated by the reaction contact zones surrounding them. Another intrusive feature, intrusive dikes, are injected when the peridotite was already in the solid-state and no contact reaction occurred, these come after indigenous dikes as confirmed by cross cutting relationships (Nicolas 1988).

Melt products within the peridotites are important features to recognize. These can come from two sources. The first being a partial melt of the peridotite itself. The criteria for this interpretation of the melt products include: the presence of interstitial plagioclase forming coronas and concave interfaces with respect to olivine grains, continuity between plagioclase rich clots, the presence of clinopyroxene and/or plagioclase deficient halos in the rock around the melt product clots and lastly, a regular distribution of melt products throughout the body. The second melt product source is magmatic impregnation. When mafic dikes are no longer able to crack the peridotite, they disperse in them. This can lead to a faux cumulate appearance of wehrlites and troctolites in dunite. A true cumulate will have olivine grains that lack a shape controlled fabric and are deformed along with the interstitial crystals, implying a similar time of formation. However, if the olivine has a strong preferred orientation (the result of plastic deformation) and the interstitial crystals are undeformed this is evidence of the peridotite being intruded by a new magma after initial deformation (Nicolas 1988).

BLUE RIDGE PROVINCE HISTORY:

The Blue Ridge Province is between the Piedmont Province and the Valley and Ridge Province of the Appalachian Mountain chain. The Blue Ridge Province is widest in the Carolinas. In North Carolina it is bounded by the Brevard fault zone to the southeast and the Blue Ridge fault system to the northwest. The Blue Ridge contains well exposed mid Proterozoic basement gneisses, late Proterozoic plutons, metavolcanic rocks and metasediments, and early Paleozoic rifted continental margin and platform deposits. The Blue Ridge consists of a series of thrust sheets with different tectonic histories.

The western sheets contain a rift facies sequence of clastic sediments deposited on crystalline basement; this was part of North America originally. The eastern sheets consist of a slope and rise sequence deposited partly on continental crust and on oceanic crust. This was not initially part of North America, meaning that the province must contain a terrane boundary (Hatcher and Goldberg 1991).

Blue Ridge rocks record the classic example of a complete Wilson Cycle beginning in the late Proterozoic and ending in the late Paleozoic (see Figure 3). This starts with the rifting of the Pre-Cambrian supercontinent and the opening of the Iapetus ocean. This forms passive margin sediments as well as rift basalts early on. Then during the early to late Ordovician, the Taconic orogeny produces obduction related thrust sheets which advance onto North America (e.g.. Hayesville thrust). The Taconic orogeny is also the event that produces the first uplift of the internal mountain chain. Later in the Paleozoic (early to mid Devonian), island arc and microcontinental fragments accreted onto North America during one or more collision events. This resulted in the Acadian orogeny. After this event, Laurentia, Baltica, Siberia and Avalonia form a large supercontinental mass. In the latest Paleozoic, this leads to the so-called Alleghenian event that deforms and metamorphoses the Blue Ridge rocks. The Alleghenian event includes extensive strike-slip faulting in the eastern Piedmont in North Carolina and is represented in the Blue Ridge by the Brevard fault zone. Shortly thereafter, convergence across the Appalachian belt continued as the supercontinent Pangea formed. Westward vergent thrusts in the foreland are driven by the Blue Ridge-Piedmont composite crystalline thrust sheet. The result of all these collisions is a large scale accretion of exotic terranes, island arcs, microcontinents and oceanic crust onto eastern North America.

The stratigraphy of the Blue Ridge is a complicated composite of allocthonous terranes. The western basement is the North American continental crust and perhaps some oceanic (ophiolitic) crust as well and a series of rift-facies or off-margin clastic sequences. In the eastern Blue Ridge the stratigraphy is uniform in character. Here the Tallulah Falls, Ashe and Lynchburg formations, which are slope-rise deposits formed in the late Proterozoic, are overlain by the younger Coweeta Group and Alligator Back formation. The first two, the Tallulah Falls and Ashe formations, consist of metagraywackes, mafic metavolcanics, and schists (including garnet-aluminous and graywacke schist) interlayered with amphibolites. The southern Appalachian ultramafics occur in these formations (Hatcher and Goldberg 1991).

Over 300 ultramafic bodies are exposed along the axis of the Blue Ridge. Most of these bodies are now serpentinized. There is curiously no evidence of any contact metamorphic reactions between them and the surrounding rocks. Their origin is the source of continuing controversy (Feiss *et al.* 1991). Whatever their origin, the fact that they were emplaced in the root zone of the Piedmont and later uplifted into the Blue Ridge Province indicates conditions of high temperature, pressure, strain and/or stress, i.e. granulite facies conditions along the Blue Ridge axis (Hatcher and Goldberg 1991)). Microfabrics of these rocks may well reflect these conditions.

OLIVINE:

This is a brief summary of olivine characteristics which will help tailor the following discussion of deformation processes and structures. Olivine is a nesosilicate with full, orthorhombic symmetry (2/m 2/m 2/m) (see Figure 4). Its structure consists of layers of Mg/FeO_6 octahedra parallel to {100}, cross-linked by independent SiO_4 tetrahedra. Divalent cations Mg and Fe occupy the M1 and M2 octahedral sites (Klein and Hurlburt 1993) Olivine has two imperfect cleavages, (010) and (100). It is a biaxial mineral (+) if Mg-rich. (001) is the optic plane with Z parallel to the [100] axis (Nicolas and Poirier 1976). Olivines have a general composition of CaO-MgO-FeO-SiO_2 and rarely MnO. There is a solid solution between the Mg-end member, fosterite (Mg_2SiO_4) and the Fe-end member, fayalite (Fe_2SiO_4) as well as between the rarer CaMg olivine, monticellite and the CaFe olivine, kirschteinite. Little solid solution occurs between these two series. Olivine can be recognized by its vitreous lustre, conchoidal fracture, H=6.5-7, G=3.27-4.37 (fairly dense), its granular nature and of course, its characteristic olive-green color. In thin section, it is clear with high relief in plane polarized light and has high birefringence when the polars are crossed (Nesse 1991).

Fosterite melts at 1890° Celsius while fayalite melts at 1205° Celsius, thus olivine crystal cores comprised of fosterite with fayalite rich rims are quite common in most olivine grains. Olivine coexists with plagioclase and pyroxene and is also found with magnetite, corundum, chromite, and as alteration minerals: serpentine and magnesite. Mg-olivine is not stable with quartz according to the following reaction: $Mg_2SiO_4 + SiO_2 = 2MgSiO_3$. In many metamorphosed rocks, olivine has a pyroxene/amphibole corona as a result of the instability of high temperature olivine in a lower temperature water rich environment (Klein and Hurlburt 1993). At very high pressures (equivalent to depth of 40 km or more), the olivine structure converts to a more dense spinel structure. The spinel has Si in tetrahedral sites and Mg, Fe in octahedral sites of the spinel structure (Klein and Hurlburt 1993).

The crystallographic preferred orientation of olivine grains in an aggregate can be discerned qualitatively using crossed polars and the gypsum plate. Upon rotation, many grains go extinct in the same field of view.

DEFORMATION PROCESSES AND STRUCTURES:

The Blue Ridge ultramafic bodies experienced granulite facies metamorphic conditions (Raymond 1995). Microstructures of these rocks should reflect these high temperature/pressure deformation conditions. In order to comprehend observations from my detailed petrographic study of these rocks, an understanding of deformation mechanisms is essential.

Crystallographic preferred orientation and texture are essentially synonymous terms. The term 'texture' is often confused with the term 'fabric,' which, following Wenk (1985), I will adopt to denote the total internal structure of a rock. Fabric includes the complete spatial and geometrical configuration of all those components that make up the rock and covers the terms texture, structure (or microstructure) and preferred orientation (Hobbs *et al.* 1976). Preferred orientations of component crystals in a rock mass usually occur as a response to a strain or deformation. Exceptions to this rule include the alignment of phenocrysts during magmatic flow or the settling of inequant grains during deposition of sediments. Likewise, stresses that produce deformation do not always produce preferred orientation. For example, in brittle deformation at low temperatures and in superplastic flow, deformation does not generate crystallographic preferred orientations. In cases where rocks deform by crystal plastic flow, however, the degree of preferred orientation is proportional to the intensity of the deformation. Thus, to begin a discussion of preferred orientation, crystal deformation regimes must be explained.

There are many relations between microstructures and deformation regimes. Taking advantage of these relations allows an estimate to be made of the environment in which the present day rock sample formed. One such relationship is between applied stress and subgrain size. Temperature is not relevant here since once a subgrain forms, its size remains constant throughout. As applied stress increases the average subgrain size decreases proportionally. Another empirical relationship is between applied stress and dislocation density within cells. The internal stress squared is proportional to the total dislocation density. Dislocation density can usually only be determined with a TEM, and even then it is difficult to assume some annihilation or rearrangement via climb has not changed the density value. Thus, this relationship, while valid, is not universally applicable (Nicolas and Poirier 1976). The following text will describe how microstructures form as a response to deformation processes. I will first introduce two similar literature cited terminologies. One of which uses deformation mechanism maps to define five mechanism regimes, the second looks at microstructures and competing hardening and recovery processes to define four distinct behaviors. This should provide a more complete coverage of plastic deformation.

PLASTIC FLOW:

Plastic flow (inelastic deformation) occurs as a response to high shear stress. The macroscopic variables of plastic deformation are the stress, temperature, strain-rate, and strain or time. Frost and Ashby (1982) define five distinct plastic deformation mechanism groups (holding grain size constant). These mechanisms are usually represented as regimes on a deformation mechanism map. Deformation mechanism maps show the relations between mechanisms at given conditions (see Figure 5). They are experimentally derived, but supported by theoretically derived flow laws for different deformation mechanisms. They use known material properties, empirical equations (and theory - see above) and gathered lab data to produce a plot. Since strain rates vary with differential stress, temperature, and grain size, one usually holds one variable constant and plots strain rate as a function of two variables. Normally, one depicts the strain rate magnitude due to the dominant deformation mechanism at each point by means of contours of strain rate on two-dimensional Cartesian axes denoting two of the three variables. Shear strain-rate-temperature-pressure (stress) or strain rate-temperature-grainsize coordinate systems are used (Handy 1989). These reveal deformation mechanism areas or regimes which are specified to certain conditions in which the mechanism will dominate. These maps allow a geologist to identify features inherent in the rock and at least estimate the P-T conditions prevailing at the time the structure formed by looking at where that inferred mechanism exists on the deformation-mechanism map (Frost and Ashby 1982).

The first of these mechanism groups defined by Frost and Ashby for the highest differential stresses is collapse at the ideal strength. The second is low-temperature plasticity by dislocation glide followed by low-temperature plasticity by twinning, power-law creep by dislocation glide, and diffusional flow. These mechanisms may occur simultaneously creating 'new' mechanisms which are really just complicated combinations.

The ideal shear strength defines a stress level above which a crystal, that is inferred to be perfect, is no longer elastic, but becomes mechanically unstable. During collapse, the crystal strength is breached and catastrophic failure results. This value of strength can be determined from the crystal structure and a calculation of the frequency at which dislocation loops nucleate and expand in an initially defect-free crystal. The shear modulus of the polycrystal is a decent proxy for the ideal strength. Handy (1989) mentions that low lithospheric pressures, high pore pressures and high strain rates promote brittle failure before yield at the ideal strength.

Low temperature plasticity (dislocation glide) is possible below the ideal strength if numerous slip systems are available. A slip systems is a combination of a specific crystallographic plane with a crystallographic direction. Slip systems are exclusively active when the pressure is high enough to prevent brittle failure and the temperature is low enough that solid-state diffusion does not factor in. Slip happens when a line defect (dislocation) slips from a small nucleating region of high stress concentration and spreads in a loop. The dislocation line defines the boundary between slipped and unslipped crystal. Slip alone usually does not produce gross changes in a crystal shape (Hobbs *et al.* 1976). This mechanism is obstacle limited. Dislocations, like all imperfections in crystal lattices, have halos of distorted crystal lattice that can repel other dislocations. In this way, a moving dislocation may be effectively 'pinned' at one location in the crystal as it approaches other imperfections in a crystal lattice like vacancies, interstitial atoms, substitutional atoms, other dislocations, or grain boundaries. Thus, the rate of flow depends on how fast a dislocation can glide along a slip plane when is impeded by the presence of other dislocations, grain boundaries, precipitates, etc. Orowan's (1940) equation ($\dot{\gamma} = \rho_m b \bar{\upsilon}$) takes into account the affect of the density of dislocations (ρ_m) on strain rate ($\dot{\gamma}$) (b = Burger's vector, a measure of the local offset of the lattice due to the dislocation (see Figure 6), and $\bar{\upsilon}$ = dislocation velocity). The dislocation density is defined as the length of dislocations in cm, divided by the cubic cm of crystal. Thus, empirically, the greater the dislocation density, the more stress is needed to move dislocations through the grain. Plasticity limitations in this case can be broken into three main categories: discrete obstacles, lattice resistance, and phonon or electron drags. Thus, the stronger and more dense the obstacles in a polycrystal are, the slower strain rate it will have. Strength of an obstacle is defined by the total free energy required to overcome the obstacle without external stress.

The Peierls force is a measure of the inherent lattice resistance to dislocation glide. The energy of the dislocation fluctuates with position in the atomic lattice (i.e. among the interatomic/molecular bonds). A dislocation advances by moving forward kink pairs which spread apart. It is the nucleation rate of these pairs that restrains glide velocity. Again, activation energies of lattice resistance have a major role in limiting plasticity. Phonon or electron drags play a role in high strain rate systems that are not really applicable in slow geological deformational settings.

The energy of a dislocation is proportional to b^2 (b = Burger's vector). In most crystals, the most common dislocations are those with the smallest Burger's vectors. Thus, slip in olivine should occur in the direction corresponding to the shortest b ([100] = 4.76 angstroms, [010] = 10.21 angstroms, [001] = 5.99 angstroms). Slip is predicted to occur in the [100] and [001] directions. According to the lattice structure of olivine, however, SiO bonds must be broken on all planes, except (010), making this a lower energy system despite the magnitude of its Burger's vector. This slip system is especially active at temperatures below 800° Celsius. Most predicted slip directions occur over a range of temperatures, strain rates, and pressures. In general, lowering the temperature lowers the boundary between slip systems as a function of strain rate. There are seven experimentally derived slip systems for olivine: (100) [001], {110} [001], (100) [010], which function at lower temperatures and higher strain rates and (010) [100], {0kl} [100], (001) [100], {101} [010] for higher temperatures and lower strain rates. (010) [100], {110} [001], and {0kl} [100] are the most common systems employed in natural conditions.

Mechanical twinning is a variation of dislocation glide that involves the movement of partial dislocations. Nucleation determines the rate of flow, not propagation since the activation energy of nucleation is proportional to rate. This mechanism is not very relevant outside of metallurgy, so it will be ignored here. Power law creep and diffusional flow are discussed in detail later.

Nicolas and Poirier (1976) define plastic flow in terms of a competition between work hardening and recovery. Work hardening is the process by which additional increments of deformation require higher differential stress due to an increase in the density of internal dislocations. This is manifested as tangles, or as a cellular structure where dislocations form three dimensional cells composed of dislocation boundaries and relatively dislocation free centers. Both of these situations impede the progress of other dislocations moving through a slip system. The work hardening coefficient is defined as the change in stress over the change in strain. If this coefficient is positive this means an increase in stress is required for strain to occur at a given strain rate.

Recovery is the process by which the dislocation density within the crystal is lowered. This is accomplished by several processes. First, is the cancellation or annihilation of two dislocations with opposite Burger's vectors. This occurs when both lie in a single glide plane, or when they lie on parallel glide planes and can climb into the same glide plane. Second is a coarsening of the dislocation network mesh thus increasing the areas of relatively low dislocation densities. Third is the climb of dislocations past obstacles via diffusion. Recovery also includes subgrain formation, or, lastly, the cross slip of screw dislocations from one glide plane to another at high temperatures. Recovery rate is defined as the change in stress divided by the change in time given zero strain rate which is proportional to the decrease in dislocation density. Recovery rate increases with temperature and decreases as hydrostatic pressure increases (Nicolas and Poirier 1976)

After recovery takes place, in the absence of deformation, primary recrystallization occurs to remove stored grain energy. This is characterized by the formation and growth to impingement of strain free 'new' grains within a strained crystal. It involves the formation and migration of high-angle boundaries. Often the nuclei of these new grains are strongly deformed portions of original grains that during initial recovery changed their dislocation structures. Thus, the new grains evolve from subgrains by the development of high angle boundaries. These new boundaries sweep through the old, deformed crystal, with the new grains growing as they do, with speeds that depend on their orientation. This produces irregular grains exhibiting a large size range. Grain configurations are often later modified by the adjustment of grain boundaries to reduce grain boundary tension.

Normal grain growth reduces grain boundary tension of the polycrystalline aggregate formed either from primary recrystallization or the heating of fine grained material. It is driven by the force of the grain boundary energy (Karato 1989). The shape usually adopted by olivine grains is an octahedron, which provides the smallest surface area to volume ratio. An aggregate will then tend to decrease the number of interfaces by increasing the grain size. Normal grain growth is inhibited by two situations. First is orientation inhibition where a large number of grain boundaries become low angle due to the otherwise induced crystallographic preferred orientation. The other is inclusion inhibition where grain boundaries become attached to minute second phase particles.

To overcome normal grain growth inhibition secondary recrystallization takes place. This decreases the grain boundary tension of the aggregate further with an increase in temperature by creating more high angle boundaries. Here new grains consume old.

If deformation is taking place at a temperature such that recrystallization occurs at the same time (dynamic recrystallization) the microstructures are governed by the rate at which recrystallization occurs compared to the rate of internal deformation (hardening). For silicates this is a function of strain rate, temperature, and OH content (Hobbs *et al.* 1976). The driving force for dynamic recrystallization is the strain energy stored in dislocations and grain size is determined by the applied shear stress (Karato 1989).

By allowing recovery/recrystallization and hardening to contribute to deformation, Nicolas and Poirier (1976) distinguished four main cases of behavior: cold working, steady-state flow, unstable flow and hot working (see Figure 7).

Cold working occurs at homologous temperatures ($T_h = T/T_{melting}$) less than 0.3 and high strain rates. Given the low temperature, the coefficients of diffusion are small. The boundary of this domain (and all others) depends on the material properties of the crystals (number of slip systems, grain size, orientation of constituent grains, heterogeneity of polycrystal, diffusion activation energy, etc.). This domain is prevalent at near surface temperature/pressure conditions often leading to cataclastic flow and brittle fracture (Nicolas and Poirier 1976).

Steady-state flow occurs when there is a balance between hardening and recovery. Here the strain rate is essentially constant under constant applied stress. Recrystallization does not play a large role of the recovery given the relatively low strain energy, climb and polygonization are dominant. This regime is usually found in a high temperature-low strain rate environment such as the deep crust and upper mantle (Nicolas and Poirier 1976).

Unstable flow refers to the high temperature-low strain rate regime. Here the recovery rate exceeds the hardening and the material becomes softer and softer in the face of deformational processes. This can only lead to failure or a different deformation mechanism regime in response to increased strain rates (Nicolas and Poirier 1976).

Hot working applies to high strain rates and high temperatures. Here strain rates can increase the strain energy enough to allow recrystallization to occur abundantly. The newly formed grains are quickly hardened and the process repeats itself. This is known as dynamic (during stress) recrystallization as opposed to static (lacking stress) recrystallization or annealing (Nicolas and Poirier 1976).

There are dislocation structures characteristic to the cold-worked state and high temperature flow. In the cold-worked state, for minerals with several slip systems (like olivine), dislocations form three dimensional tangles and, as strain and dislocation density increase, these tangles become a cellular structure. Individual crystals exhibit undulose extinction, glide polygonization, kink bands and twinning. High temperature flow, depending on the mechanism, typically displays a polygonized substructure consisting of numerous, "dislocation free" subgrains separated by dislocation walls which formed by climb. When there are many slip systems available these subgrains are fairly equiaxed. The extent of misorientation between the subgrains and the original grain is usually between 1 and 12°. Along grain boundaries, climb usually alleviates the build-up of dislocations. Diffusion around grain boundaries contributes to grain-boundary sliding and migration, giving a pressure solution appearance or even corrugated edge. Recrystallization is normally rampant at high temperatures, but it is hard to tell whether the new grains formed in response to stress (syntectonic/dynamic) or merely thermal activation during a post deformation anneal (static) (Nicolas and Poirier 1976).

CREEP:

High-temperature plasticity is known broadly as power-law creep because the relationship between strain rate and stress is a n-power equation where n has a value between 3 and 10. In steady-state creep, defined as when hardening and recovery processes are in balance (Nicolas and Poirier 1976), if the activation energy is small, then given the necessary high thermal conditions, creep-like behavior can occur.

Exponential creep, which employs dislocation glide, is restricted to a narrow range of high stresses and strain rates near the transition between crystal-plasticity and brittle behavior (Handy

1989). The power-law between strain rate and stress gives way to an exponential relationship between strain rate and stress when dislocations move by glide plus climb and strain rates are faster than predicted by the relationship equation (generally given the term 'hot-working'). Dynamic recrystallization in concurrence with power-law creep also produces speedy strain rates which exceed those predicted by the equation (Frost and Ashby 1982).

Climb-plus-glide is a valuable way for dislocations to move through a crystal resulting in creep. At very high temperatures, the diffusive motion of single ions or vacancies to or from the dislocation is the rate-controlling process. This is known as Weertman creep (after Weertman 1955 as cited in Frost and Ashby 1982). Diffusive mass transfer (diffusional flow) involves stress induced changes in chemical potential throughout a polycrystal. A change in chemical potential of atoms at grain surfaces requires a stress with a deviatoric element. Hydrostatic pressure uniformly changes potential. At high temperatures a diffusive flux of matter leads to strain as long as it is accompanied by sliding displacements in the boundary planes. This is diffusion controlled. Solid solution may change the diffusion coefficients by imposing a drag on boundary dislocations (Frost and Ashby 1982). The strain is due to the glide of dislocations issued from Frank-Read sources, but the strain rate is controlled by climb which allows leading dislocations in nearby tangled planes to annihilate (Nicolas and Poirier 1976). At high homologous temperatures, lattice-diffusion controls climb. Lattice diffusion is the movement of ions or vacancies through cells that are defined as low dislocation density areas bounded by dislocation walls within a crystal. The velocity of climb depends on diffusion coefficients which are experimentally derived. At lower temperatures core diffusion is dominant. Core diffusion is the movement of ions or vacancies along cell boundaries (Frost and Ashby 1982).

Intracrystal diffusion (lattice diffusion) at high temperatures results in Nabarro-Herring creep (Frost and Ashby 1982). The activation energy for creep is equal to the activation energy for the self-diffusion independent of shear stress. There is a linear relationship between stress and strain rate which suggests Newtonian viscosity (equal to shear stress divided by strain rate) (the shear stress here is a measure of the radius of the Mohr circle - i.e. = differential stress). Also, this type of creep requires the sources and sinks of vacancies to be grain boundaries and a low dislocation density inside the grains, hence stresses must be small or else dislocations would be spontaneously nucleated within the grain. Nabarro-Herring creep only effectively works at small grain sizes because strain rate is inversely proportional to grain diameter cubed (Nicolas and Poirier 1976).

At lower temperatures grain-boundary diffusion is more important and Coble creep results (Frost and Ashby 1982). Here the activation energy equals the energy needed for grain-boundary diffusion, usually half that required for lattice diffusion. Coble creep is inversely proportional to grain diameter squared (Nicolas and Poirier 1976).

Another creep sub-mechanism is called Harper-Dorn creep. This only has been seen to occur when diffusional creep is suppressed by large grain sizes. This mechanism exhibits linear viscous creep where the dislocation density did not change with stress (Frost and Ashby 1982). In general, however, we can neither determine the diffusive path nor determine whether grain boundaries were dry or had extensive fluid phases along them (H_2O in lower temperature crustal deformation and CO_2 in higher temperature, mantle deformation). Thus we refer to diffusive mass transfer rather than identifying this creep mechanism as Coble or Nabarro-Herring creep, (Steven Wojtal in comments 1998).

Handy (1989) discusses the relationship between the broad categories of grain size sensitive (GSS) and grain size insensitive (GSI) creep. He investigates the effects of pressure, temperature, grainsize and time on these relations. Both GSI and GSS power law creep regimes are strongly temperature dependent. Though GSS creep at a nearly constant strain rate involves flow at lower stresses and viscosities, most rocks have too large a grainsize for the diffusion-accommodated processes inherent in GSS creep to compete effectively with the dislocation glide and climb in GSI creep. A significant reduction in grain size must occur first. The transitional domain (boundary) between these two regimes is very temperature dependent. Frost and Ashby (1982) found that most natural tectonites deformed at high (greater than 0.2) homologous temperatures show evidence of dynamic recovery and recrystallization such as strong lattice preferred orientations, sutured grain boundaries, dislocation substructures and relatively large grain sizes define a GSI fabric. GSS fabrics, defined by weak lattice preferred orientations, equant polygonal grains and finer grain sizes are found rarely. Exceptions to this rule include polyminerallic rocks which have undergone syntectonic metamorphic reactions or were deformed at high homologous temperatures and low ambient stresses. Small grain size and superplastic deformation are more likely to result from reactions occurring during underthrusting (Rubie 1983).

Handy concludes that GSI power law creep predominates at relevant geological strain rates, stresses and temperatures in the crust and mantle. Rubie mentions solid-solid univariant reactions which reduce grain sizes may allow for superplasticity in the crust and mantle. Nucleation of these new smaller grains requires a large amount of overstepping of the activation energy for grain growth which is much less dependent on temperature and pressure (Rubie 1983).

The climb of dislocations in olivine becomes important above 1000 degrees Celsius for a strain rate of 10^{-3} s^{-1}. This creates a substructure with (100) tilt walls associated with [100] Burger's vector (b) along with (001) tilt walls at [001] slip direction. With increasing temperatures the dislocation pattern changes from dense tangles to helices, loops and networks with b=[100] being dominant. At temperatures greater than 1050 degrees Celsius and a similar strain rate of around 10^{-3} s^{-1}, recrystallization at grain boundaries occurs, then with increasing temperature intragranular recrystallization occurs reducing the dislocation density within a grain by a few orders of magnitude (Nicolas and Poirier 1976).

LATTICE PREFERRED ORIENTATION:

Lattice preferred orientation of olivines forms when inequant grains rotate as well as when slip within grains accompanies the rotation. This happens at low temperatures. At higher temperatures, lattice preferred orientations form when plastic flow occurs by dislocation creep (including recrystallization), not diffusion or superplastic creep mechanisms. Lattice preferred orientations follow the strain ellipsoid and rotate with respect to the flow plane as a response to increasing strains. Thus it is due to the deformation geometry, not the stress orientation (Zhung and Karato 1995). When dynamic recrystallization occurs by subgrain rotation, the resulting lattice preferred orientation is similar to that due to deformation, but when the recrystallization is due to grain boundary migration a totally different preferred orientation could result. Lattice preferred orientation follows strain regardless of recrystallization, deformation alone is necessary (Zhung and Karato 1995). If the olivine is recrystallized with no stress (static annealing) there is a relationship between the new strain-free grains and the old deformed grains within which the new ones grew. There will be a 20-40° inclination between them (Hobbs *et al.* 1976).

Ave' Lallemant and Carter (1970) studied the preferred orientations of olivines which recrystallized in three situations: new grains enclosed by host grains, new grains along host boundaries, and new grains in completely recrystallized rocks. The first situation produced a preferred orientation of new grains which was essentially the same as the host grains. The second showed orientations related to the axial stress in a symmetric way. The third situation showed that irrespective of host grain orientation, the preferred orientation of new grains is related to axial stress. Complete recrystallization with increasing temperature and decreasing strain rate occurred by the following inferred process. First, new grains nucleated at a host grain boundary. Second, new grains nucleated within the host and the first grains continued to grow at the expense of the host. The first new grains' orientation is influenced by stress, while the next new grains' orientations within the host are dominated by the host orientation as stated above. Finally, grain-boundary recrystallization continued until the host was consumed as well as new grains with orientations oriented unfavorably with respect to stress. This process aligned [010] parallel to the compressive stress (Nicolas and Poirier 1976).

To develop textures and preferred orientation by intracrystalline slip requires large strains. Assuming a random starting orientation, a migration of [010] towards the direction of compressive stress has been seen in laboratory experiments (see Figure 8). Conversely, [001] and [100] migrate to the foliation plane, where elongation is occurring. The slip system (010)[100] was active in this high strain setting, which is dominant at high temperatures and low strain rates where recovery and recrystallization is favored. It was also observed that strain of single crystals was not homogeneous, which is in good agreement with the self-consistent theory described below. These lab experiments derived a two-stage process for the development of textures and preferred orientations. First, from 0% to around 30% strain, the dominant mechanism of deformation is external rotation of anisometric grains. Then after 30% strain, intracrystalline slip becomes most important. At the beginning of this stage, rotation has oriented many grains favorable with slip systems in directions normal to the compressive stress.

POLYCRYSTAL DEFORMATION MODELS:

Since olivine commonly occurs as granular aggregates of grains, a discussion of polycrystal deformation is relevant. Most models assume that shear-strain components are accommodated mainly by slip and normal-strain components by climb. Slip produces a rigid body rotation of crystals, whereas climb does not contribute to texture development. The rotations due to activation of slip systems result in preferred orientation. In pure shear [010] shows the greatest preferred orientation and in simple shear the [010] maximum is rotated 30 degrees from the shear plane normal (see Figure 9).

These parameters are defined by the Taylor (1938) theory which suggests that deformation of an isotropic polycrystal is homogenous. This means a shape change of a particular crystal is the same as the change of the whole aggregate. This however requires five independent slip systems, which are lacking in olivine. Furthermore, olivine aggregates are also quite anisotropic. Thus, a relaxed theory assuming some heterogeneous deformation is commonly adopted for olivine. Since simple shear is often observed in peridotites, it is assumed that climb is rate controlling . In peridotites, simple shear neither hardens nor softens much as a preferred orientation is developing, thus a steady-state Arrhenius-type flow model is a decent approximation.

An alternative to the Taylor theory for predicting textures is termed a self-consistent theory (Molinari *et al.* 1987). Here, each crystal is embedded in a homogenous anisotropic medium. Deformation in each grain is affected by compatibility and equilibrium conditions within its neighborhood. This allows local heterogeneous deformation while maintaining macroscopic wholeness. Here, favorably oriented crystals can deform fast while those that are not so oriented might not deform at all. There is no slip system restriction in this viscoplastic behavior, which is important in olivine with a strong rate sensitivity and a small stress exponent. Individual grains can deform at different rates.

These theories differ in the nature in which they explain/predict strain compatibility between grains and/or stress equilibrium conditions. It is still not clear whether olivine deforms in single slip or polyslip, though it is known different slip systems are used in nature. Neither of these theories take into account recrystallization which must complicate the applicability (Takeshita *et al.* from Barber and Meredith 1990).

BUCK CREEK ULTRAMAFIC BODY:

The following text and discussion is about the Buck Creek ultramafic body and in particular the Corundum Knob area. I hope to make useful references to the above background material when describing my and others' observations in order to make important inferences about those observations in discussion.

LITERATURE DESCRIPTIONS:

The Buck Creek ultramafic body is located in Clay County, NC in the Blue Ridge Mountains. The body is nearly entirely enclosed within amphibolite, (mafic), schist and gneiss. Taken together these rocks compose the Chunky Gal Mountain mafic-ultramafic complex (see Map 2). Here, the ultramafic parts consists mainly of one large dunite body; it is accompanied by other small bodies that are almost entirely serpentinized. This dunite mass is conformable within the schist and gneiss, suggesting a similar time of deformation and emplacement in the root zone of the Piedmont. There are no fault contacts, and foliation in the schists and dunite trends across gradational boundaries. The crystallographic preferred orientations of olivines in the dunite body may predate the deformation which caused the foliation of the regional rocks, i.e. during the Ordovician Taconic orogeny. According to geothermometry results, the Taconian metamorphism reached granulite facies conditions, with temperatures as high as 725° Celsius. In addition, these peak metamorphic conditions coincided with the formation of alteration mineral assemblages in the hinges of major folds. This was followed by a Devonian retrograde event, which led to more widespread alteration, and especially affected/formed the chlorite-talc schists. A late Paleozoic greenschist facies metamorphism produced the serpentines (Raymond 1995).

This body is about 1.22 square kilometers in size. Ninety percent of the mass is dunite, with troctolite (olivine-plagioclase rock), troctolite-amphibolite, and amphibole gneiss as well. The complex has a tabular form that dips about 50° to the north, and could be described as a sill dipping northward. The regional foliation of the envelope rocks is parallel to the margins of the complex. Contacts everywhere are concordant (Kuntz 1964).

The surrounding mafic rocks include gneisses and schists. There are two distinct types of mafic gneisses in the Blue Ridge belt; the Carolina gneiss and the Roan gneiss. The first of these contains mica, garnet and kyanite schists and gneisses. The other is made of hornblende gneiss and schist similar to diorites (McElhaney and McSween 1983).

The Buck Creek body contains some lherzolite as well as metatroctolites, and edenite/margarite schists locally. Alteration minerals include, serpentine, tremolite, talc, magnetite, anthophyllite, pyrrhotite and chlorite. Textures seen in the Buck Creek dunite include: porphyroclastic, equigranular-mosaic, equigranular-tabular, mesh seen in serpentines alone, and schistose.

PUBLISHED MODELS:

A summer Research Experience for Undergraduates (REU) program, of which I was a part in 1997, looked at the Buck Creek ultramafic rocks in an attempt to shed new light on proposed models of its origin and emplacement. The following text describes some of these models. Later, I will describe our observations/evidence we gathered to support or refute these ideas, this ultimately led to our own proposed model.

There are several models attempting to explain how the Buck Creek complex came to exist in the Blue Ridge mountains. Hartley and Penly (1974) suggest the Buck Creek body was an ultramafic sill emplaced in the lower crust. The body would have originated in a gabbroic magma chamber in the upper mantle. As this magma rose, the olivine crystals settled out leaving more gabbroic magma at the top. When the magma mush encountered an appropriate space to create a sill, the chamber spread with a gabbroic envelope around the dunite olivine mush. If this event occurred at the beginning of an orogeny, no contact metamorphism would exist today.

McElhaney and McSween (1983) proposed that the Buck Creek dunites originated as cumulates from an oceanic spreading center. The dunites we found had a similar Ti concentration as that of high Ti ophiolites and gabbros from a mid-ocean ridge spreading center. McElhaney and McSween proposed the body was subducted and emplaced at pressures greater than 6 kilobars and as high as 12 kb. This is unlike the typical ophiolite which experienced around 5 kb and 500° Celsius.

Lacazette and Rast (1989) hypothesized that the Buck Creek complex was part of a tectonic melange emplaced in a block-in-matrix fabric during shear deformation. Thus the dunites were juxtaposed with the amphibolites and were not closely related in origin.

THE SUMMER STUDY:

FIELD/LAB OBSERVATIONS:

We conducted our field study in the Corundum Knob area along the southern most edge of the Buck Creek complex (see Map 3). This is a convenient location because it is near the mafic/ultramafic contact in outcrop, exhibits nearly all the rock types found in the complex, and has ample outcrop thanks in part to an assay performed around the time of World War II for abrasives (corundum). In the field, I identified four rock types, dunite, troctolite, edenite/margarite schist and amphibolite, each with sub-types based on texture and field composition. The most abundant rock type was dunite. This was further subdivided into *layered*, with veins or patches of alteration, *massive*, with a granular (sugary) texture and lastly, *altered*, where no longer are alteration minerals confined to veins, but serpentines, anthophyllite, talc and chlorite are nearly all that is left of the original dunite. The next most abundant rock type of the body was troctolite which is a bluish (some green varieties were seen) plagioclase/olivine rock. It usually contains substantial spinel, orthopyroxene and clinopyroxene, which are often present as coronas around the plagioclase and olivine grains. Some troctolites exhibited a simplectic, interwoven texture while others appeared pitted with rings around the olivines. The next rock type seen were edenite/margarite schists which are hydrated metatroctolites. These compositionally varied between being nearly all edenite (Ca, Al amphibole) or all margarite (Ca brittle mica) or an even mix between the two. Spinels forming green halos from chromite along with zoisite and corundum were seen in these schists. The last rock type found was the hornblende/plagioclase amphibolite. These ranged in texture from a gneiss to a schist.

In the field the contacts between these different rock type units sharp to gradational; however, upon further analysis there are chemical, mineralogical and physical/structural gradations across all the rock type boundaries (see Map 4). Between the dunite and troctolite there are several degrees of gradation. Some were sharp at the scale of a hand sample and at the other extreme there was a substantial edenite/margarite schist reaction layer between them. The contacts between the amphibolite and the other rock types were generally sharp with localized complex zones of interlayered dunite, metatroctolite, edenite margarite schist and amphibolite.

Our field mapping revealed several features and patterns that allowed us to infer how the Buck Creek complex deformed. There is an interference pattern between the dominant folds and several refolded areas (N70W for the dominant fold axis and N30W for the refolded axes). This is easily seen in the map patterns of the troctolites and the edenite/margarite schists. Along the southern edge of the body, two distinct half-moons appear to be reflected across an imaginary mirror plane that would fit the cleft in the knob. The normal to this mirror plane is inferred to be the first fold axis, trending roughly N70W with little to no plunge. Troctolites and edenite/margarite schists also occur in long, lenticular bodies which are boudin-like forms along the sides of the body. This geometry may result because they were more brittle and resistant to ductile deformation when compared to the dunites. Also, the troctolite and edenite/margarite schists form lens shaped bodies in map section which are thickest at the hinge regions. The dominant foliation was seen in the schists and rarely in the dunites. This is later disrupted by another deformation event which produced crenulation in the schists. There are several late stage brittle faults seen mostly across the troctolite layers which are host to the most altered rocks found in the region.

The Buck Creek body, and specifically Corundum Knob, represents a cumulate body with amphibolite (mafic) underlying and locally on top of interlayers of dunite with troctolite (ultramafic). There is a linear gradational trace in MgO-CaO-Al_2O_3 content between cumulate dunites, to troctolites, to gabbros, to basalts similar to that of other metamorphic peridotites of oceanic crust origin (Collins *et al.* 1998).

MY PETROGRAPHIC STUDY:

The fourteen oriented dunite samples I gathered were cut parallel to the barely discernible foliation. The olivine grains do not show a great degree of elongation in any direction (i.e. weak directional preferred orientation). They are anhedral and nearly equidimensional. As will be later explained, through recrystallizing and annealing dunite tends to lose its prominent foliation trace, but may maintain a crystallographic preferred orientation. The thin sections were made with the long edge parallel to the longest dimension of the grains. The texture is equigranular-mosaic (or allotriomorphic, according to Kuntz 1964) (see Plates 1, 2). In many samples there is a bimodal grain size distribution with large relict grains surrounded by smaller more spherical grains (described as porphyroclastic by Kuntz 1964) (see Plate 3). The grain boundaries are straight and usually smooth with some occasional suturing. Stable 120° triple junctions are common. Within the large grains or porphyroclasts are several deformation features. Foremost are the deformation (kink) bands running perpendicular to the long dimension of the large grains. There is also distinct undulose extinction and parting parallel to (010),

(001) and (100). The twinning in the olivine grains is parallel to (001). The predominant pattern of twins in the olivine is a single twin plane with two twin lamellae (Kuntz 1964). Nearly all the olivine grains are also irregularly cracked and fractured in A-shaped patterns. Very few, if any subgrains are present in these aggregates. This is odd due to the supposed metamorphic environment these rocks experienced. Such a phenomena is probably due to complete recrystallization either in a static or dynamic setting.

The other primary minerals existing in these rocks are rare, totaling less than 5%. The most abundant is orthopyroxene (enstatite?) followed by clinopyroxene, amphibole, spinel and calcic plagioclase. These occur as interstitial phases, often in triple junctions, not as coronas. The pyroxenes occur as stubby crystals between adjacent olivine grains, never penetrating any grains. The amphiboles are non-pleochroic and are also stubby occurring in the same habit as the pyroxenes. The plagioclase is present as a rare interstitial component. It is found in clots and there is no continuity between the crystals. It appears to have deformed along with the olivine as evidenced by a high degree of twinning (see Plate 4).

In plane polarized light, alteration minerals are evident along cracks between and within the clear olivine grains. Yellow-green, pleochroic chlorite occurs in confused aggregates of platy crystals between olivine grains and surrounding the opaque minerals. Talc occurs in felty masses in the most heavily altered areas mixed with tremolite and the serpentines (chrysotile, antigorite) which are green and sometimes needle-like. These alteration minerals do not penetrate the olivine grains themselves, but merely grow as short cross-fibers from the walls of the cracks (see Plates 5, 6). Magnetite (and other opaque oxides/sulfides?) are interspersed throughout the rocks and are themselves being weathered to limonite/hematite. In a few heavily altered sections the orientation of the alteration mineral fibers defined the macroscopic and microscopic foliation of the rock (see Plate 7). They appear to have slowly devoured the primary minerals from the outside in.

The different assemblages of alteration minerals formed at different times under different conditions. The talc and chlorite was probably formed during the first retrograde event and the serpentines were formed later; the evidence for this being cross cutting relationships. Alteration is still occurring in these unstable rocks. This is seen as dark brown reaction crusts on the outside of the rock samples.

ANALYSES AND FIGURES:

I performed a quantitative analysis of this preferred orientation (see Plate 8) using a universal microscope stage and the method described by Phillips (1971). As is customary, I plotted data on pole figures showing the orientations of the three crystallographic axes with respect to the foliation of each sample. There is a consistent point maximum of [010] or [001] perpendicular to the foliation. Also, there are [100], [001], and [010] point maxima at angles to the foliation of some samples (see Figure 10). The orientation of the weak foliation in these rocks varies with position within the Buck Creek body (see Map 5). Foliation in the rocks to the west of A-A' (N30E fold trace) dips westward. Foliation to the east of A-A' dips eastward. The orientation of the different point maxima relative to foliation also varies corresponding to the rocks position on the inferred folds. For instance, the point maximum for [010] is normal to the foliation south of C-C', whereas north of C-C' [010] is more nearly parallel to the foliation. This could signify a shift in shear type deformation across a fold (i.e. simple shear vs. pure shear) (see figure 11).

In addition, I performed a grain size count using a linear integrating stage, and analyzed these data using the Spektor chord analysis (Underwood 1970, p 126-129). Figure 12 gives the calculated volume percentages for various grain sizes. All the samples exhibit at least a bimodal distribution. Some plots show more than two peaks indicating a concentration of more than two dominant grain sizes. The mean diameter of the smaller, most abundant grain size was 0.85 ± 0.05 mm. These are the largest peaks on each graph. The mean larger grain size was 2.6 ± 0.15 mm. These are represented by the smaller peaks. I measured rare grains as large as 8.6 mm.

DISCUSSION:

SUMMER RESEARCH:

The purpose of the summer research and my own study was to help substantiate or disprove other existing models of how the Chunky Gal mafic/ultramafic complex formed and/or was emplaced. The following text outlines how the observations we made allowed us to devise a model of our own, then how my specific research, drawing from data we gathered, either substantiated or not our interpretation.

The contact between the mafic amphibolites and the dunites is sharp in some locations (i.e. along the southwestern side of the body). In other locations (i.e. along the southern edge of the body the contact is complex and the dunites are interlayered troctolites, edenite/margarite schists and amphibolites. In most locations, we found the contacts between the dunite and amphibolite to be mineralogically and compositionally gradational. We found no evidence of any contact metamorphism along the contact, which is inherent in the Hartley and Penly (1974) model. This means the body was either emplaced under very hot conditions or that later metamorphism completely erased any evidence. We found no mylonites, evidence of a shear zone such as Lacazette and Rast (1989) describe in their melange model (Stonesifer et al. 1998). We saw a tholeitic path (high Fe and Mg content), inherent in mid-ocean ridges, which rules out a calc-alkaline parent (Collins *et al.* 1998). Thus, we interpreted the protolith to be a layered mafic igneous complex. Slusser *et al.* (1998) found the compositions of amphibolites suggest A signature of a basaltic magma chamber, with regular gradation from plagioclase rich rocks to a cotectic assemblage of pyroxene-plagioclase-olivine. The linear gradational trace in MgO-CaO-Al_2O_3 content between dunites, to troctolite, to gabbros, to basalts (Collins *et al.* 1998) is typical of peridotite metamorphic association. Further, Slusser *et al.* (1998) identified a mid-ocean ridge signature for the Zr, Y, Ti, and Sr numbers in the amphibolites surrounding and present on the top of the knob. This suggests an oceanic crust origin such as that beneath a spreading ridge.

Simons *et al.*(1998) analyzed the rare earth elements (REEs) concentrations in Buck Creek dunites and the surrounding metamorphic rocks to see if they indicate a possible protolith signature. These elements are not very mobile during metamorphism. The La/Sm number was greater than 1 in all samples, which implies a mid-ocean ridge basalt or back-arc environment. Simons *et al.* (1998) also determined the REE signature of two nearby ultramafic bodies. According to the REE patterns, the inferred depleted source of the Buck Creek rocks was similar to one nearby ultramafic body, but not another neighboring one. Thus the Buck Creek body is not part of a massive ultramafic sheet, but one of many small bodies in the Blue Ridge Province, which may or may not be related.

Slusser *et al.* (1998) determined that the original mineral assemblage of troctolite (plagioclase, olivine, pyroxene, spinel) requires a low pressure to remain present without prograde alteration, while Hartley and Penly's (1974) ultramafic sill model requires a much higher pressure to mask the contact metamorphism inherent in their interpretation.

Emilio *et al.* (1998) performed geochemical analyses to determine the grade of metamorphism experienced by the Buck Creek body. Buck Creek rocks are useful for this study because troctolite, amphibolite, and dunite preserve both dry and wet metamorphic assemblages over a range of grades and protoliths. The troctolite, edenite/margarite schist, and chlorite/talc schists are gradational between the anorthite and dunite end-members. Kyanite seen in the edenite/margarite schist indicates that those rocks had seen a very high pressures and temperatures, similar to the hot dry melt which effected the troctolites and the preserved the sapphirine + clinopyroxene assemblage still seen presently therein. Emilio *et al.* (1998) proposed a new range of 800° Celsius at 10 kb to 800-900° Celsius at 11.5 kb for metamorphic conditions in the Buck Creek rocks.

Several distinct field observations support inferences about how the Buck Creek dunite deformed. The Buck Creek ultramafic body was probably moved upward from great depths as a solid mass because there is no evidence of melt. Due to the structural interference pattern of the rock units, we inferred that the deformation of the Buck Creek body occurred as a polyphase deformation. During the first or primary deformation, tight to isoclinal folds formed; the hinge of one of these early isoclinal folds is apparent along the southern margin of the Buck Creek body, where half-moon shaped outcrops of troctolite and edenite/margarite schist define a N70W trending fold axis and a gently north-dipping hinge surface. The limbs dipped moderately 35-40° NE. The dominant foliation in the surrounding rocks is axial planar to these folds. Upright to asymmetrical, open to tight folds with N30E trending axes fold this foliation and the early folds. These second folds are locally associated with upright NE trending crenulation cleavages especially visible in the schistose rocks. The interaction of these two phase deformation features produced a saddle-shaped map trace very similar to a type 2 map interference pattern recognized by Ramsay (1967).

OUR MODEL:

From the above lines of geochemical, mineralogical and structural observations, we proposed the following time scale model for the existence of the Buck Creek complex in the Blue Ridge mountains (see Figure 13). First during the late Precambrian (570 Ma?) the Buck Creek complex forms at a mid-ocean ridge. From the high TiO_2 content and LREE depleted signature of the cumulate, we infer that this mass formed at a normal mid-ocean ridge, i.e. within a large ocean basin. Around 500 Ma (Penobscottian orogeny?), the body was subducted to at least 18 km as evidenced by the orthopyroxene-clinopyroxene-spinal simplectic coronas around the plagioclase and dunites. This must be an anhydrous environment to preserve the original minerals. The body thus becomes basal to the Tallulah Falls/Ashe metamorphic suite. At about 440 Ma (Taconic orogeny), the body was subjected to deeper burial and initial deformation during the collision. It was emplaced on the hanging wall of the Hayesville thrust as a fragment of a deep ophiolite. Here it experienced the first stage folding with the troctolites formed at the noses of the folds. Somewhere around 400-360 Ma (Acadian orogeny?), the Chunky Gal thrust formed and uplifted the body to amphibolite facies (600-700° Celsius, 5 kb) conditions and separates it from the Lake Chatuge body. It is now emplaced within the Tallulah Falls formation as a mafic/ultramafic crustal fragment. Here it also experiences the second stage folding, with the retrograde tremolite bearing metamorphic assemblage forming. Later brittle deformation forms faults within the body, cutting the troctolites perceptively and allowing hydrous alteration. These zones show the most prevalent alteration (containing serpentine, talc, chlorite) (Slusser *et al.* 1998).

DUNITE DISCUSSION:

The purpose of all the preceding text was to provide an understanding against which to compare and contrast my observations. This is done in an attempt to shed some light on the history and deformation of the Buck Creek dunite. The first observations I am going to discuss are simply qualitative. These include structures within grains, relationships between mineral grains, and the composition of the dunite.

These rocks were mostly olivine. In some samples this was masked by intense alteration, but fresh samples gave a clear indication of the primary mineral assemblages. The absence of significant pyroxene, amphibole, and other common primary ultramafic minerals defines these rocks as dunites. According to Raymond(1995), dunite is the olivine end member of the ultramafic rocks. These rocks probably came from a very pure mantle source. The initial grains must have been closely packed somehow to prevent the interstitial phases to form large portions of the rock. The rock is certainly a cumulate and the absence of undeformed plagioclase clots rules out later magmatic impregnation. There are no pyroxene/amphibole coronas around the olivine grains indicating dry metamorphic conditions (Klein and Hurlburt 1993). Dunite in association with lherzolite and harzburgite comprises the lowermost tectonite of most ophiolite sequences. It is curious that the lherzolite and harzburgite rocks are not found on Corundum Knob.

Many of my rock samples had polygonal grains with 120° triple junctions and long edges between grains of olivine. This is similar to the equigranular-mosaic texture described by Raymond for alpine ultramafic bodies. There were very few, if any subgrains seen in these dunites, this is probably due to nearly complete recrystallization. Another prevalent feature of these dunites is the bimodal grain size distribution. From a qualitative standpoint, the large relict grains contained deformation features including: deformation bands, deformation lamellae, undulose extinction, kinks, twins and cleavages. These features form as a result of deformation at low temperature or high strain rate producing a former, dominant, equigranular-tabular texture. The smaller, more spherical surrounding grains (former subgrains?) were, in comparison, free of these deformation structures. This again is a typical alpine ultramafic texture defined by Raymond (1995) as porphyroclastic. Porphyroclastic textures are also the dominant microstructure of ophiolites. The relict grains and the new grains had very similar extinctions not displaying the 20-40° inclination produced by static annealing.

Since preferred orientation is a prevalent and long lasting feature it is perhaps one of the most useful tools of comparison. The experiment by Carter and Ave' Lallemant (1970) showed how recrystallized grains and relict grains are related in crystallographic preferred orientation. For most cases there is very little difference so I will not take recrystallization into account.

In the Buck Creek dunites I examined, the preferred orientation of [100] matches that observed in recrystallized textures plotted by Mercier (1985) (rocks were deformed by slip, uniaxial compression at 1300° Celsius). Buck Creek dunites usually have a strong [001] point maximum normal to the rock's foliation and point maxima of [100] and [010] at angles of around 20-30° to the foliation. Takeshita et al. (1990) measured textures like this, with the [010] and [100] directions inclined at angles to foliation (see Figure 11), in samples deformed in simple shear. Nicolas and Poirier (1976) state that simple shear requires a single sense of rotation compared with two senses in pure shear. Climb in both cases is rate controlling. Slip planes and lines become oriented during flow parallel to the plane of simple shear. The slip system (010) [100] is responsible for this movement at high temperatures. Twiss and Moores (1992) further help to substantiate this conclusion by revealing that a [010] maximum inclined to the foliation is consistent with dominant glide on (010) [100], with a strong simple shear component.

Whereas, if the [001] maximum were normal to the foliation, {110} [001] would be the dominant slip system used, especially at lower temperatures (~ 700° Celsius) (Twiss and Moores 1992). It should be noted that three of my texture diagrams show there is a relevant concentration of [001] points at a normal to the foliation, therefore I will not discount the {110} [001] slip system. A slip system is preferred by which slip plane is oriented parallel to the compressive stress, or which is oriented parallel to the shear direction. It is unclear whether olivine deformation employs polyslip or simply uses one system at a time.

The textures in the Buck Creek dunite are most similar to textures seen in dunites deformed by hot working (dynamic not static recrystallization) with dominant rotational shear flow, using the slip direction [100] and slip plane (010) (Nicolas and Poirier 1976). The fact that these Buck Creek dunites probably did not experience high temperatures without some shear deformation is significant in their history. They were not later heated after the different thrust emplacing events. These comparisons also showed that my plots looked like those they displayed of porphyroclastic and equigranular-mosaic/tabular textures, making my observations more substantiated.

The crystallographic preferred orientations and dislocation substructures along with the absence of evidence of diffusive mass transfer (i.e. pressure solved grains, 'beards around grains, significantly sutured boundaries, etc.) led me to infer that dislocation creep was the dominant late stage deformation mechanism at work in the Buck Creek olivine.

The bimodal grain size distribution is especially important. The smaller grain size is most abundant. This averaged 0.85 mm ± 0.05 mm. The larger, relict grains were 2.6 mm ± 0.15 mm. Since it is difficult to determine exactly how much of the relict grain was consumed during recrystallization, its size is not applicable to a grain size deformation mechanism map or as a paleopiezometer. The size of the new, smaller grains however have direct correlations with the deformation mechanism that produced them, which helps to narrow down the conditions of deformation.

Assuming temperature was fairly constant during this deformation (around 800° Celsius as discussed above), a deformation mechanism map such as that of Handy (1989), or Frost and Ashby (1982) can be used to gain some insight on the stress and strain-rate conditions at the recrystallized grain size. At the constant grain size diameter of about 1 mm the mechanism proposed for deformation is grain size insensitive creep, not exponential-law creep, brittle failure nor grain size sensitive creep for strain rates of 10^{-10} s^{-1} according to Handy's map. This is supported by the presence of the GSI creep (dislocation glide/climb process) fabric I saw in these dunites. This includes strong lattice preferred orientations, dislocation substructures, large grain sizes, and some sutured grain boundaries, which are recrystallization and dynamic recovery features. In GSS creep where diffusional processes are inherent, very weak if any lattice preferred orientation is seen and the grain sizes are very small.

Frost and Ashby's map holds grain size constant at 1 mm and shows that at low shear stresses (< 10^{-3} MN/m^2) all reasonable strain rates and 800° Celsius, the dominant mechanism is plasticity, not power-law creep or diffusional flow. In thin section no evidence of diffusional flow was seen, for example few, if any, beard overgrowths or pressure solved corrugated edges were on any olivine grain.

Twiss (1977) describes a technique which relates stress during steady state creep to both subgrain size and dynamically recrystallized grain size. The relation results from equating the dislocation strain energy in the grain boundary to that in the enclosed volume, only the effective isotropic elastic moduli and Burgers vector are needed to apply it. The relation takes the form of the equation: $\sigma = B\, d^{-0.68}$ where σ is in MPa, d is in mm and $B \equiv K\Gamma b^{p}$: for olivine, B is given as 14.6. Inserting 0.85 mm as d and using the given B computes a value of σ = 16.3 MPa or 0.163 kbar. This technique is limited to rocks which have undergone very little annealing, this limits its applicability to the Buck Creek dunites because of the amount of recovery that has taken place there. The rocks should preferably be quenched under constant stress or by physical inhibition of grain growth by different neighboring phases. This technique usually renders a minimum value for stress and I will accept it as such.

These results have implications about the interpretations of how the Buck Creek body was deformed. These rocks possessed a very weak directional preferred orientation and lacked evidence of strong foliation that one might anticipate given the tight shapes of the folds presented by Stonesifer *et al.* (1998) for the Corundum Knob area or the pervasive shearing zones of the tectonic melange model of Lacazette and Rast (1987). This could mean that the fold shapes in detail are incorrect or that grain shapes themselves do not record all the strain the entire aggregate experiences. According to the self-consistent theory for polycrystal deformation presented by Molinari *et al.* (1987), the deformation is heterogeneous and thus the grains I looked at might not show the entire range of deformation figures to be found elsewhere in the body. Looking at the crystallographic axes preferred orientations across several of these folds it appears that pure shear may have played a larger role in the deformation along the southern edges of the folds (across C-C') and simple shear more so on the northern side of C-C'. This is explained by the fact that olivine aggregates are anisotropic and therefore can not realistically deform homogeneously. The crystallographic preferred orientations of these rocks are strong, this means the strain they experienced was substantial. The fact that they probably deformed by a dislocation creep mechanism is consistent with the elevated temperatures/pressures inherent in the thrust fault emplacement model.

CONCLUSIONS:

The research done for this paper proved very useful in making correlations between my own observations and those of other geologists. First looking at general ultramafic bodies' characteristics and then comparing them with both my REU summer research and this olivine fabric study allowed the following conclusions to be made.

The mafic and ultramafic portions of this mass are probably related in protolith. Geochemical/mineralogical data from across the contacts between the different rock types indicates a gradation, not a sharp difference. The different elemental signatures indicate they were formed at a mid-ocean ridge. They were later subducted and uplifted into the root zone of the mountains. This produced large scale deformation that pervaded the entire body, producing the primary folding. The early deformation microstructures are almost completely overprinted by later recrystallization; some of the relict grains evident in the porphyroclastic rocks are probably the few remaining indicators of long past conditions. This makes it difficult to determine what initial conditions of deformation were. However, the structures, grain size distribution and crystallographic preferred orientation of the olivine grains that exist now gave an abundance of information with which to make inferences about later stage deformation.

The olivine grains deformed via dislocation creep, employing at least the (010) [100] slip system or the {110} [001] slip system or both. These systems are common in high temperature-low strain rate conditions (hot working including dynamic recrystallization, not static annealing). Diffusion mass transfer was not prevalent due to the absence of pressure solution features and corrugated grain boundaries. The recrystallized grain size pointed to minimum stresses of ~16.3 MPa. The orientation of the slip directions with the foliation plane is consistent with deformation via simple shear rather than pure shear.

The Buck Creek body did experience high strain levels as evidenced by the microstructures seen in the dunite. The fabric of the dunites does not indicate high levels of shear or folding inherent in both the melange model of Lacazette and Rast (1987) and the polyphase deformation model of Slusser *et al.* 1998. Given the anisotropy of olivine aggregates this is not entirely unexpected.

ACKNOWLEDGMENTS;

First and foremost, I would like to thank Steven Wojtal for all his patient suggestions on this project. Thanks also to Pete Munk for his dedication in getting my thin sections (even sample TT8) ready no matter when I needed them. Thanks to Virginia Peterson, who prompted the idea in the first place. Finally, I thank Silken, whose portraits inspired me late at night.

BIBLIOGRAPY:

Bai, Quan & Kohlstedt D. L. "High Temperature Creep of Olivine Single Crystals, 2. Dislocation Structures." *Tectonophysics*, vol. 206, 1992.

Collins, J., Becker, A., Palmer, J., Simons, K., Frey, B., Gaskin, P., Lucas, S., Manooch, S., O'Leary, J., Slusser, T., Stonesifer, K., Thornberry, T., Ryan, J. G., Bek, R., Emilio, M., Peterson, V. L. "Geochemical Results from a Section of the Buck Creek Mafic/Ultramafic Complex, NC." Geological Society of America Abstract no. 15604, 1998.

Cristescu, N. Rock Rheology. ©1989, by Kluwer Academic Publishers.

Emilio, M. C., Ryan, J. G., Peterson, V. L. "Study of the Metamorphic Evolution of the Buck Creek Mafic/Ultramafic Complex, NC.." Geological Society of America Abstract no. 11977, 1998.

Feiss, P. Geoffrey, Maybin, Arthur S., III, Riggs, Stanley R. & Grosz, Andrew E. "Mineral Resources of the Carolinas." from, The Geology of the Carolinas. Horton J. Wright, Jr. & Zullo, Victor A., eds. ©1991, by The University of Tennessee Press.

Frost, Harold J., & Ashby, Michael F. Deformation-Mechanism Maps. The Plasticity and Creep of Metals and Ceramics. ©1982, by Pergammon Press.

Hadley, Jarvis B. "Preliminary Report on Corundum Deposits in the Buck Creek Peridotite Clay County, North Carolina." United States Geological Survey Bulletin 948-E, 1945.

Handy, Mark. "Deformation Regimes and the Rheological Evolution of Fault Zones in the Lithosphere: the Effects of Pressure, Temperature, Grainsize and Time." *Tectonophysics*, vol. 163, 1989.

Hatcher, Robert D., Jr. & Goldberg, Steven A. "The Blue Ridge Geologic Province." from, The Geology of the Carolinas. Horton J. Wright, Jr. & Zullo, Victor A., eds. ©1991, by The University of Tennessee Press.

Hobbs, Bruce E., Means, Winthrop D., & Williams, Paul F. An Outline of Structural Geology. ©1976 , by John Wiley & Sons, Inc.

Karato, S. "Grain Growth Kinetics in Olivine Aggregates." *Tectonophysics*, vol 168, 1989.

Karato, Shun-ichiro, & Toriumi, Mitsushiro, eds. Rheology of Solids and of the Earth. ©1989, by Oxford University Press.

Klein, Cornelis & Hurlburt, Cornelius S., Jr. Manual of Mineralogy. ©1993, by John Wiley & Sons, Inc.

Lacazette, Alfred J., Jr., & Rast, Nicholas. "Tectonic Melange at Chunky Gal Mountain, North Carolina." from Geological Society of America Special Paper 228, 1989.

McElhaney, M. Stuart, & McSween, Harry Y., Jr. "Petrology of the Chunky Gal Mountain Mafic-Ultramafic Complex, North Carolina." Geological Society of America Bulletin, v. 94, July 1983.

Mercier, J.-C. C. Olivine and Pyroxene. from Preferred Orientation in Deformed Metals and Rocks: an Introduction to Modern Texture Analysis. Wenk, Hans-Rudolf ed. ©1985, by Academic Press, Inc.

Molinari, A., Canova, G. R., & Ahzi, S. A Self-Consistent Approach of the Large Deformation Polycrystal Viscoplasticity. *Acta. Metallurgy* vol. 35, 1987.

Nesse, William P. Introduction to Optical Mineralogy. ©1991, by Oxford University Press.

Nicolas, A. Structures of Ophiolites and Dynamics of Oceanic Lithosphere. ©1988, by Kluwer Academic Publishers

Nicolas, A., & Poirier, J.P. Crystalline Plasticity and Solid State Flow in Metamorphic Rocks. ©1976, by John Wiley & Sons, Ltd.

Phillips, Wm. Revell. Mineral Optics. ©1971, by W. H. Freeman and Company.

Priest, S. D. Hemispherical Projection Methods in Rock Mechanics. ©1985, by George Allen & Unwin (Publishers) Ltd.

Putnis, Andrew. Introduction to Mineral Sciences. ©1992, by Cambridge University Press.

Raymond, Loren A. Petrology, The Study of Igneous, Sedimentary, Metamorphic Rocks. ©1995, by Wm. C. Brown Communications, Inc.

Rodgers, John. The Tectonics of the Appalachians. ©1970, by John Wiley & Sons, Inc.

Rubie, David C. "Reaction-Enhanced Ductility: the Role of Solid-Solid Univariant Reactions in Deformation of the Crust and Mantle." *Tectonophysics*, vol 96, 1983.

Simons, K., Ryan, J. G., Frey, B., Peterson, V. L. "Rare Earth Element Systematics of the Buck Creek Mafic/Ultramafic Complex, NC." Geological Society of America Abstract no. 15258, 1998.

Slusser, T., Gaskin, P., Becker, A., Lucas, S., Collins, J., Palmer, J., Simons, K., Frey, B., Manooch, S., O'Leary, J., Stonesifer, K., Thornberry, T., Peterson, V. L., Ryan , J. G., Emilio, M. "Constraints on Current Models for the Origin of the Buck Creek Mafic/Ultramafic Complex, Western, NC." Geological Society of America Abstract no. 12035, 1998.

Slusser, T., Ryan, J. G., Peterson, V. L. "Geochemical Constraints on Amphibolites in the Buck Creek Mafic-Ultramafic Complex, NC." Geological Society of America Abstract no. 11985, 1998.

Stonesifer, K., Frey, B., Manooch, S., Thornberry, T., Becker, A., Collins, J., Gaskin, P., Lucas, S., Palmer, J., Simons, K., Slusser, T., Peterson, V. L., Emilio, M., Ryan, J. G. "Lithologies and Structure of the Buck Creek Mafic/Ultramafic Complex, NC." Geological Society of America Abstract no. 11846, 1998.

Takeshita, Toru, Wenk, Hans-Rudolf, Canova, Gilles R., & Molinari, Alain. "Simulation of dislocation-assisted plastic deformation in olivine polycrystals." from Deformation Processes in Minerals, Ceramics and Rocks. Barber, D. J., & Meredith P. G., eds. ©1990, by Unwin Hyman Ltd.

Twiss, Robert J. "Theory and Applicability of a Recrystallized Grain Size Paleopiezometer." *Paleogeophysics*, vol 115, 1977.

Twiss, Robert J., & Moores, Eldridge M. Structural Geology. ©1992, by W. H. Freeman and Company.

Underwood, E. E. Quantitative Stereology. ©1970, by Addison-Wesley Publishing Co.

Wenk, Hans-Rudolf, ed. Preferred Orientation in Deformed Metals and Rocks: An Introduction to Modern Texture Analysis. © 1985, by Academic Press, Inc.

Zhung, Shuqing & Karato, Shun-ichiro. "Lattice Preferred Orientation of Olivine Aggregates Deformed in Simple Shear." *Nature,* vol. 375, 1995.

Layered Bodies

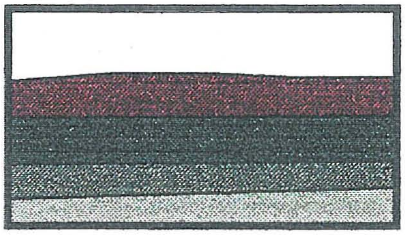

Layered

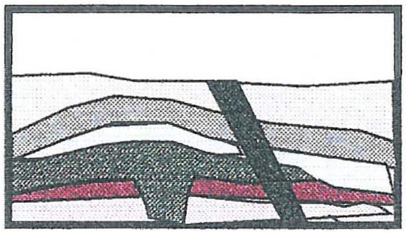

Dikes and Sills

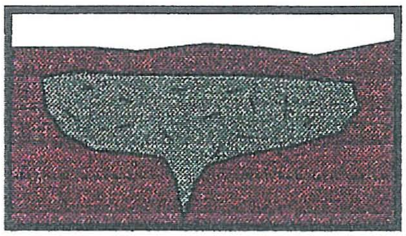

Lopolithic bodies

Ophiolites

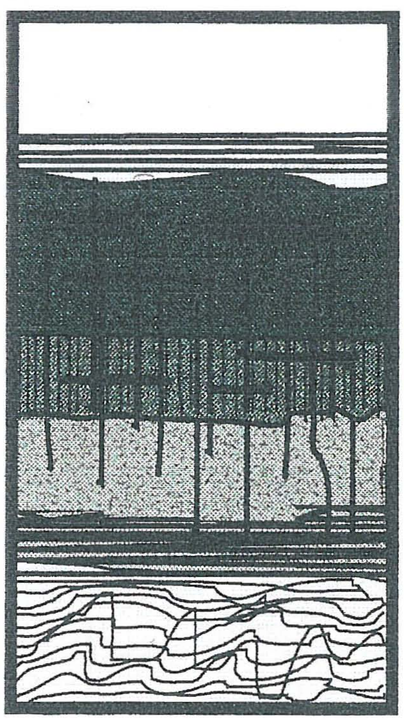

Sedimentary Rocks

Volcanic Rocks

Dike and Sill complex

Non-cumulate

Cumulate

Plutonic complex

Metamorhpic Ultramafic Tectonite

Figure 2

Alpine Ultramafic Textures

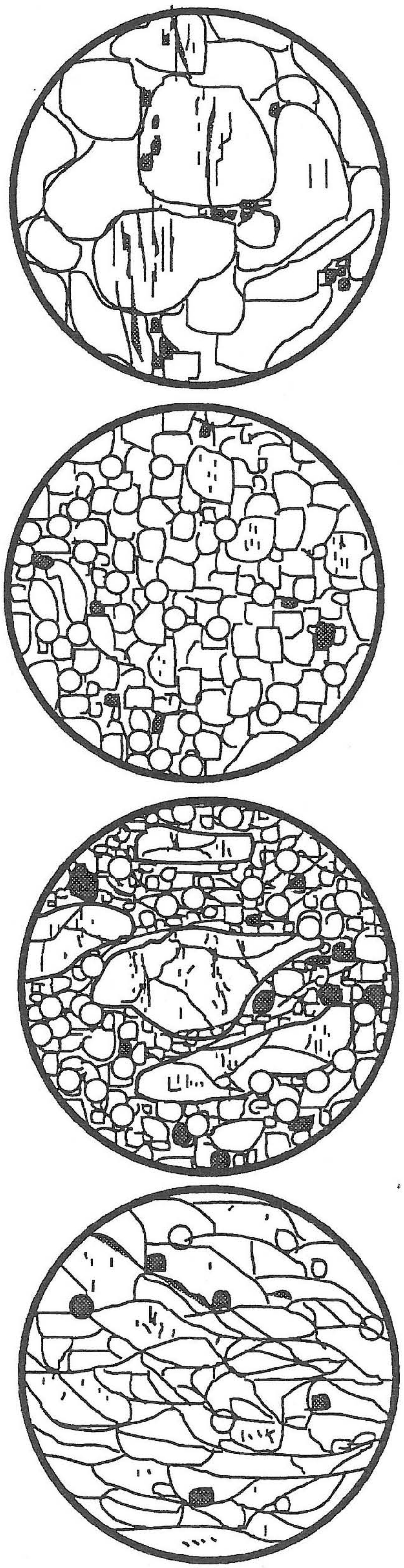

Protogranular

Equigranular-mosaic

Porphyroclastic

Equigranular-tabular

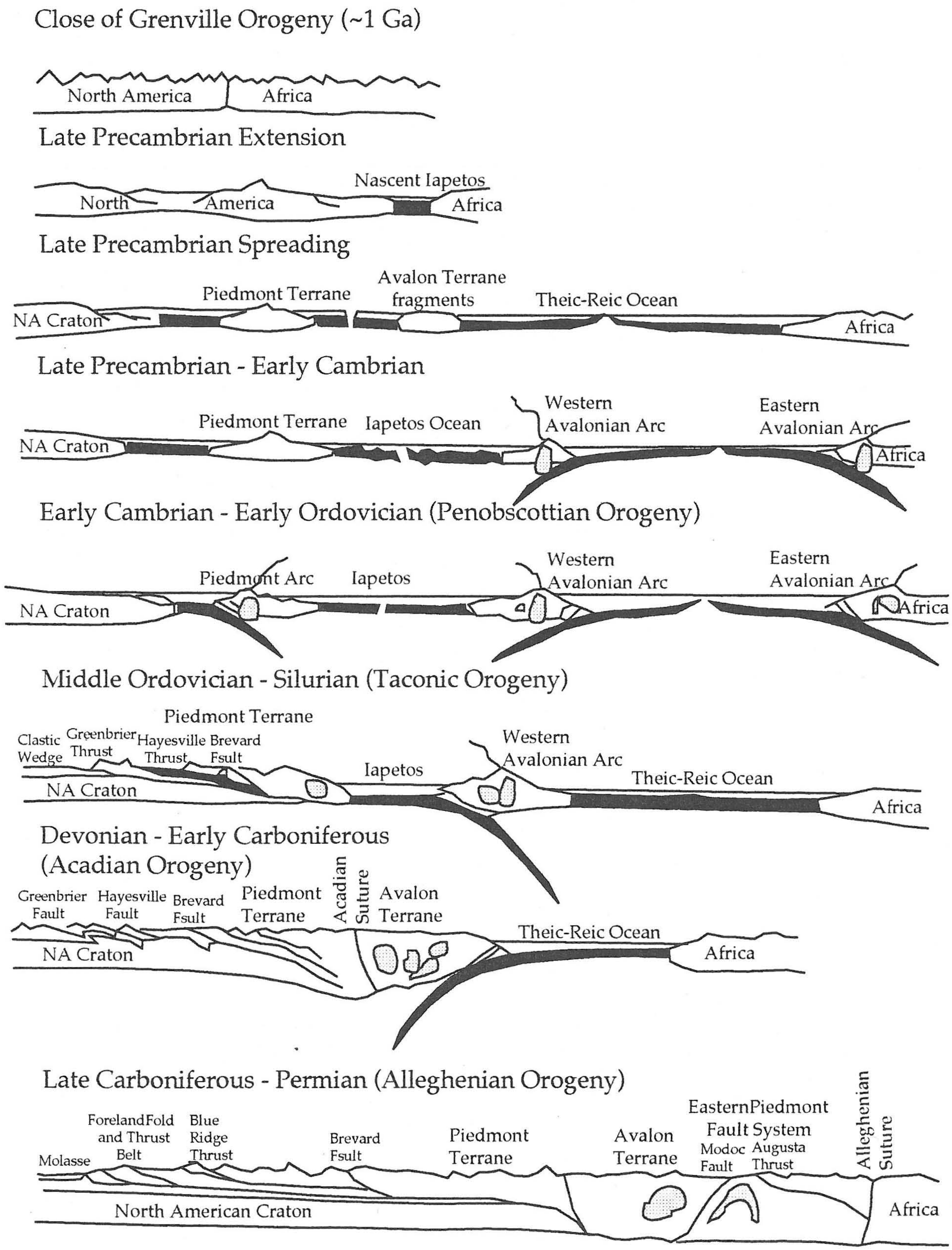

Sequential Development of the Appalachians in the Carolinas, Georgia and Tennessee. Note the location of the Hayesville Thrust Fault.

from Hatcher et al. 1991

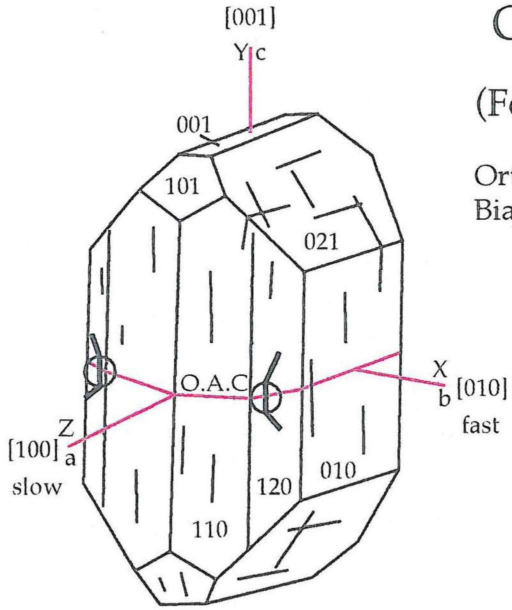

Olivine

$(Fe,Mg)_2SiO_4$

Orthorhombic
Biaxial (+ or -)

Between Fo_{100} and Fo_{85} olivine is biaxial + with 2Vz = 82 -90°

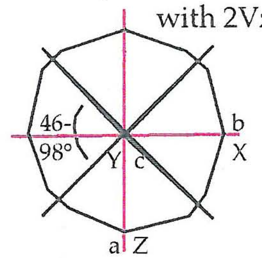

001 section
2Vx=46-98°

Crystallographic habit and optical direction of forsterite

poor cleavage on {010} and {100}
twinning is not common, but maybe present as simple or multiple twins with diffuse boundaries on composition planes {100}, {011} or {012}

G= 3.22 - 4.39
H= 6.5 - 7
ηa= 1.636 - 1.827
ηb= 1.651 - 1.869
ηc= 1.669 - 1.879
δ = 0.033 - 0.052

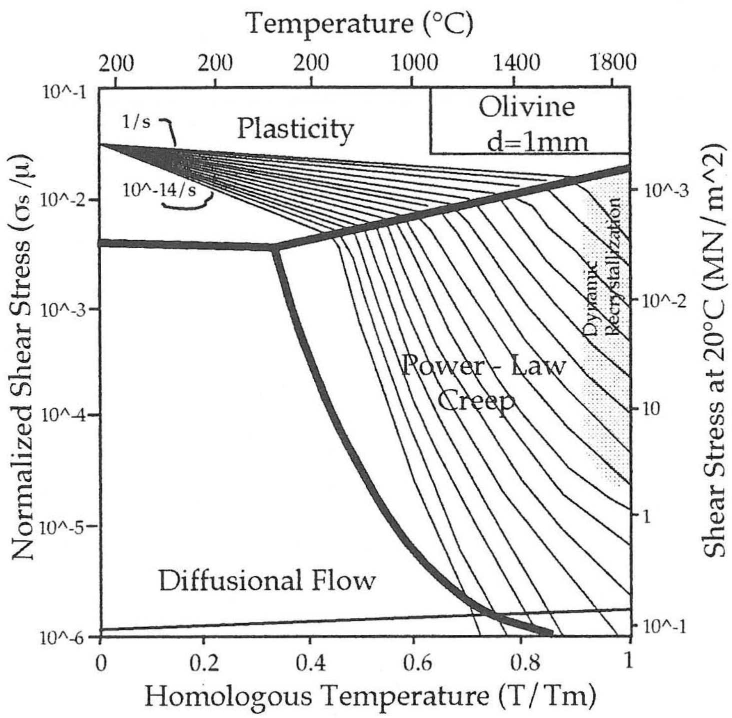

from Frost and Ashby 1982

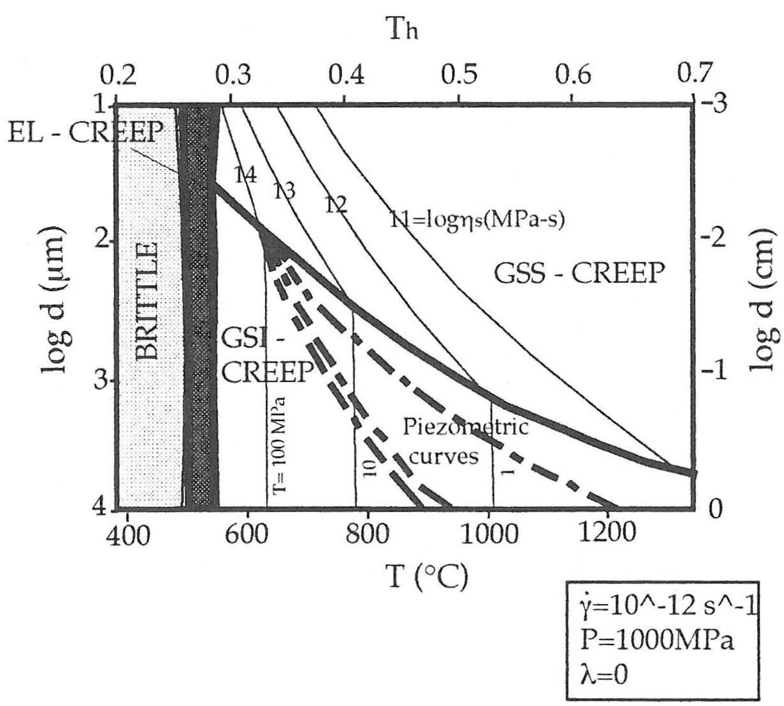

from Handy 1989

Burger's vector's role in slip

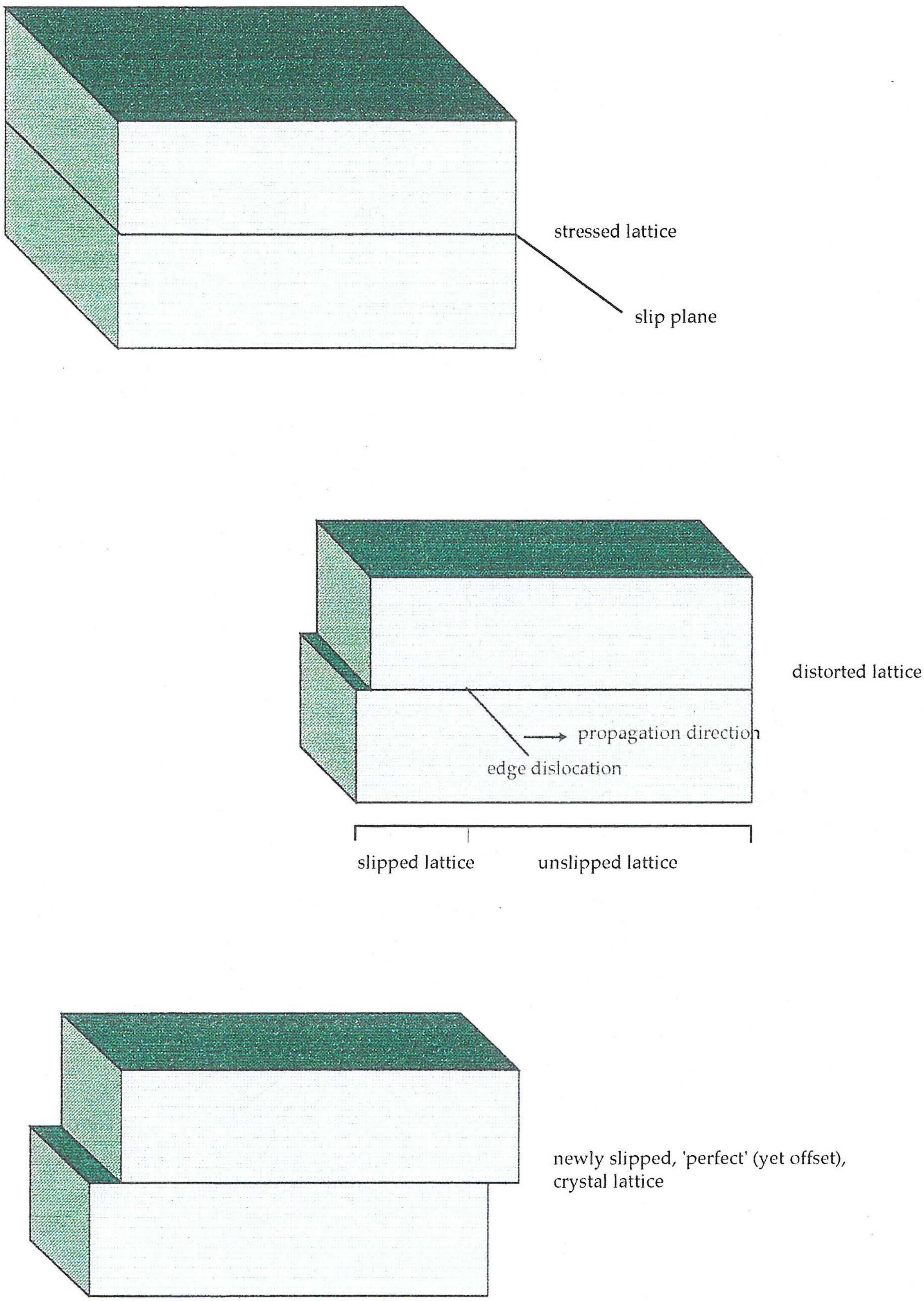

$\vec{b}$ = Burger's vector (depends on dislocation type and inter atomic structure)

Deformation Regimes

		$\dot{\varepsilon}$ = Constant		σ = Constant	
COLD WORKING LOW T/T_m HIGH $\dot{\varepsilon}$	$h\dot{\varepsilon} - r > 0$ Strain Hardening, Recovery	$\frac{\Delta \sigma}{\Delta t} > 0$	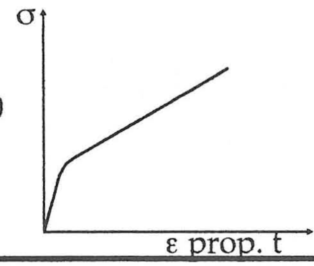	$\frac{\Delta \dot{\varepsilon}}{\Delta t} < 0$	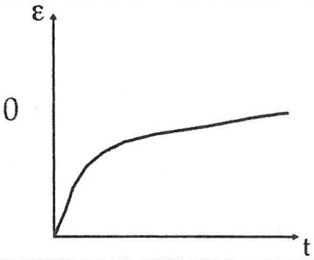
STEADY-STATE FLOW HIGH T/T_m LOW $\dot{\varepsilon}$	$h\dot{\varepsilon} - r = 0$ Strain Hardening, Recovery	$\frac{\Delta \sigma}{\Delta t} = 0$	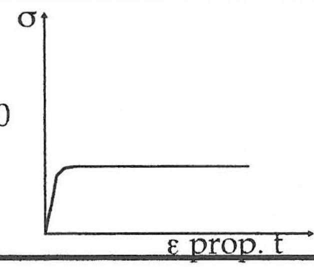	$\frac{\Delta \dot{\varepsilon}}{\Delta t} = 0$	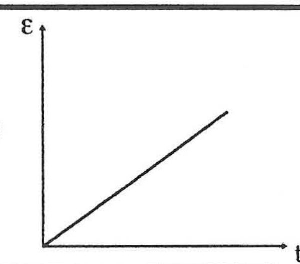
UNSTABLE FLOW HIGH T/T_m LOW $\dot{\varepsilon}$	$h\dot{\varepsilon} - r < 0$ Strain Hardening, Recovery	$\frac{\Delta \sigma}{\Delta t} < 0$	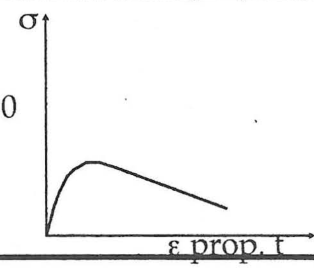	$\frac{\Delta \dot{\varepsilon}}{\Delta t} > 0$	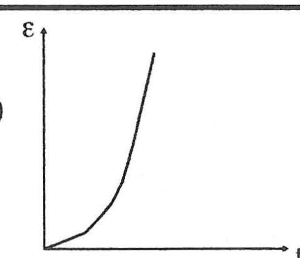
HOT WORKING HIGH $\dot{\varepsilon}$ HIGH T/T_m	Strain Hardening, Recovery + Recrystallization		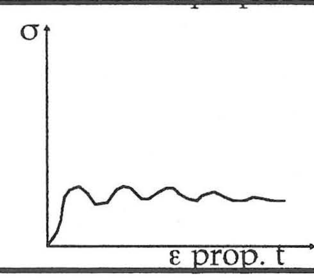		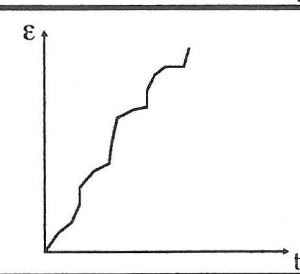

$\dot{\varepsilon}$ = strain rate, h = hardening coefficient,
ε = strain, t = time, σ = stress, r = recovery rate

from Nicolas and Poirier 1976
page 134

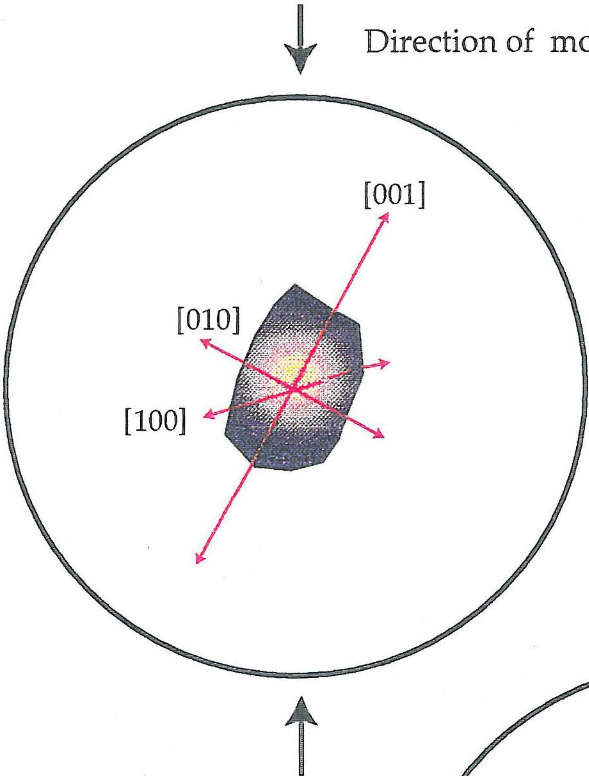

Starting random orientation of a olivine grain in an aggregate.

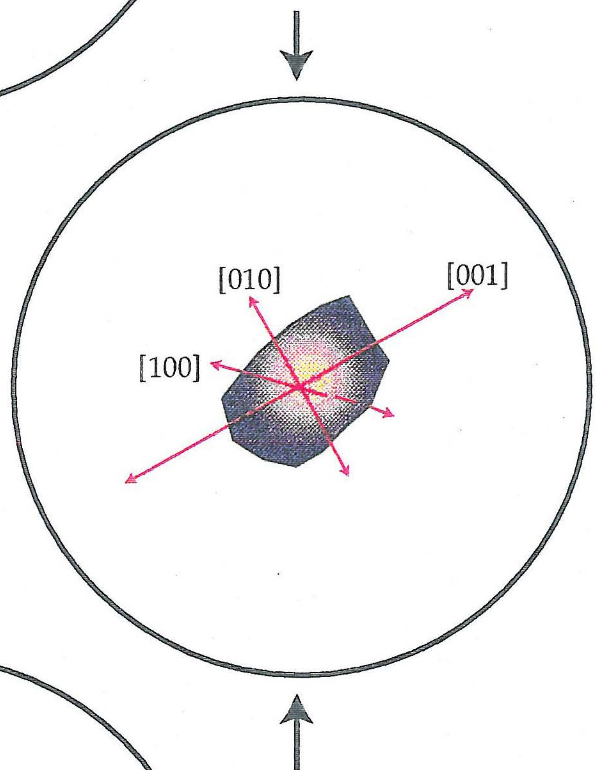

[010] direction rotates and becomes aligned with the direction of most compressive stress. It will be an active intracrystalline slip direction.

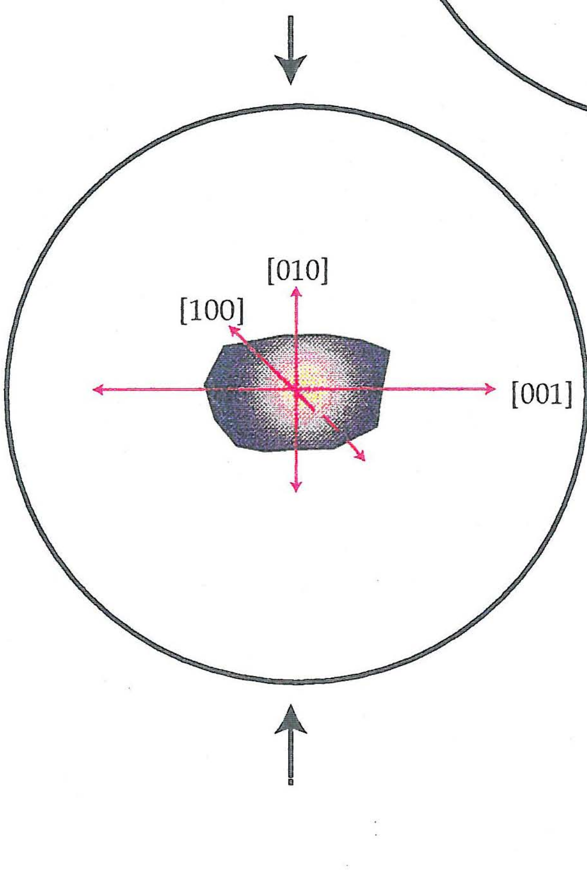

[001] and [100] are now aligned perpendicular to the direction of most compressive stress, (i.e. to the foliation plane) the grain is elongating this way.

It should be noted that [010] is exclusive in this behavior, only at high strain conditions.
information from Nicolas and Poirier 1976

Simple Shear deformation

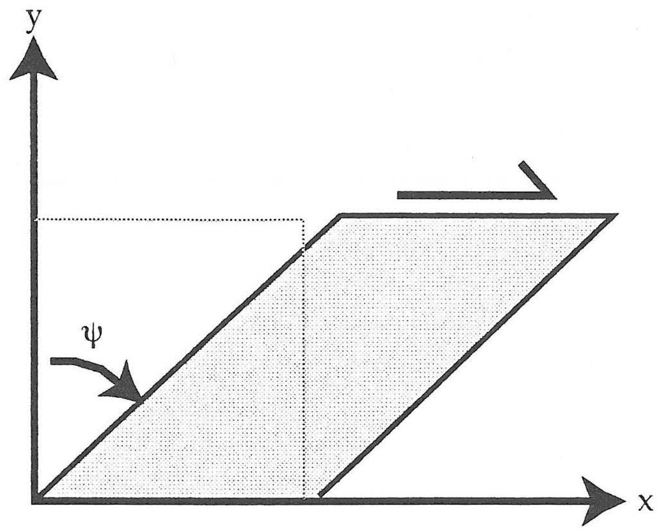

from Wojtal structural handout 1996

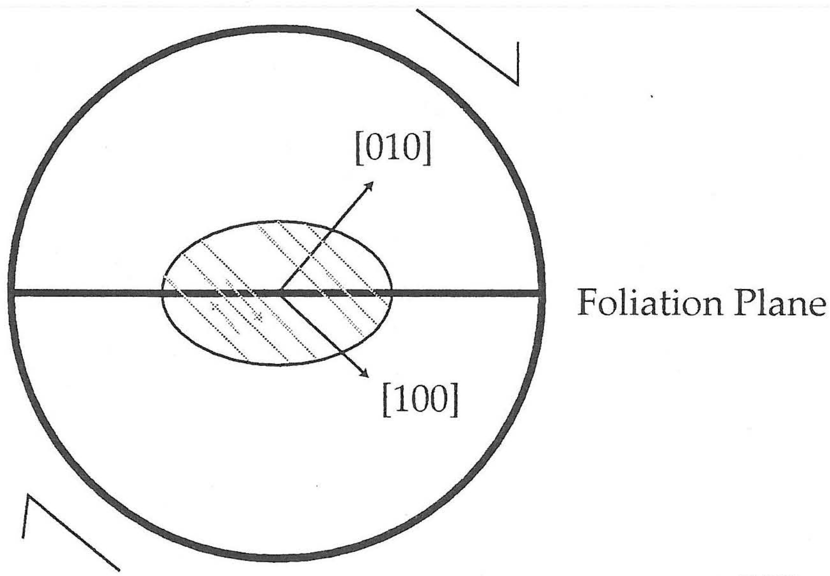

from Takeshita *et al.* in
Barber and Meredith 1990.

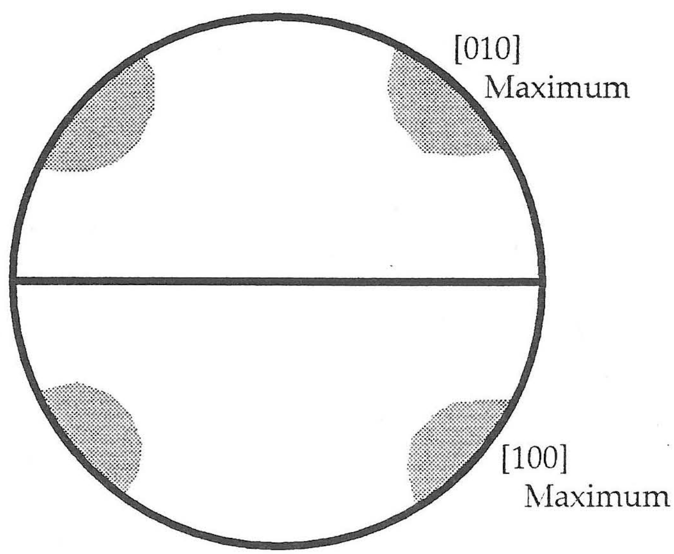

Pole figure of probable slip direction maximum
shows maximum at n° to foliation

Figure 10

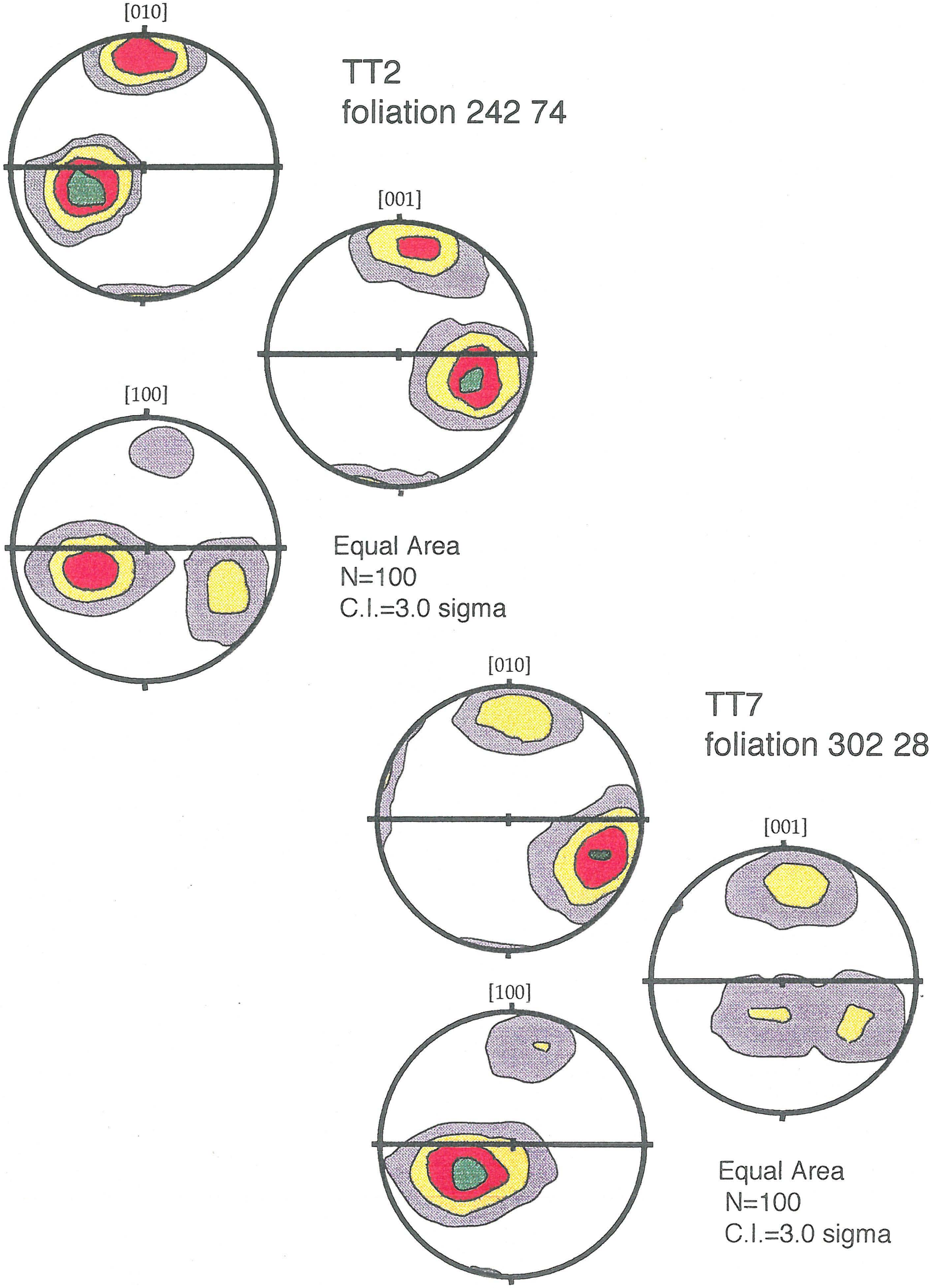

Horizontal line: trace of the foliation plane

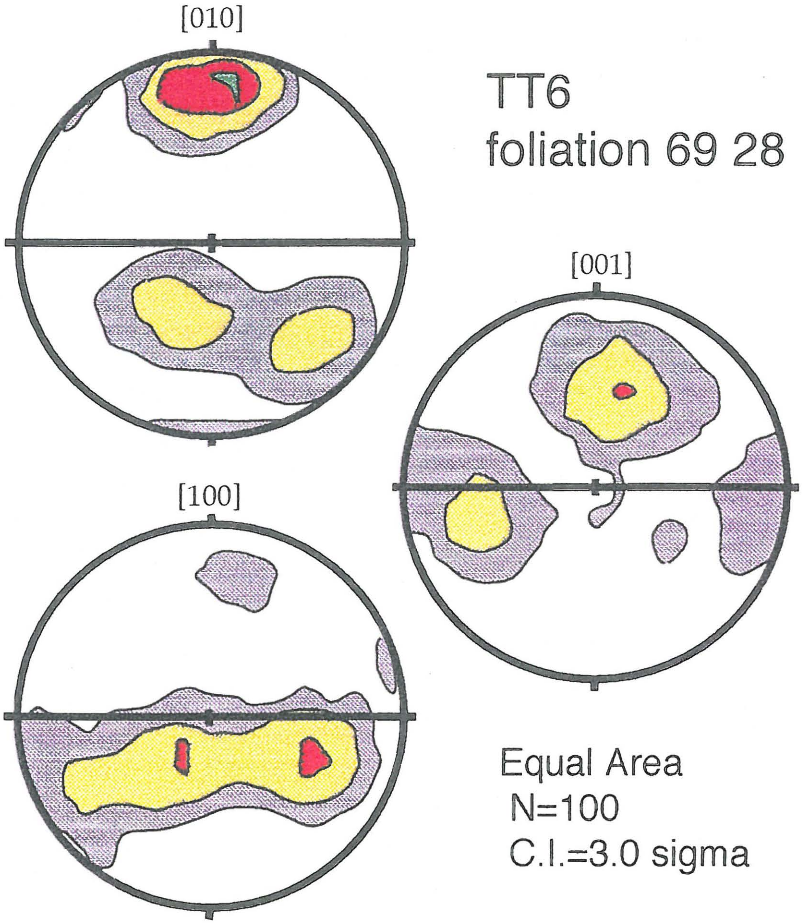

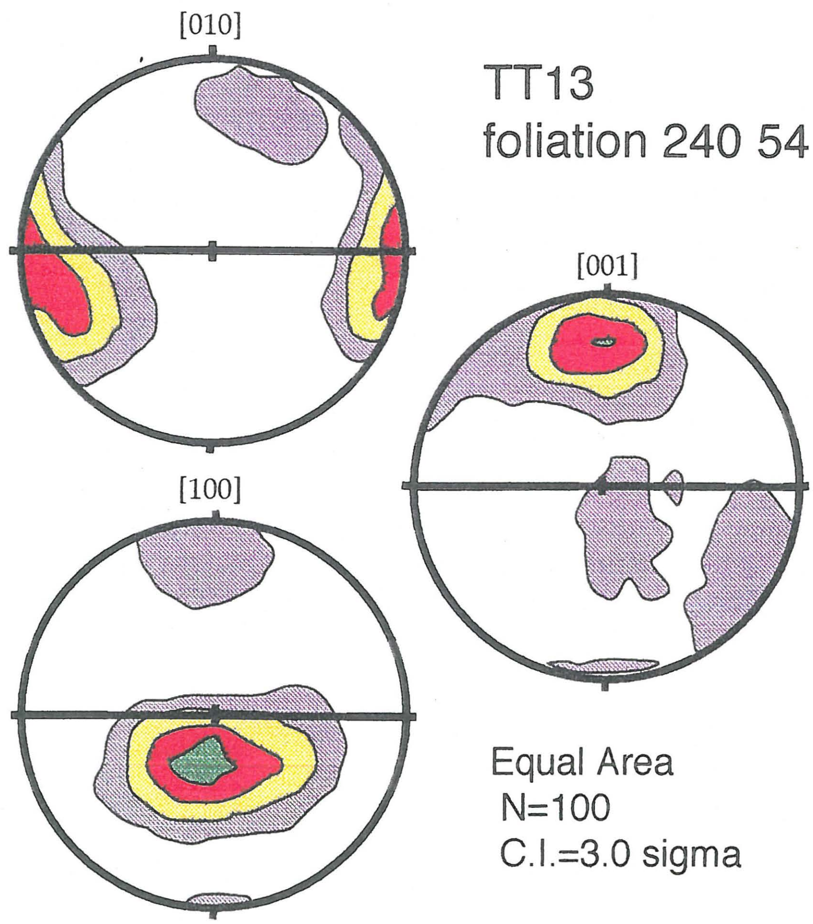

Horizontal line: trace of the foliation plane

Predictions for Preferred Orientations of Crystallographic Axes

Simple Shear

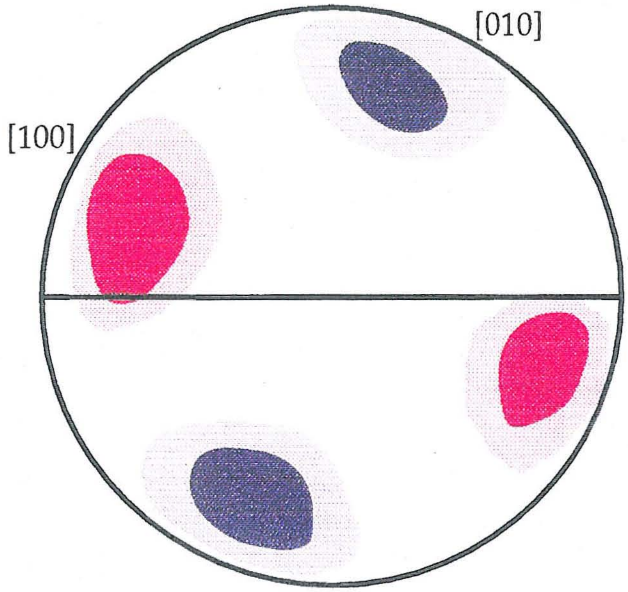

important to note: location of directional maxima depends on shear orientation, however maxima are always at an angle to the foliation.

Pure Shear

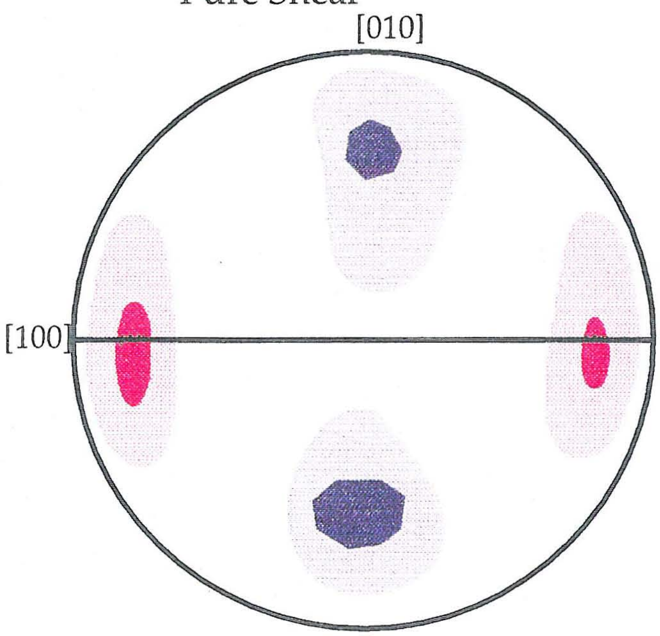

important to note: [100] maximum is strictly parallel to foliation, [010] maximum is perpendicular.

from Takeshita *et al.* in Barber & Meredith 1990

Figure 12

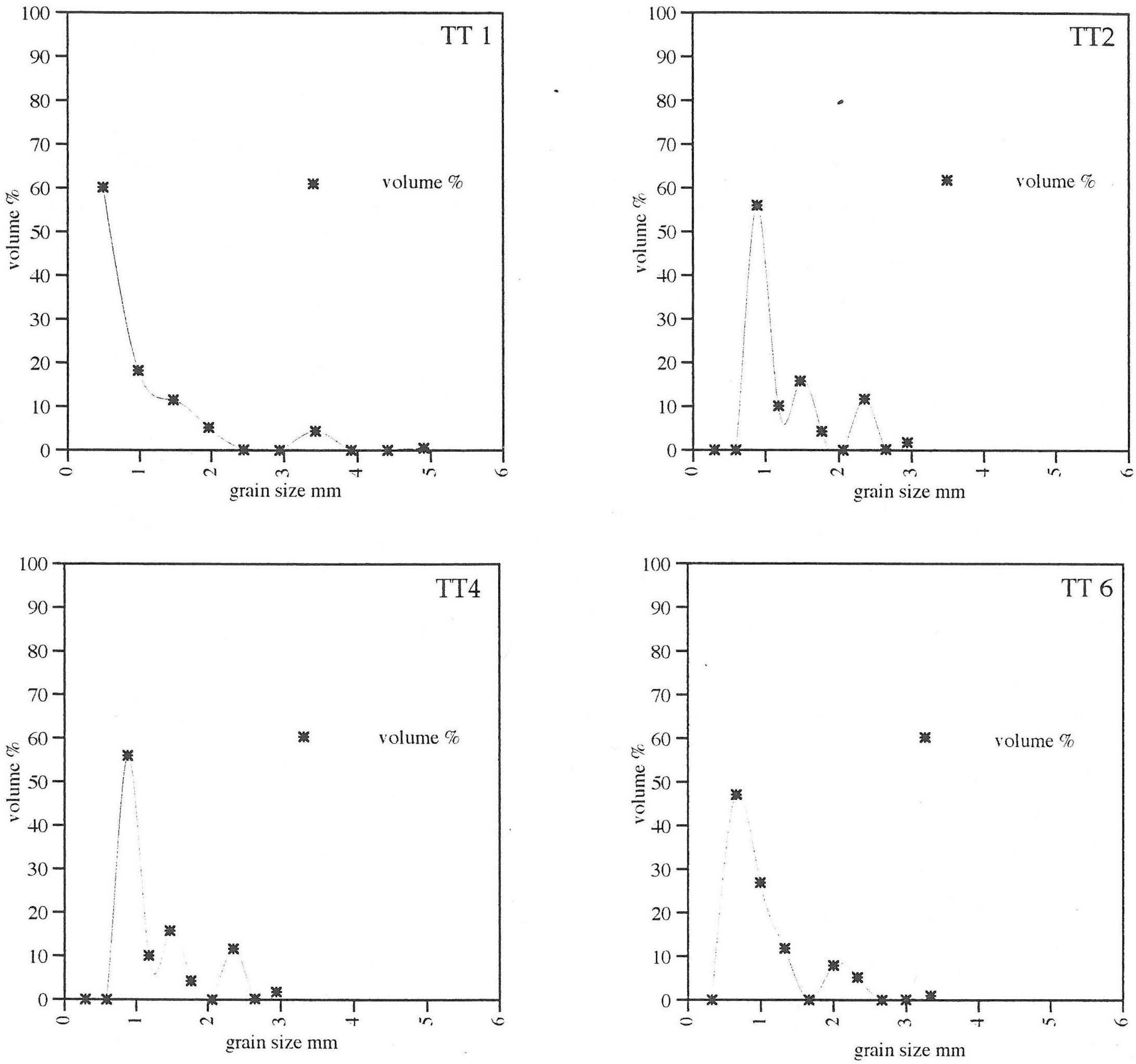

TT 1
volume %
grain size mm
TT2
volume %
grain size mm
TT4
volume %
grain size mm
TT 6
volume %
grain size mm

Figure 12

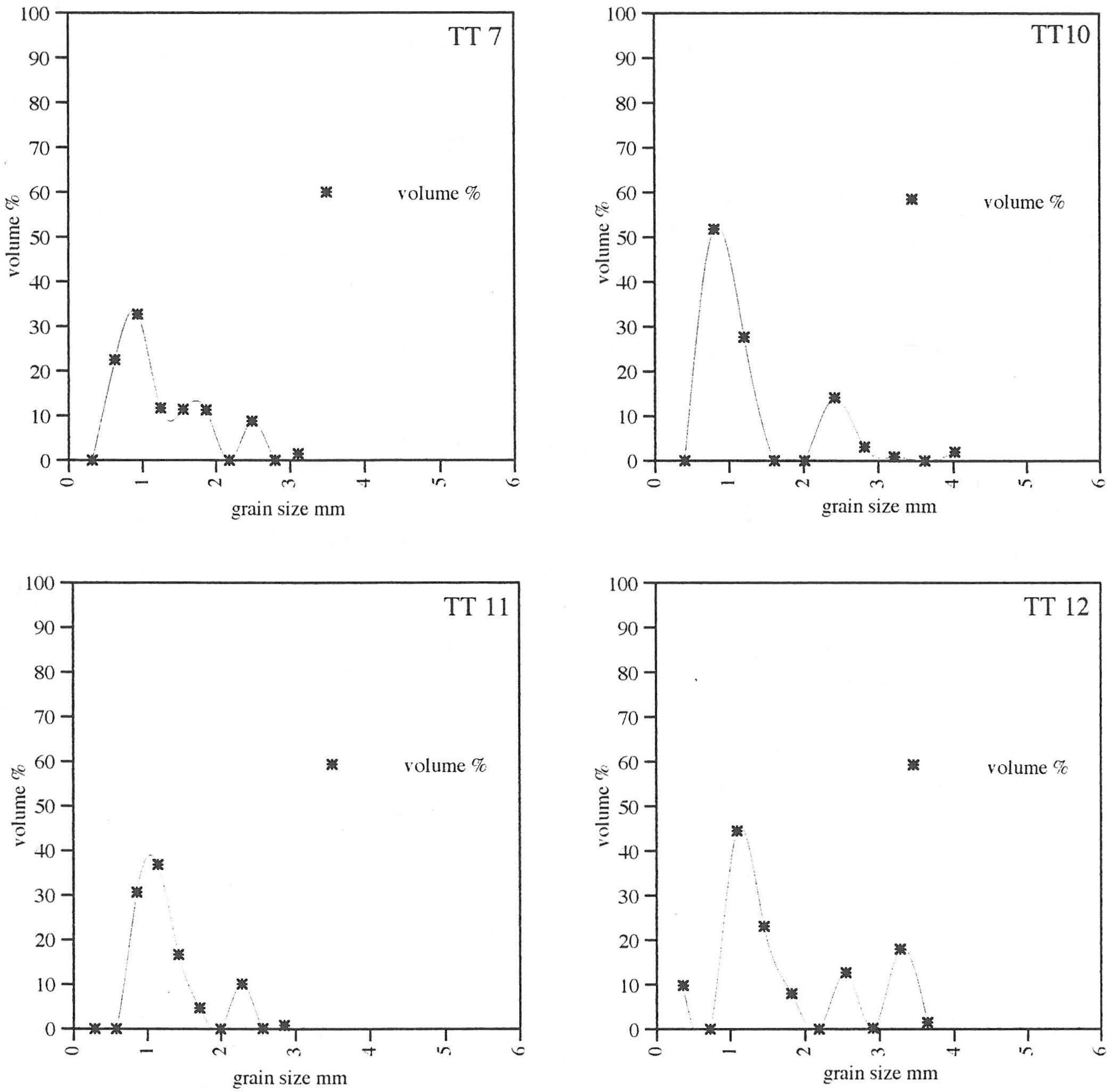

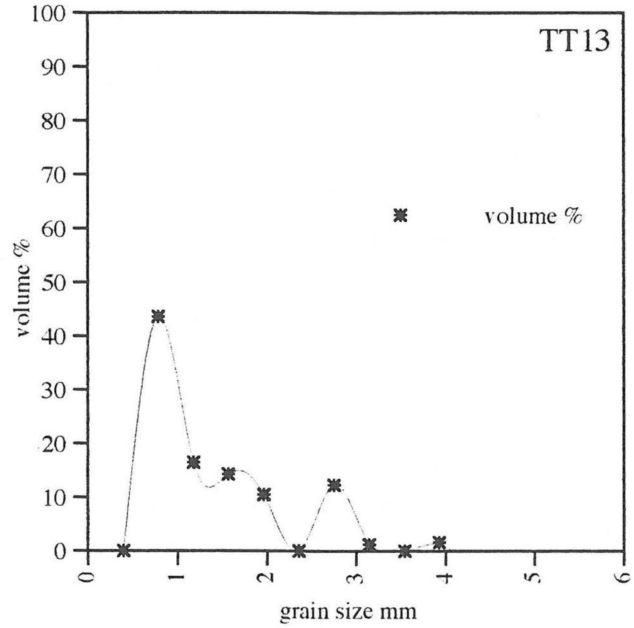
TT13
volume %
volume %
grain size mm

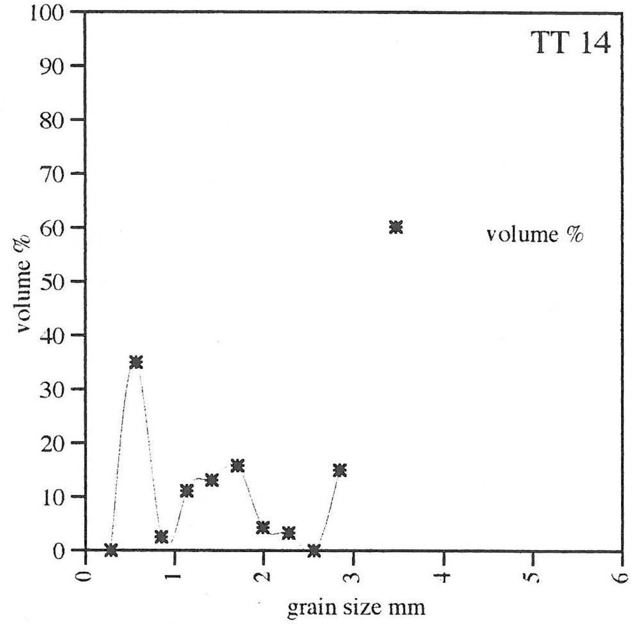
TT 14
volume %
volume %
grain size mm

Late Precambrian (570 Ma?)

1) Formation of Buck Creek mafic/ultramafic cumulates beneath a Precambrian oceanic spreading center.
-- The high TiO2 and LREE depleted signatures of the cumulates suggests formation in a large ocean basin.

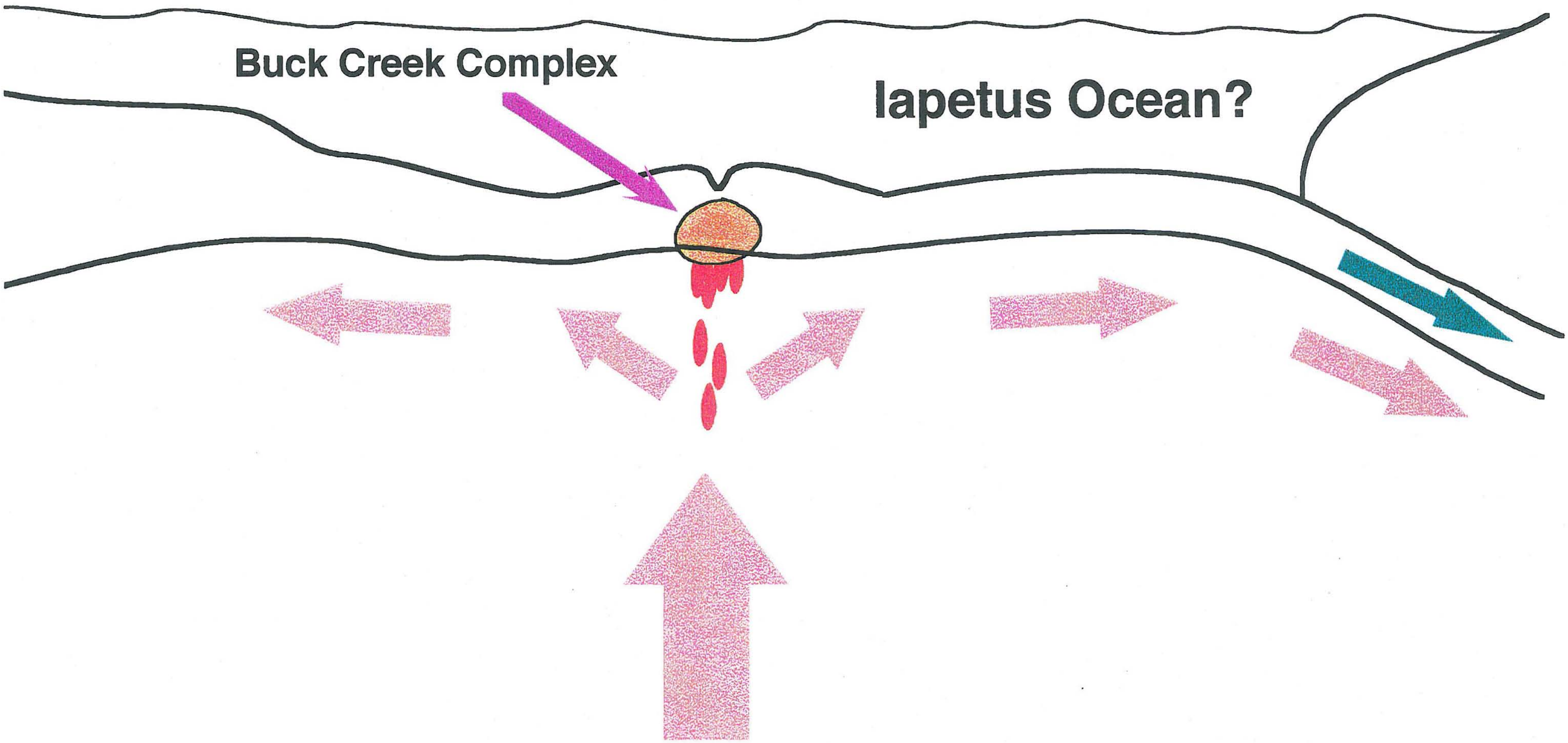

500 Ma (Penobscottian?)

2) Subduction of Buck Creek cumulates to at least 18 km, to produce OPX-CPX-Spinel symplectic coronas (Tenthorey et al. 1996).
-- Relatively anhydrous conditions persist to preserve primary mineralogies of troctolites and dunites

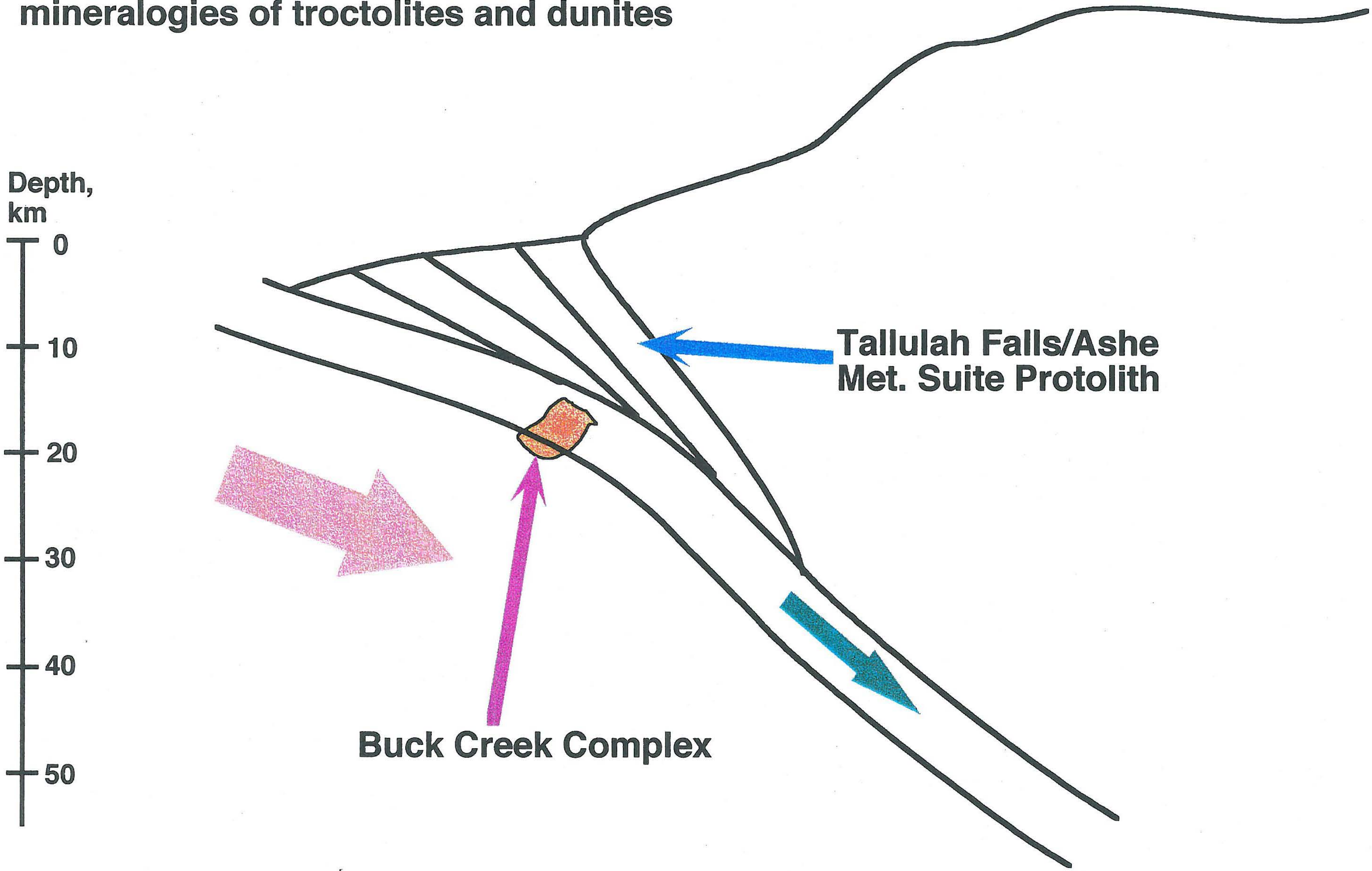

440 Ma (Taconic Orogeny)

3) Deep Burial and Initial Deformation of the Buck Creek complex during collision in the Taconic Orogeny.

--Buck Creek (and Lake Chatuge) complex emplaced on the hangingwall of the Hayesville Thrust as a fragment of old, subducted ocean crust (a deep ophiolite?).

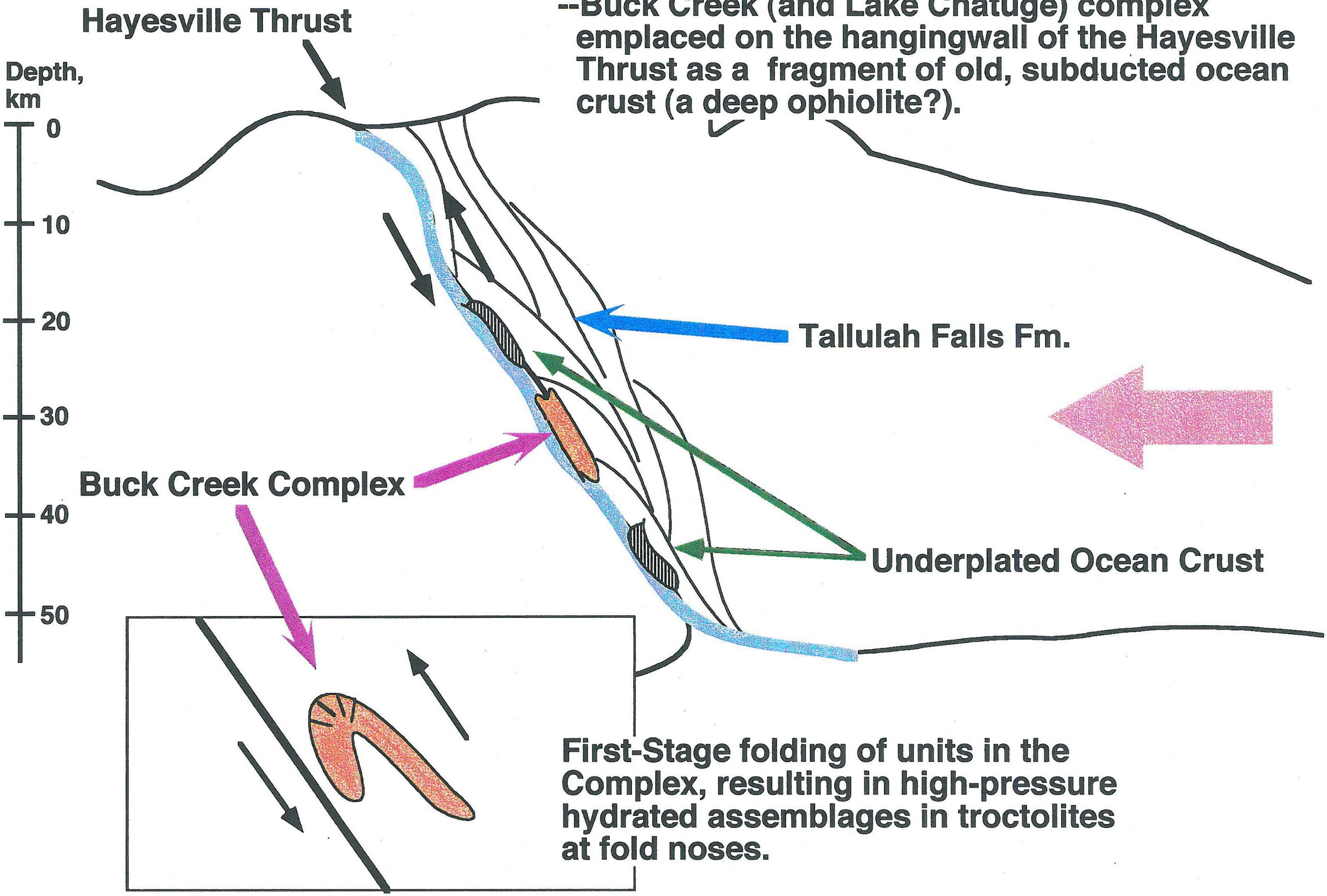

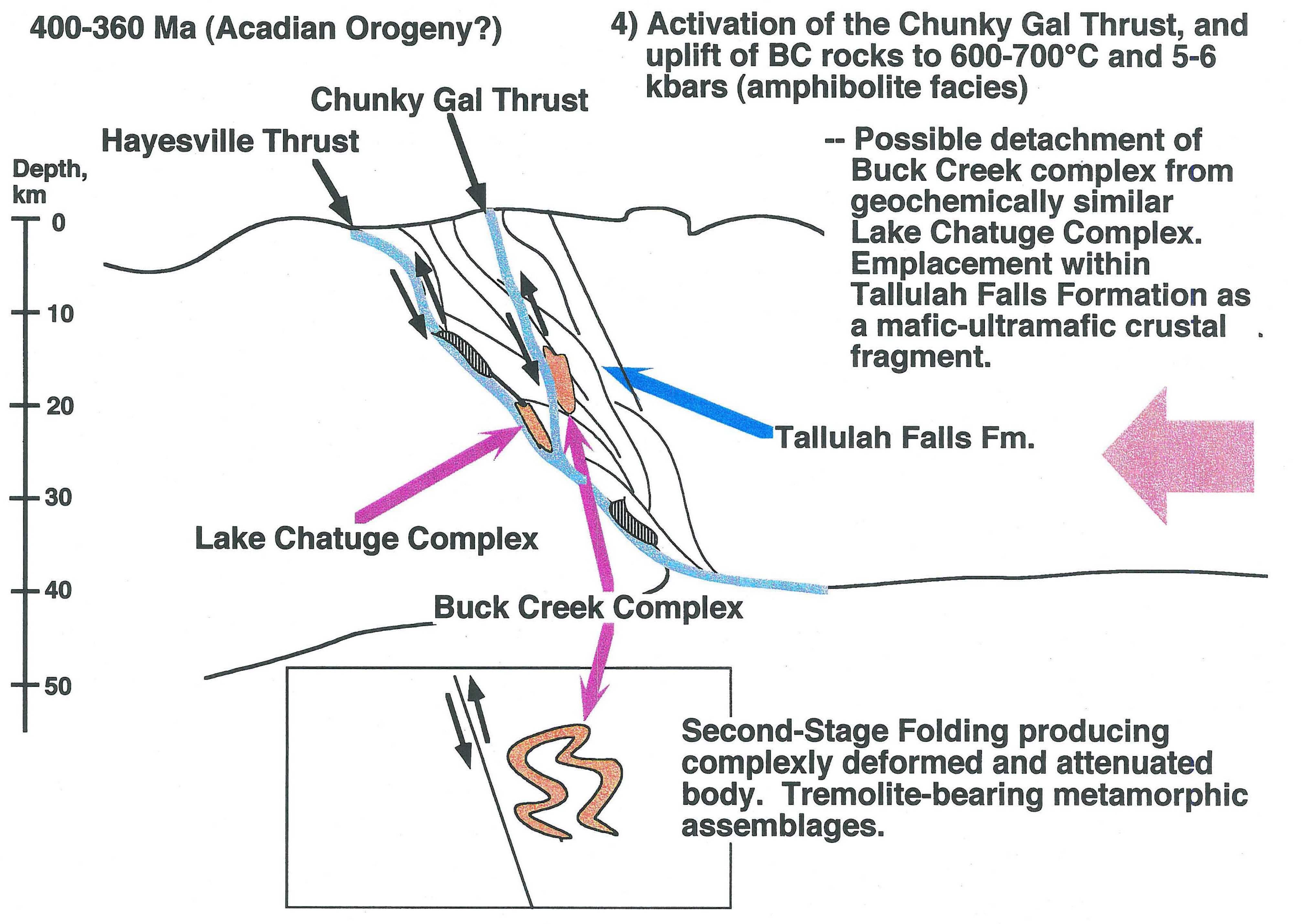
400-360 Ma (Acadian Orogeny?)
4) Activation of the Chunky Gal Thrust, and uplift of BC rocks to 600-700°C and 5-6 kbars (amphibolite facies)
-- Possible detachment of Buck Creek complex from geochemically similar Lake Chatuge Complex. Emplacement within Tallulah Falls Formation as a mafic-ultramafic crustal fragment.
Chunky Gal Thrust
Hayesville Thrust
Depth, km
0
10
20
30
40
50
Tallulah Falls Fm.
Lake Chatuge Complex
Buck Creek Complex
Second-Stage Folding producing complexly deformed and attenuated body. Tremolite-bearing metamorphic assemblages.

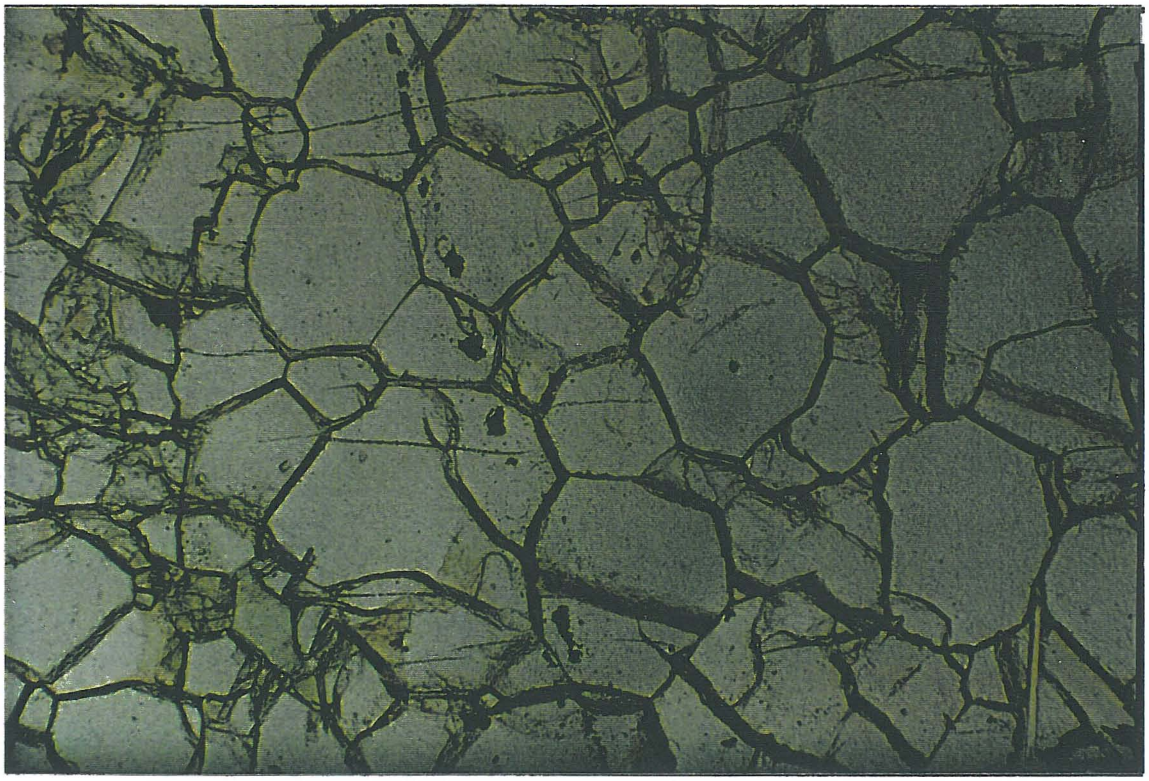

above: Equigranular-mosaic texture in plane polarized light from sample TT6

0.2 mm

below: Same equigranular-mosaic texture in crossed nicols from sample TT6

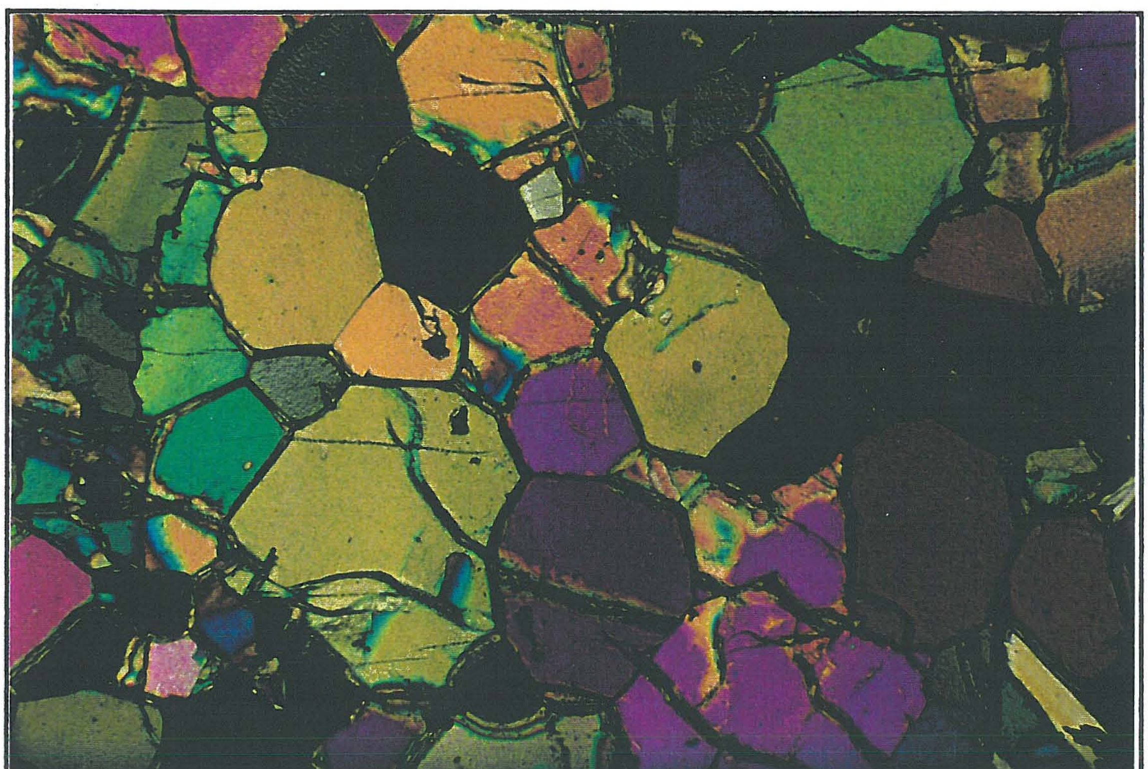

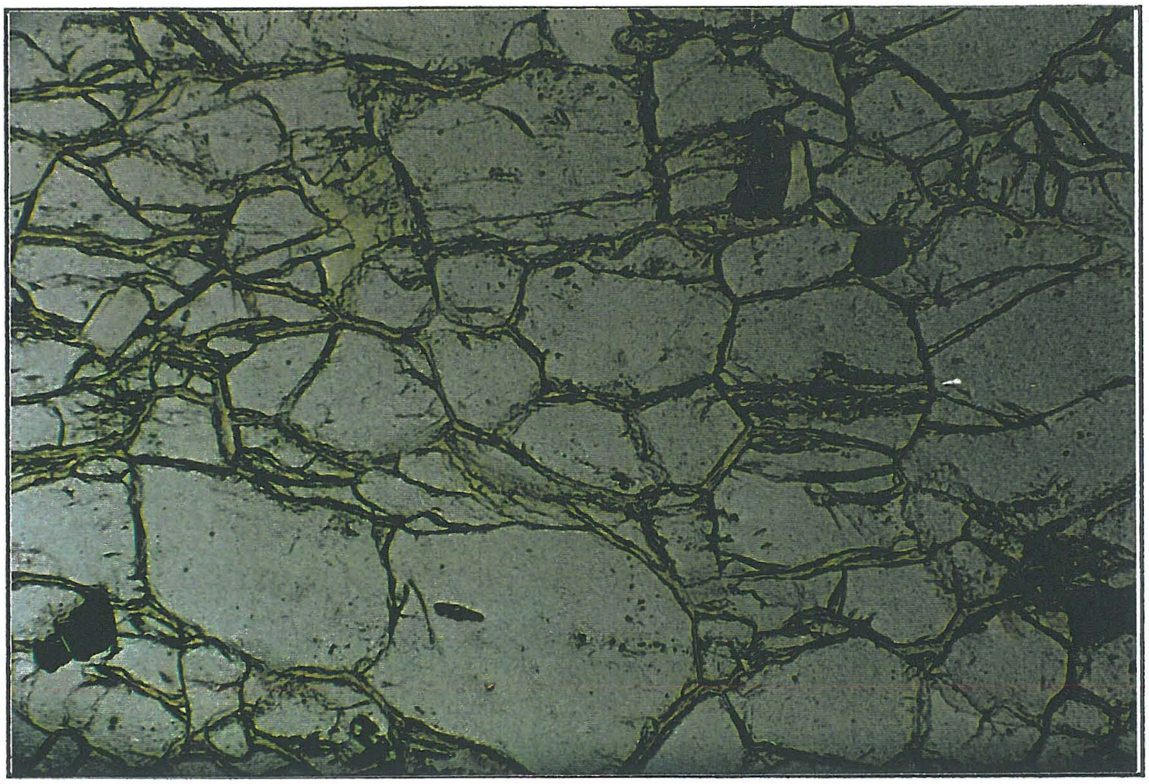

above: Rare equigranular-tabular texture in plane polarized light from sample TT7

0.2mm

below: Same equigranular-tabular texture in crossed nicols from sample TT7

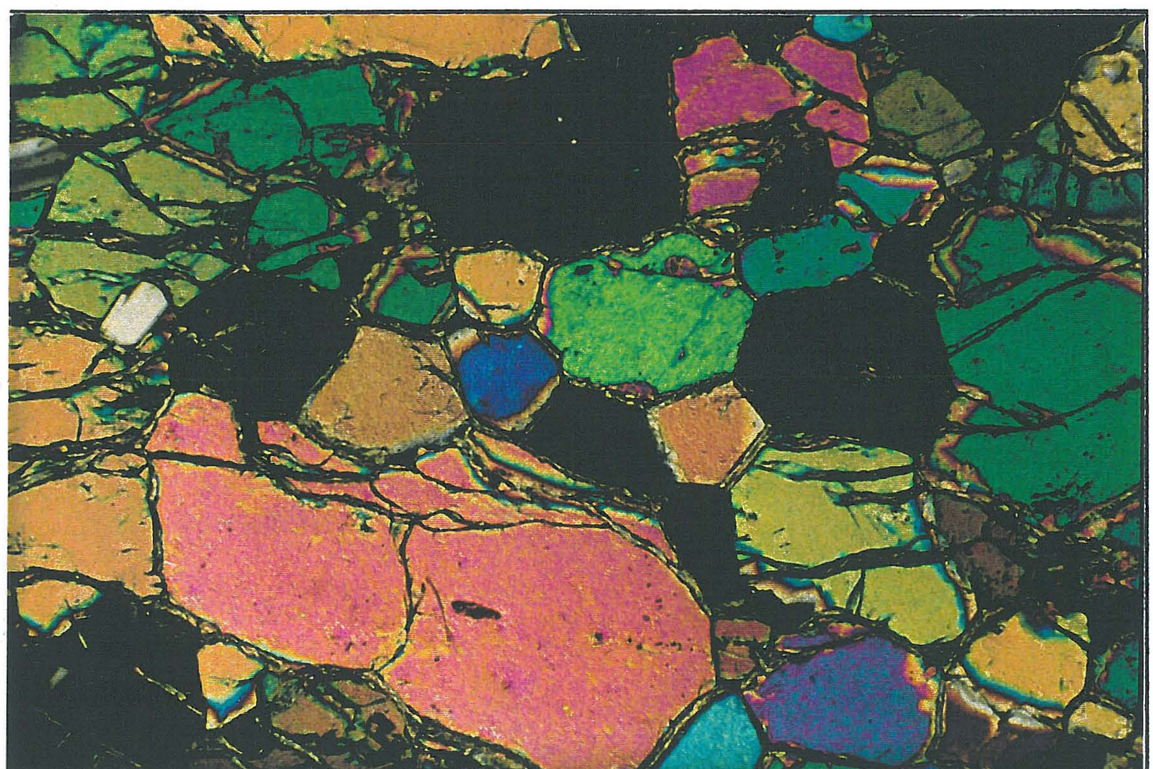

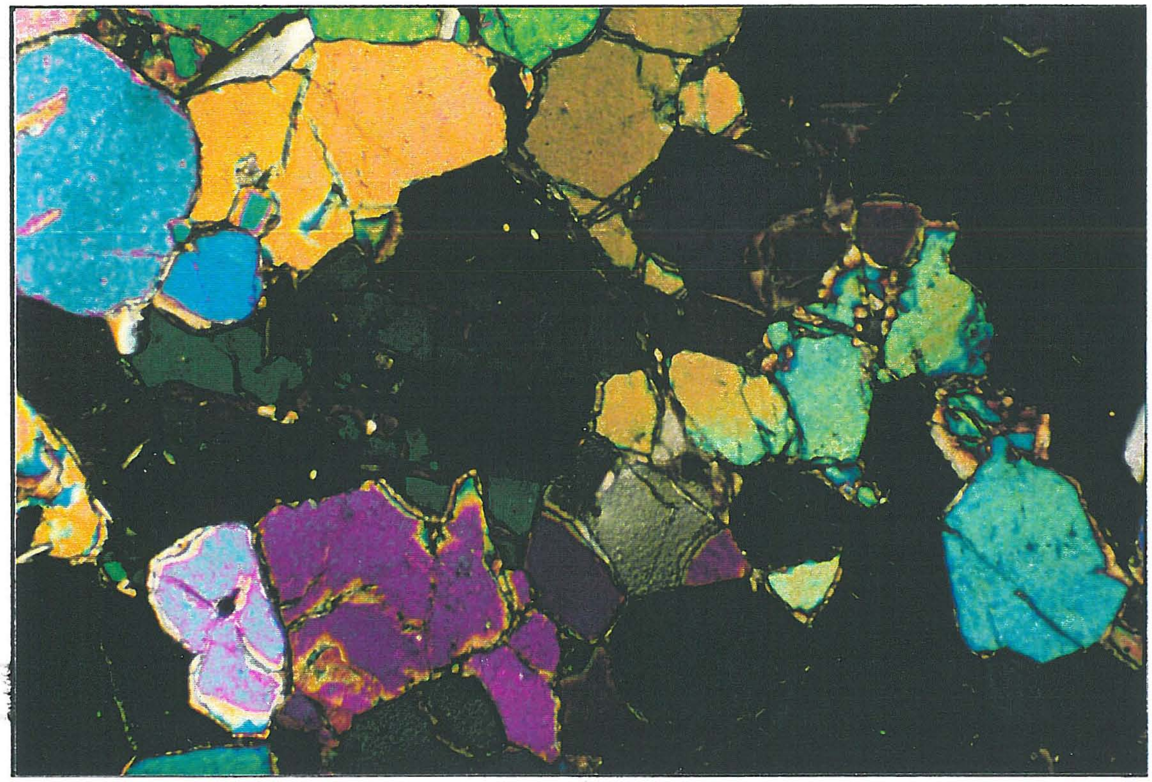

above: Porphyroclastic texture in crossed nicols from sample TT2

below: Porphyroclastic texture in crossed nicols from sample TT6

0.2mm

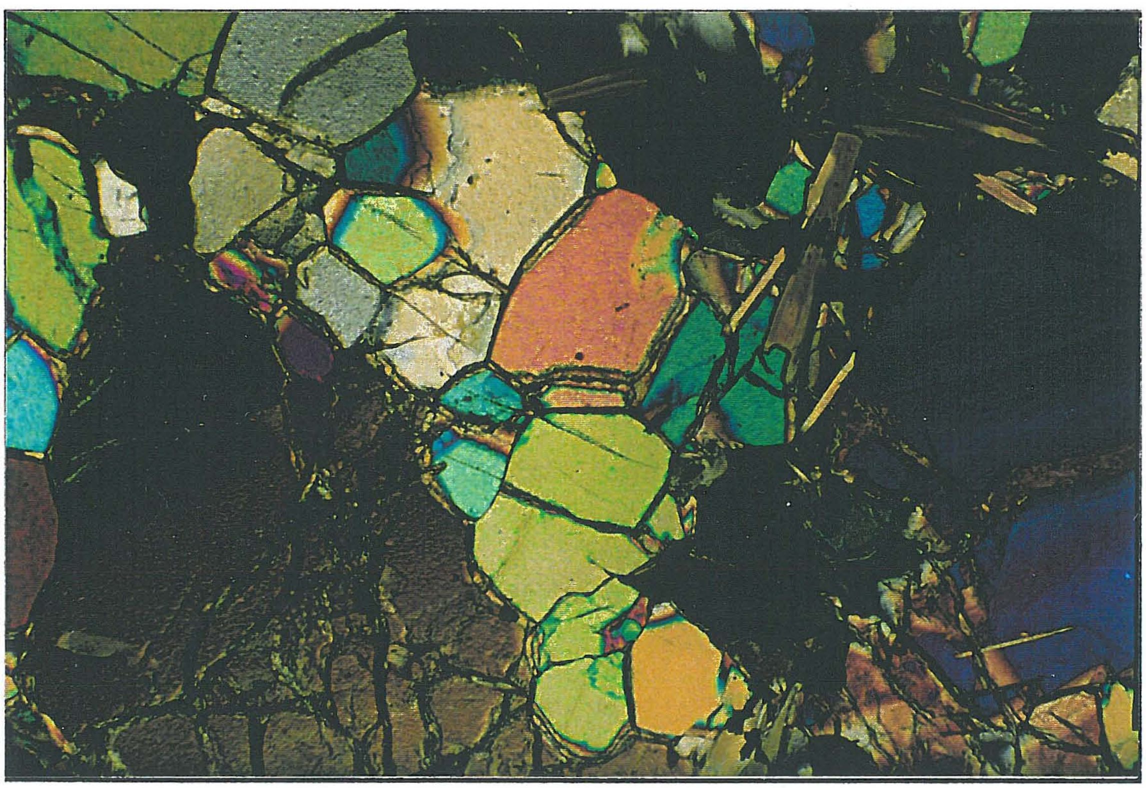

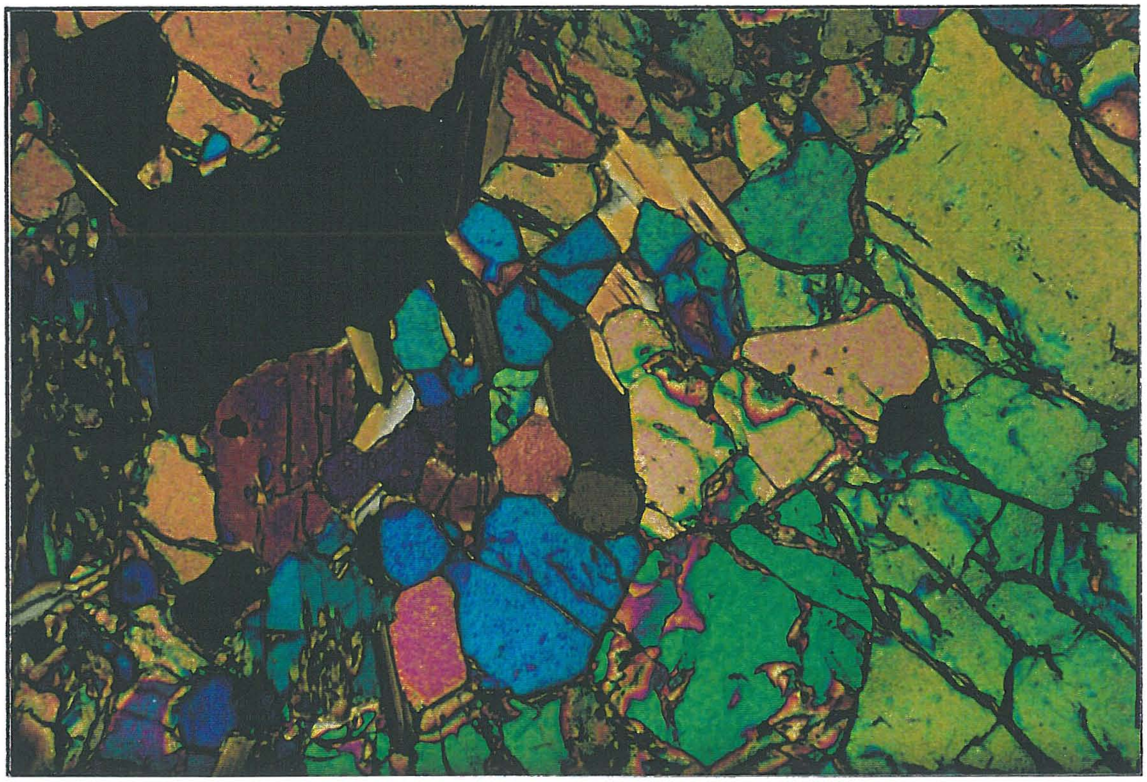

above: Interstitial plagioclase clots in crossed nicols from sample TT2

below: Rare interstitial orthopyroxene grain in crossed nicols from sample TT1

0.2mm

0.1mm

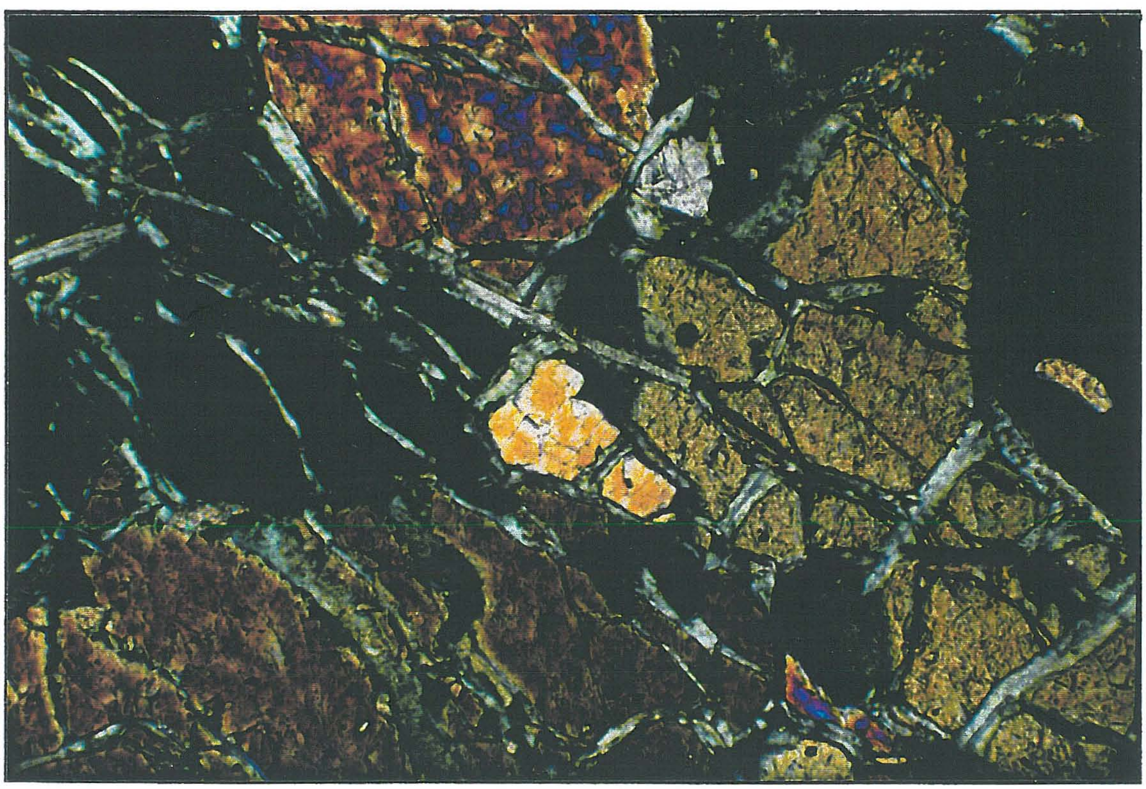

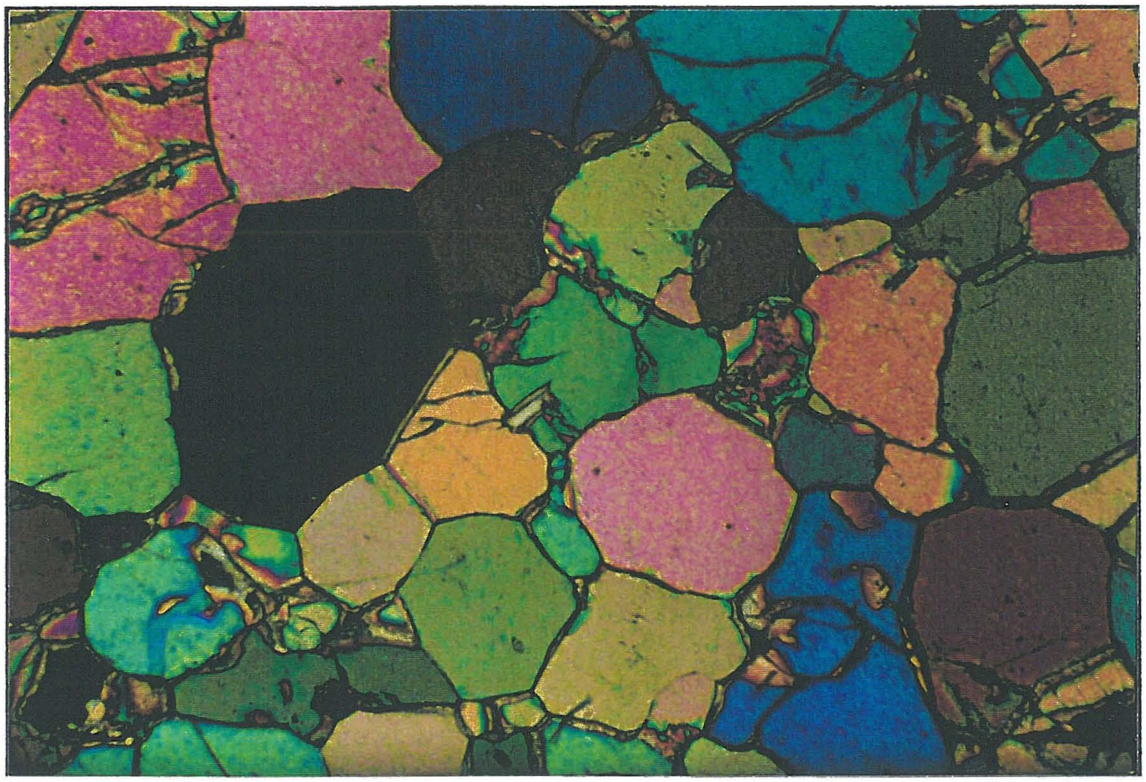

above: Unaltered dunite (equigranular-mosaic texture) in crossed nicols from sample TT2

0.2mm

below: Slightly more alteration along cracks in crossed nicols from sample TT12

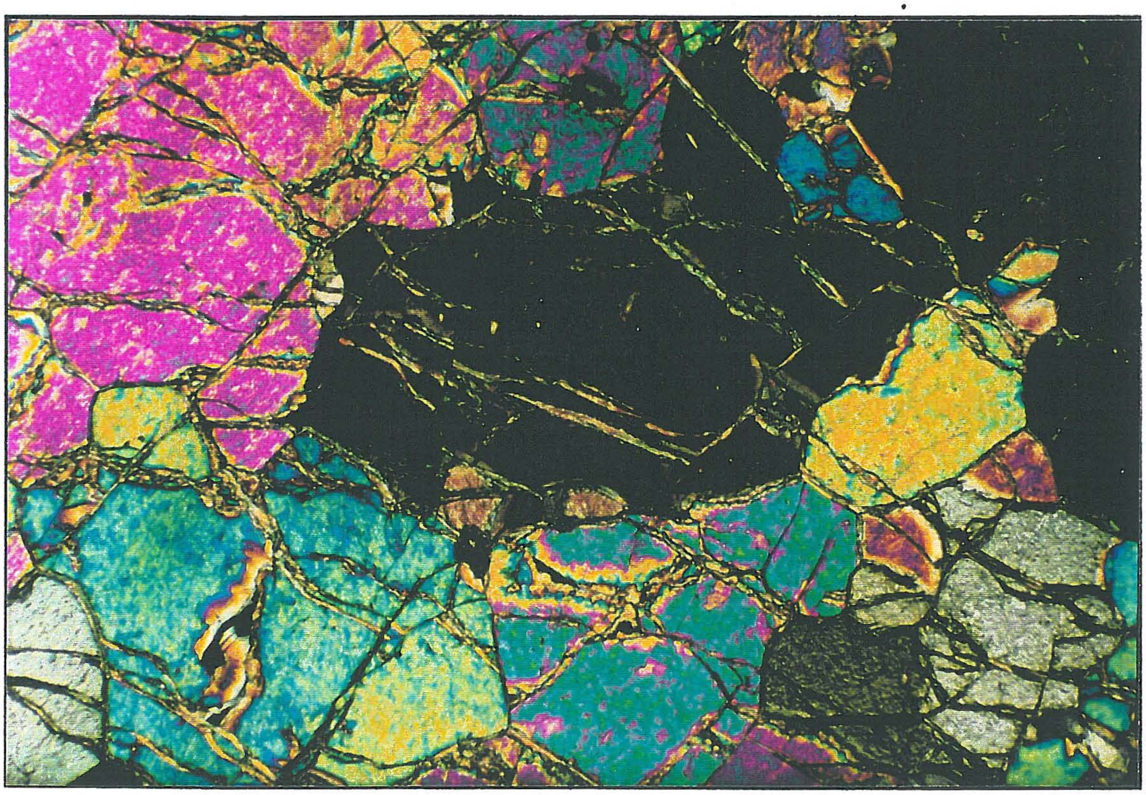

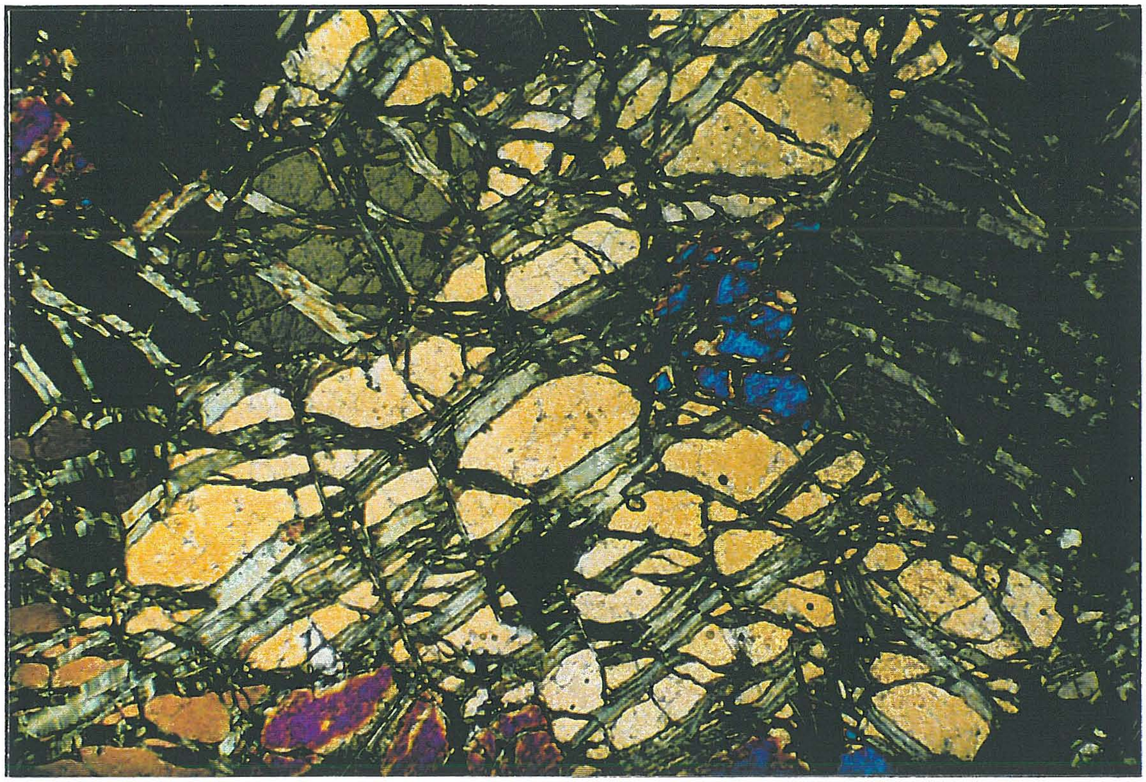

above: Serpentine significantly filling cracks of grains in crossed nicols from sample TT14

0.2mm

below: Relict olivine grain in alteration matrix in crossed nicols from sample TT5

0.1mm

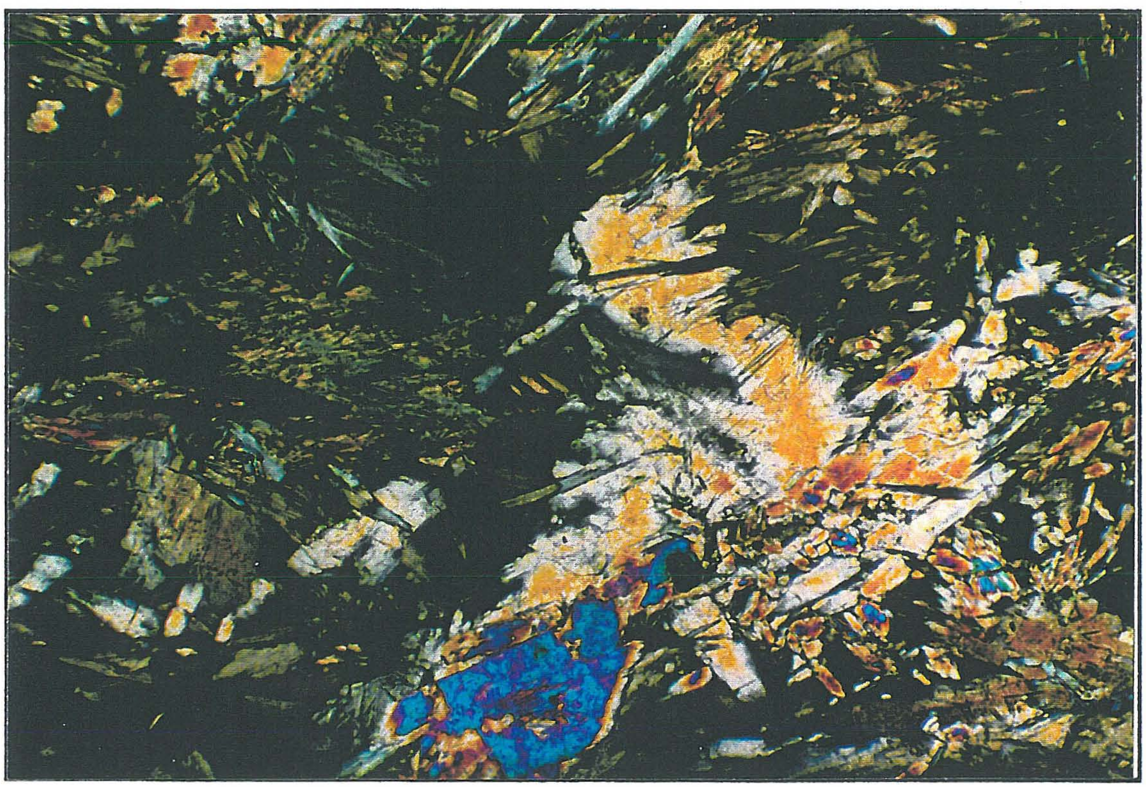

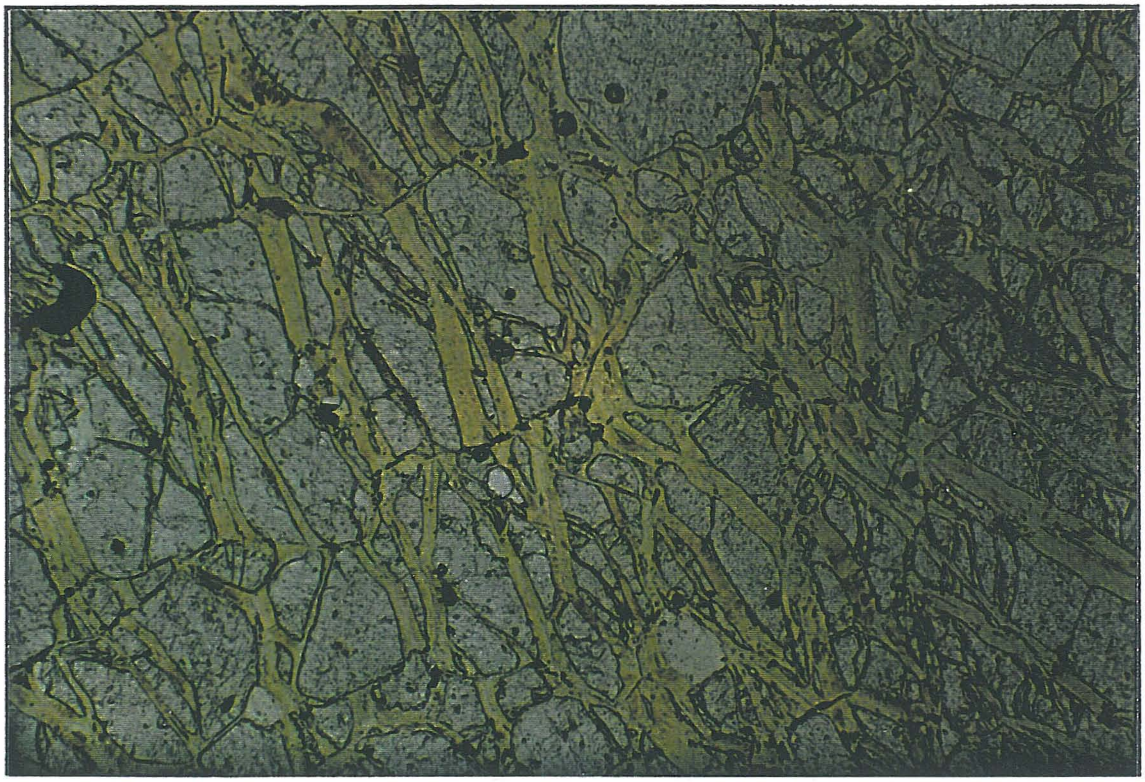

above: Serpentine in cracks defining a fabric in plane polarized light from sample TT1

0.2mm

below: Same view in crossed nicols from sample TT1

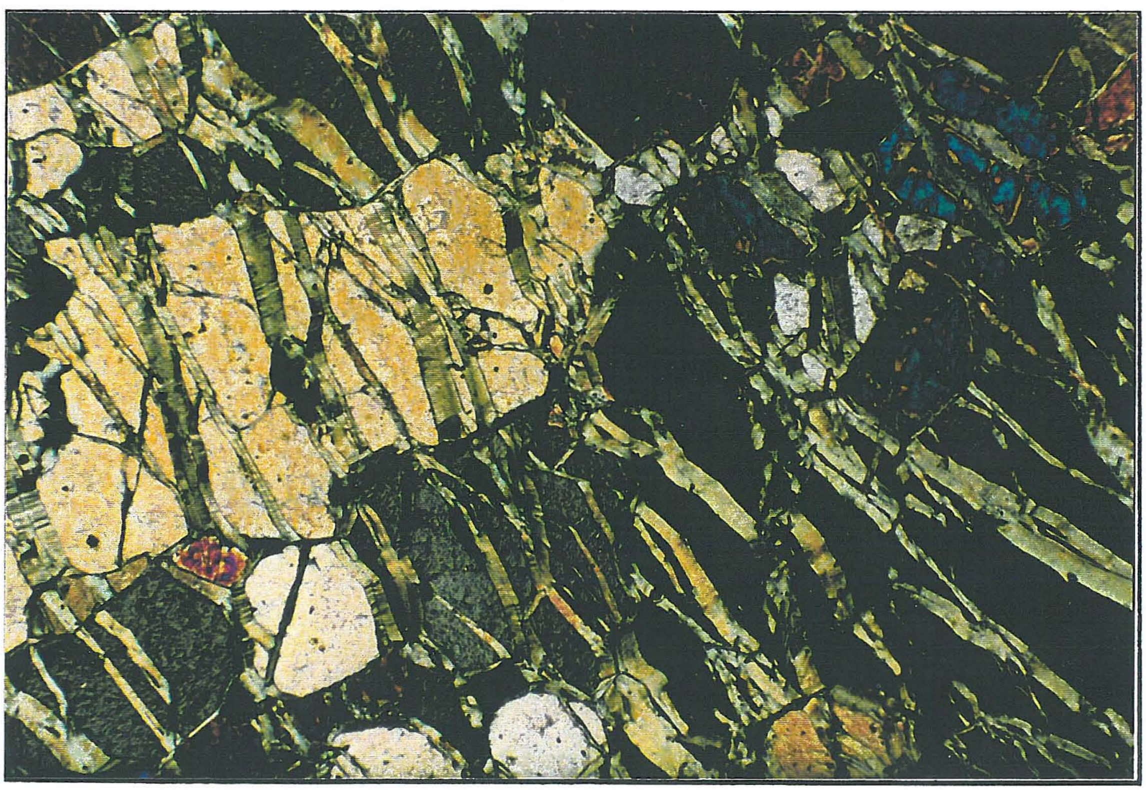

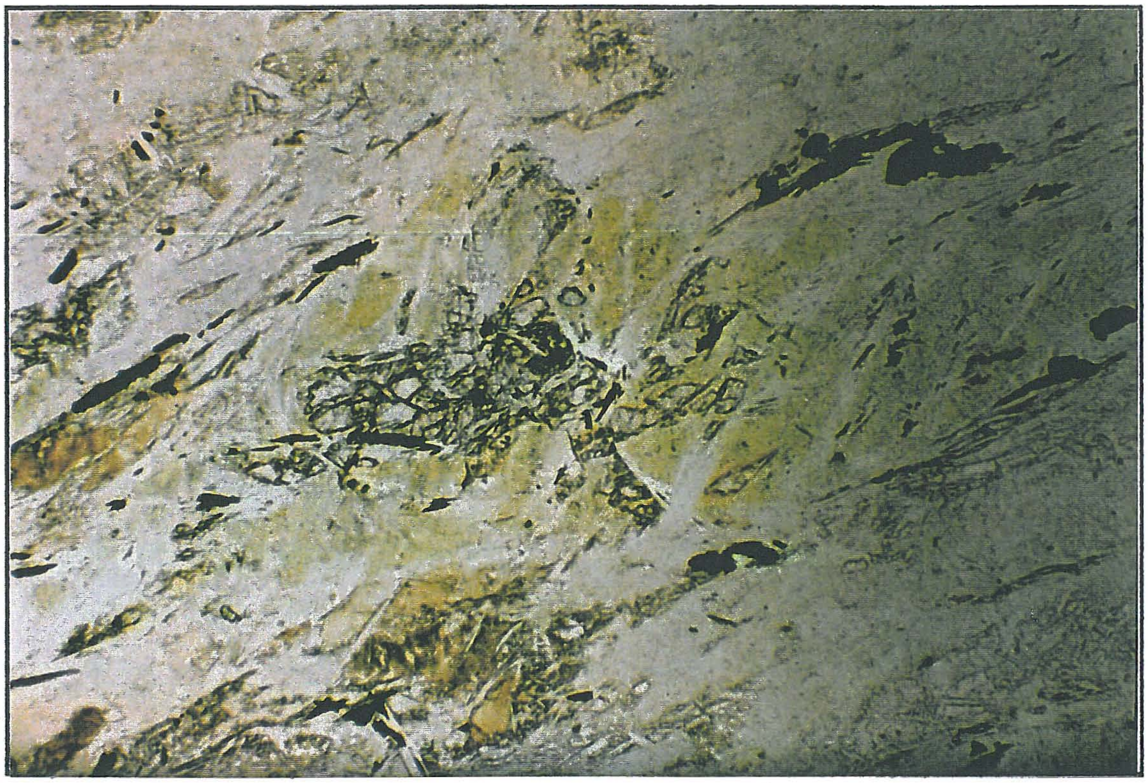

above: Chlorite, serpentine, talc, anthophyllite, etc. in plane polarized light sample TT5

below: Preferred orientation of several olivine grains with gypsum plate from sample TT2 0.2mm

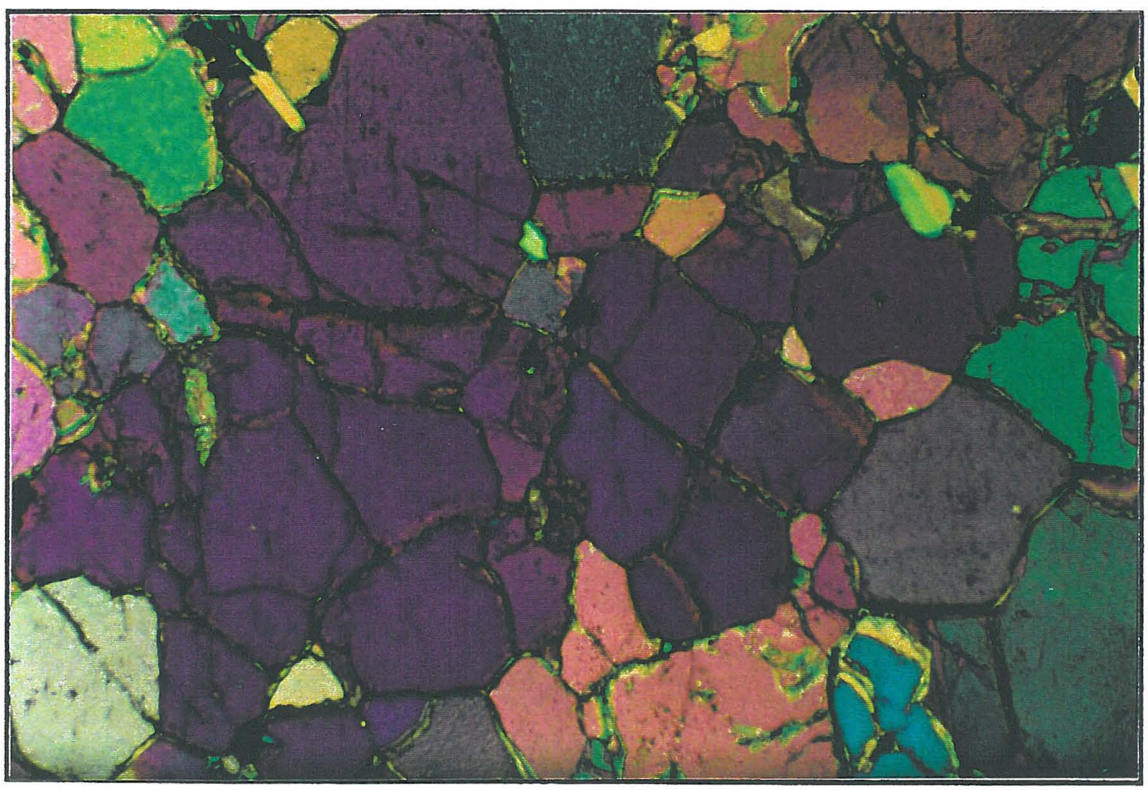

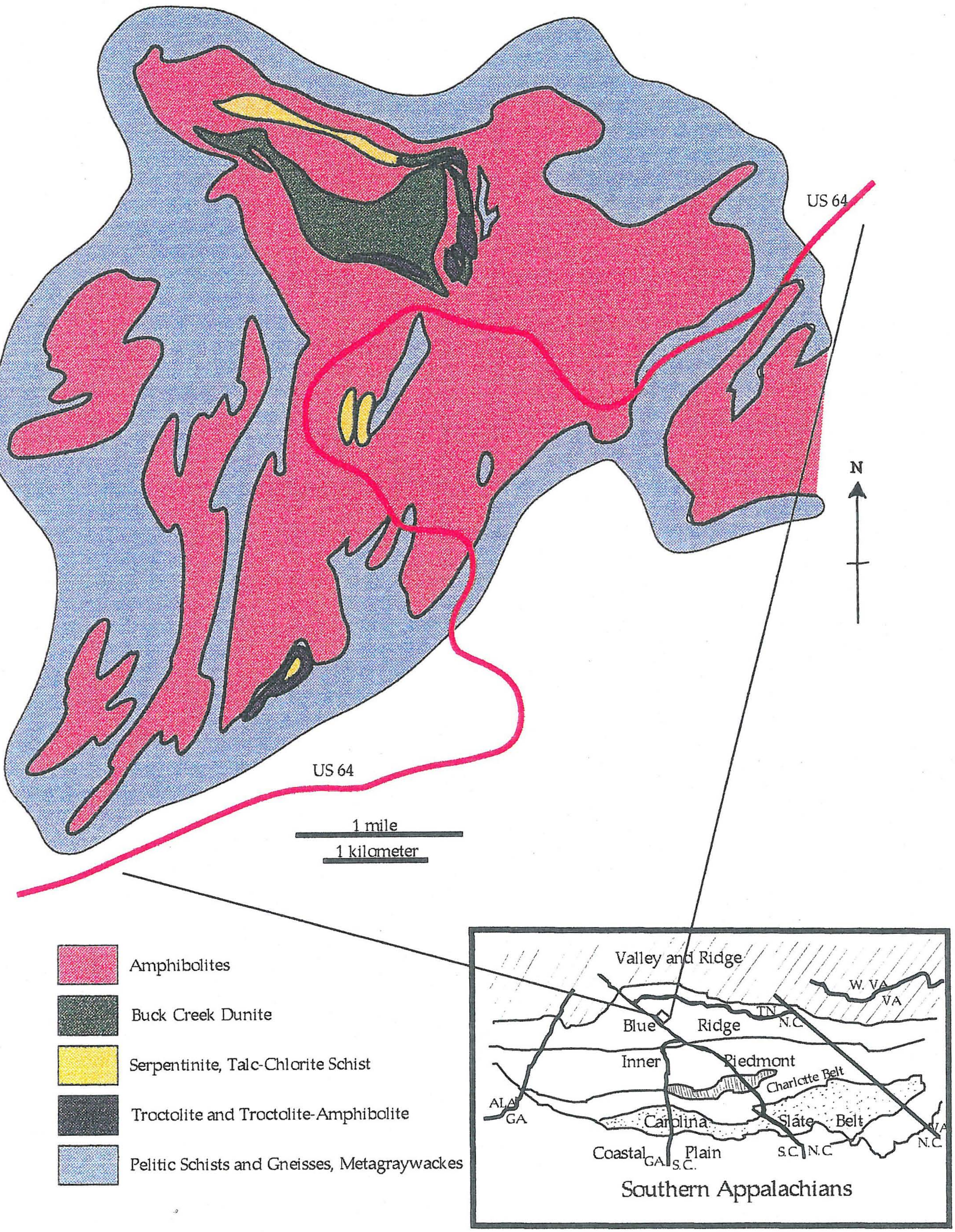
US 64
US 64
N
1 mile
1 kilometer
Amphibolites
Buck Creek Dunite
Serpentinite, Talc-Chlorite Schist
Troctolite and Troctolite-Amphibolite
Pelitic Schists and Gneisses, Metagraywackes
Valley and Ridge
W. VA
VA
TN
N.C.
Blue
Ridge
Inner
Piedmont
Charlotte Belt
ALA
GA
Carolina
Slate
Belt
VA
N.C.
Coastal
Plain
GA
S.C.
S.C.
N.C.
Southern Appalachians

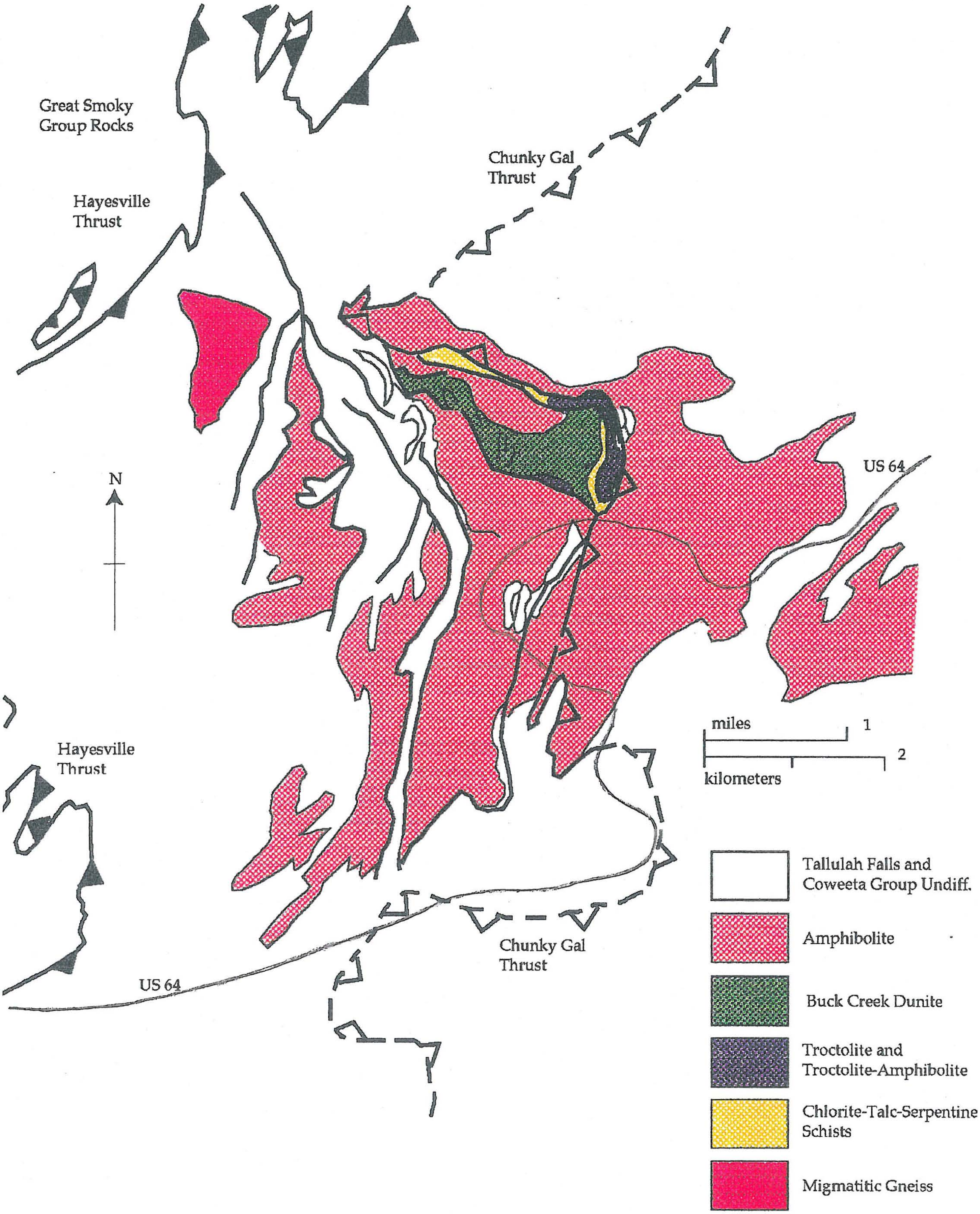
Great Smoky
Group Rocks
Hayesville
Thrust
Chunky Gal
Thrust
N
US 64
miles
1
2
kilometers
Hayesville
Thrust
Chunky Gal
Thrust
US 64
Tallulah Falls and
Coweeta Group Undiff.
Amphibolite
Buck Creek Dunite
Troctolite and
Troctolite-Amphibolite
Chlorite-Talc-Serpentine
Schists
Migmatitic Gneiss

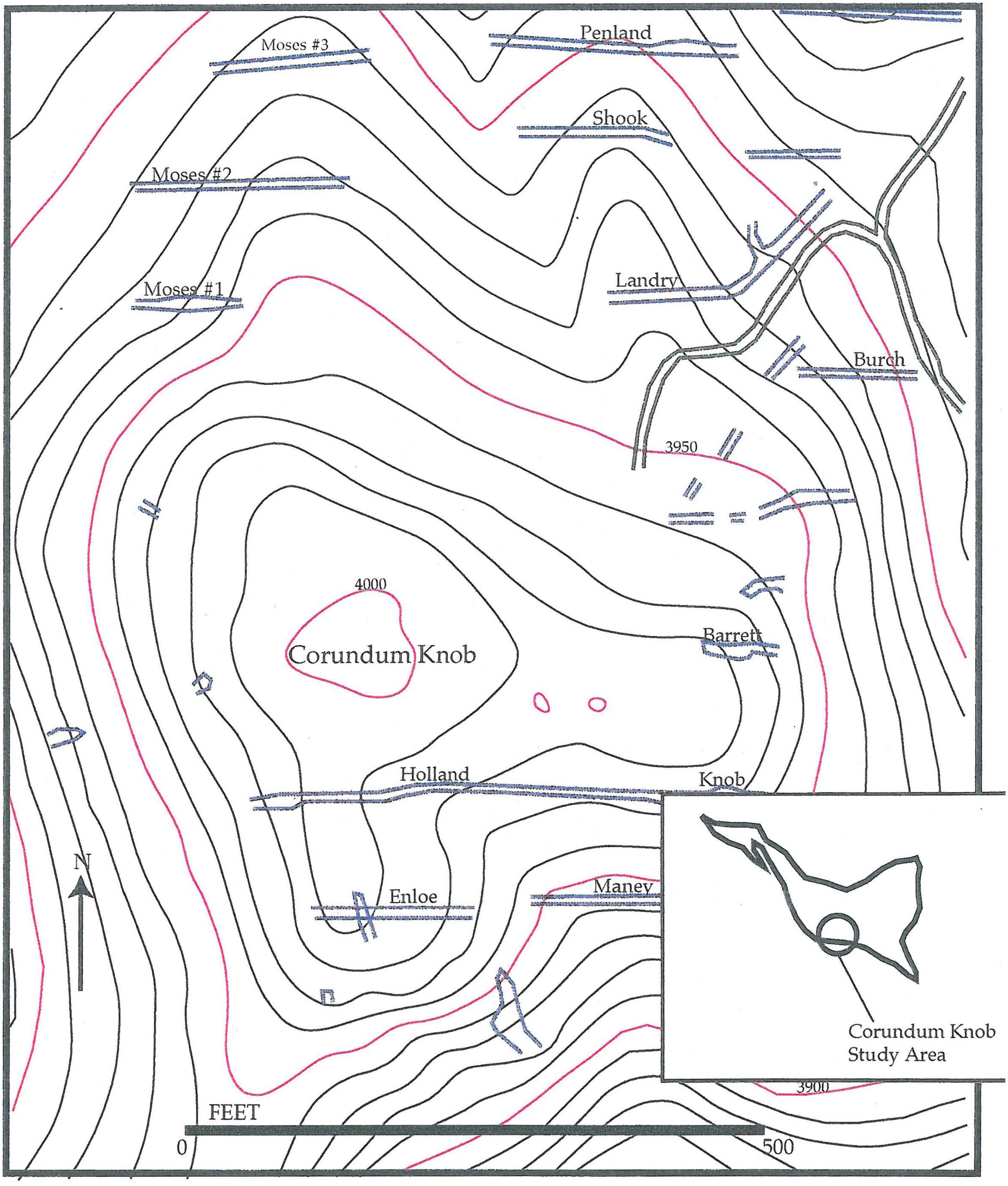
Moses #3
Penland
Shook
Moses #2
Moses #1
Landry
Burch
3950
4000
Corundum Knob
Barrett
Holland
Knob
N
Enloe
Maney
Corundum Knob
Study Area
3900
FEET
0
500

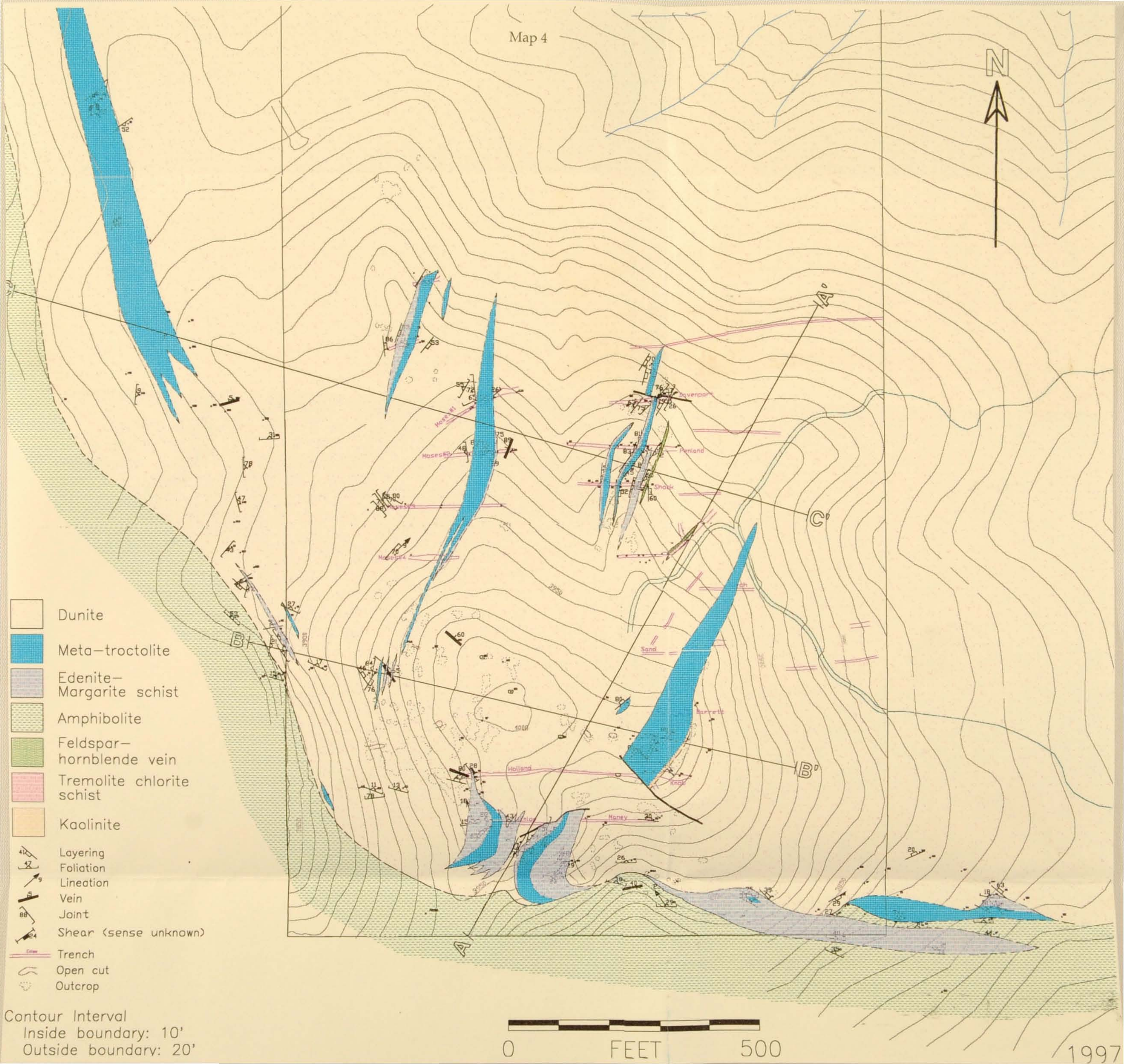
Map 4
N
Dunite
Meta-troctolite
Edenite-Margarite schist
Amphibolite
Feldspar-hornblende vein
Tremolite chlorite schist
Kaolinite
Layering
Foliation
Lineation
Vein
Joint
Shear (sense unknown)
Trench
Open cut
Outcrop
Contour Interval
Inside boundary: 10'
Outside boundary: 20'
0
FEET
500
1997
A
A'
B
B'
C
C'
Davenport
Penland
Shook
Moses#1
Moses#2
Moses#3
Moses#4
Sand
Barrett
Holland
Money
Knob
3950
4000

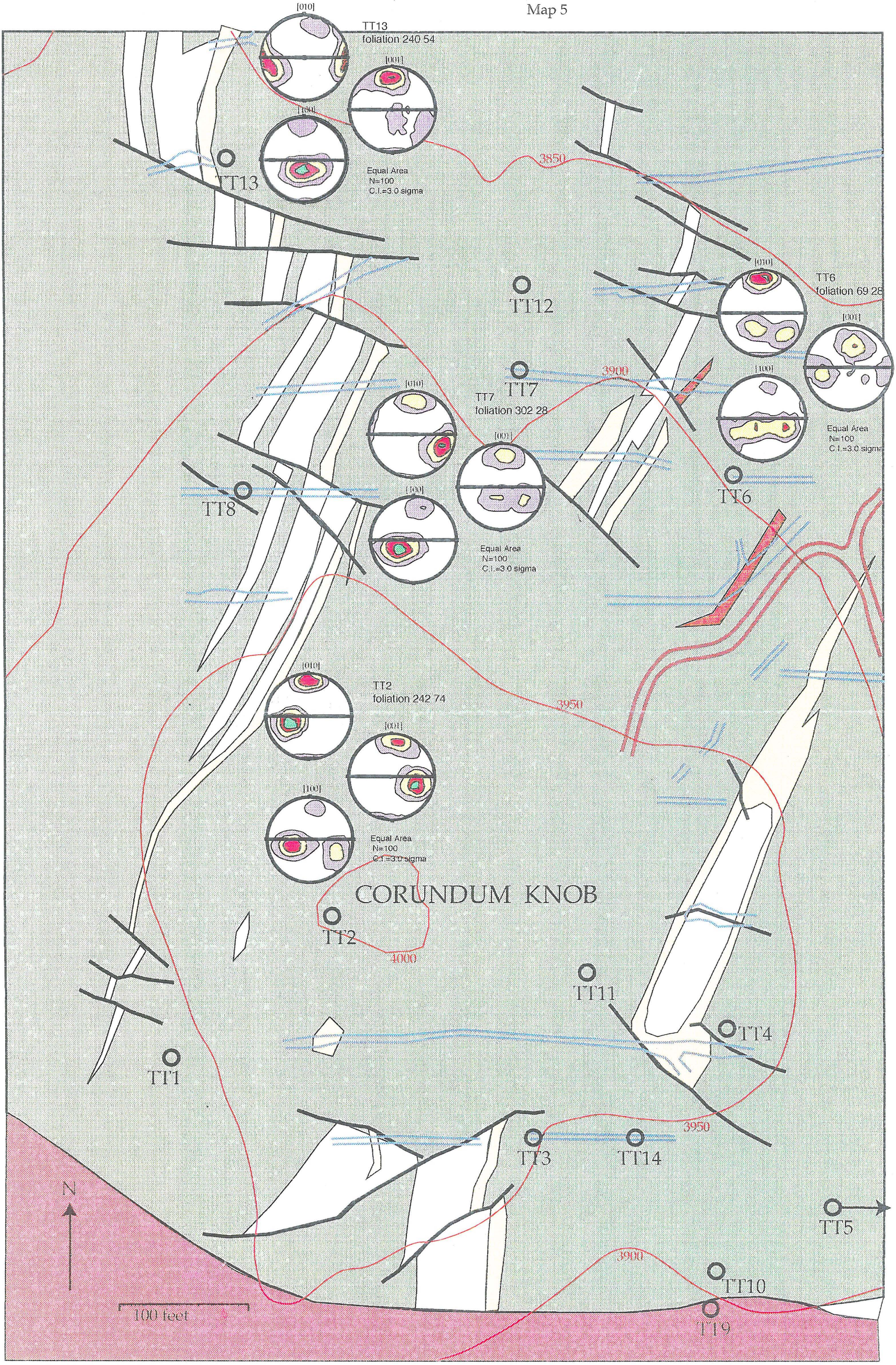
[010]
TT13
foliation 240 54
[001]
[100]
Equal Area
N=100
C.I.=3.0 sigma
TT13
3850
TT12
[010]
TT6
foliation 69 28
[001]
[100]
Equal Area
N=100
C.I.=3.0 sigma
TT7
3900
[010]
TT7
foliation 302 28
[001]
[100]
Equal Area
N=100
C.I.=3.0 sigma
TT6
TT8
[010]
TT2
foliation 242 74
[001]
[100]
Equal Area
N=100
C.I.=3.0 sigma
3950
CORUNDUM KNOB
TT2
4000
TT11
TT4
TT1
3950
TT3
TT14
N
TT5
3900
TT10
100 feet
TT9

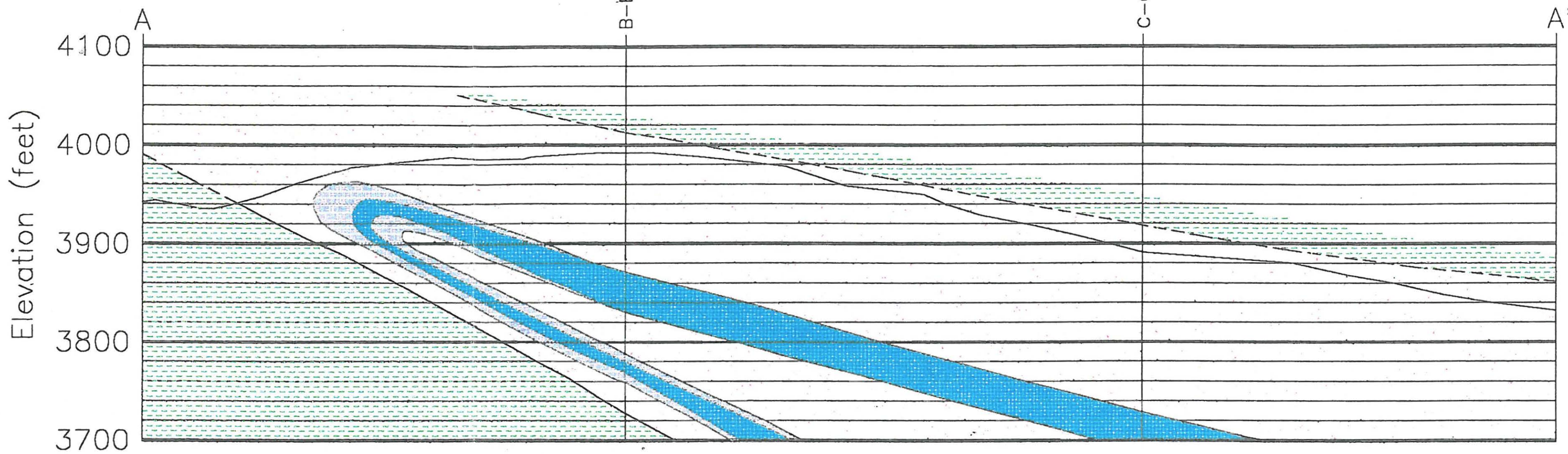
A
B-B
C-C'
A'
4100
4000
3900
3800
3700
Elevation (feet)

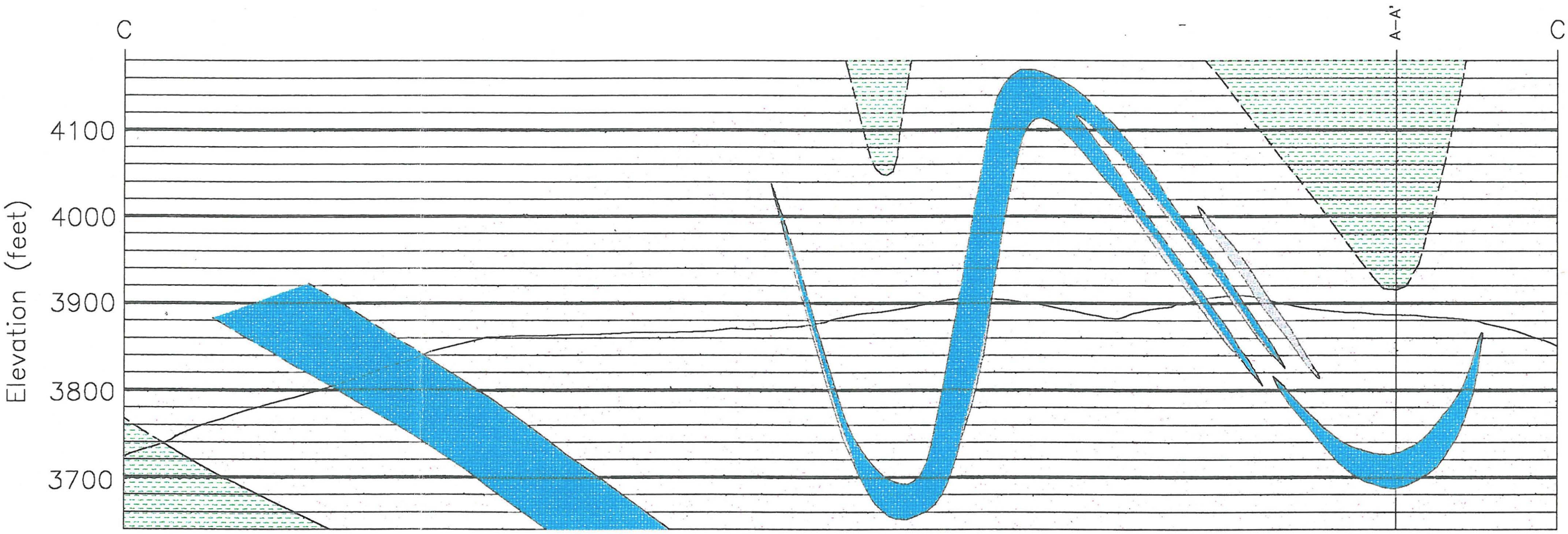
C
A-A'
C'
4100
4000
3900
3800
3700
Elevation (feet)

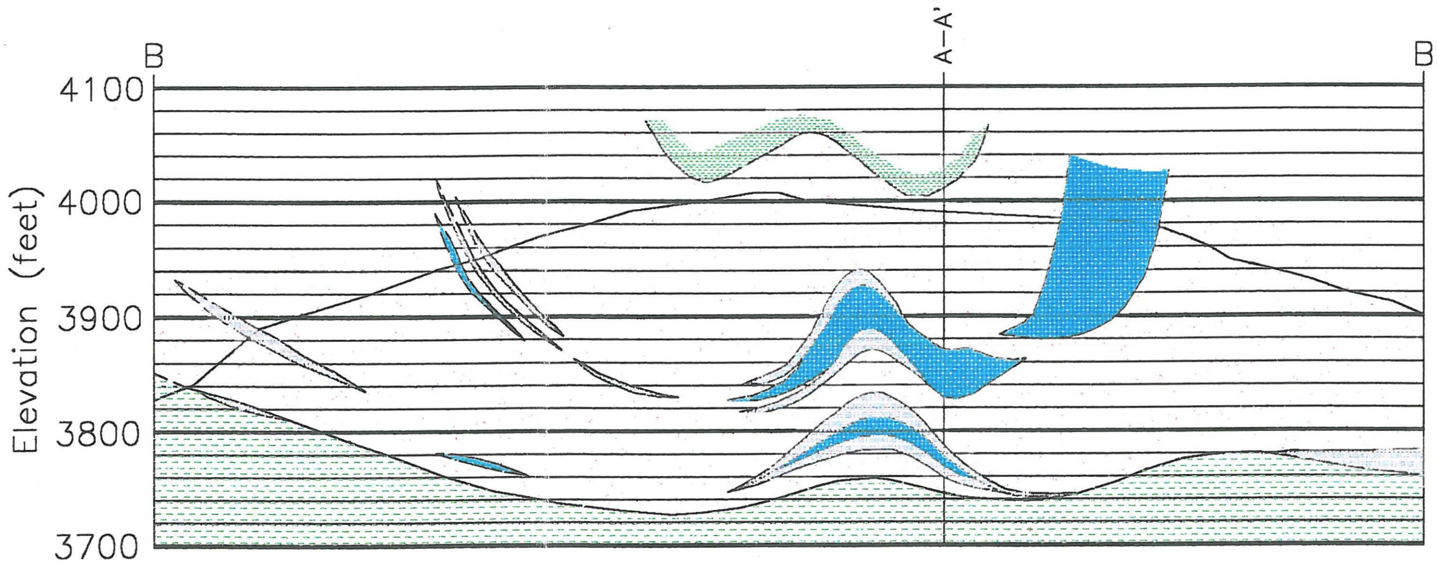
B
A-A'
B'
4100
4000
3900
3800
3700
Elevation (feet)